

สารยับยั้งเอนไซม์แอสทิลโคลินเอสเทอเรสจากรากมะสัง *Feroniella lucida*



นางสาวฉลวยลักษณ์ ภูพิชญนันท์

สถาบันวิทยบริการ
วิทยานิพนธ์นี้เป็นส่วนหนึ่งของการศึกษาตามหลักสูตรปริญญาวิทยาศาสตรมหาบัณฑิต
จุฬาลงกรณ์มหาวิทยาลัย
สาขาวิชาเคมี ภาควิชาเคมี

คณะวิทยาศาสตร์ จุฬาลงกรณ์มหาวิทยาลัย

ปีการศึกษา 2550

ลิขสิทธิ์ของจุฬาลงกรณ์มหาวิทยาลัย

ACETYLCHOLINESTERASE INHIBITORS FROM ROOTS OF *Feroniella lucida*



Miss Chalouyluk Phoopichayanun

สถาบันวิทยบริการ

จุฬาลงกรณ์มหาวิทยาลัย
A Thesis Submitted in Partial Fulfillment of the Requirements
for the Degree of Master of Science Program in Chemistry

Department of Chemistry

Faculty of Science

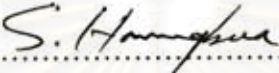
Chulalongkorn University

Academic Year 2007


Copyright of Chulalongkorn University

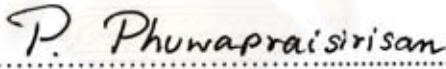
Thesis Title ACETYLCHOLINESTERASE INHIBITORS FROM ROOTS
OF *Feroniella lucida*
By Miss Chalouyluk Phoopichayanun
Field of Study Chemistry
Thesis Advisor Assistant Professor Preecha Phuwapraisirisan, Ph.D.

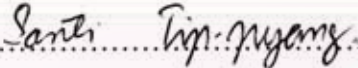
Accepted by the Faculty of Science, Chulalongkorn University in Partial
Fulfillment of the Requirements for the Master's Degree


.....Dean of the Faculty of Science
(Professor Supot Hannongbua, Ph.D.)


THESIS COMMITTEE

.....Chairman
(Professor Udom Kokpol, Ph.D.)

.....Thesis Advisor
(Assistant Professor Preecha Phuwapraisirisan, Ph.D.)

.....Member
(Associate Professor Santi Tip-pyang, Ph.D.)

.....Member
(Luksana Dubas, Ph.D.)

.....Member
(Wimolpun Rungprom, Ph.D.)

จลวยลักษณ์ ภูษิณนันท : สารยับยั้งเอนไซม์แอซีทิลโคลีนเอสเทอเรสจากรากมะสัง
Feroniella lucida (ACETYLCHOLINESTERASE INHIBITORS FROM
 ROOTS OF *Feroniella lucida*) อ. ที่ปรึกษา: ผศ. ดร.ปริษา ภูวไพริศิศา, 63 หน้า

จากการศึกษาทางเคมีของสารที่ออกฤทธิ์ยับยั้งเอนไซม์แอซีทิลโคลีนเอสเทอเรสจากส่วน
 สกัคบิวทานอลของรากมะสังซึ่งเป็นพืชสมุนไพรที่อยู่ในวงศ์ Rutaceae นำไปสู่การแยกสารพิวเว
 โนคูมารินใหม่ได้ 4 ชนิด คือ feronielloside, feronielllic acid A, feronielllic acid B and
 feronielllic acid C รวมทั้งสารคูมารินที่มีรายงานแล้ว 12 ชนิด คือ glucopsoralen, bergaptol-O-
 β -D-glucopyranoside, aesculetin glycoside, 2'', 3''-epoxyanisolactone, anisolactone,
 marmesin, feroniellin A, feroniellin C, xanthoarnol, gosferol, 7-demethylsaberrosine และ
 haploperoside D โครงสร้างทางเคมีของสารคูมารินที่แยกได้เหล่านี้สามารถพิสูจน์ได้ด้วยวิธี
 ทางสเปกโทรสโกปี การเปรียบเทียบกับข้อมูลที่มีรายงานมาแล้วและการวิเคราะห์ทางเคมี จากนั้น
 นำสารคูมารินทั้งหมดที่แยกได้ไปทดสอบหาฤทธิ์การยับยั้งเอนไซม์แอซีทิลโคลีนเอสเทอเรสได้
 ด้วยวิธีของ Ellman ซึ่งเป็นวิธีทางสเปกโทรสโกปี พบว่า gosferol แสดงฤทธิ์ยับยั้งเอนไซม์ได้ดี
 ที่สุดที่ระดับความเข้มข้น 8.3 mM รองลงมาคือ xanthoarnol และ marmesin ที่ยับยั้งเอนไซม์ได้ดี
 ที่ระดับความเข้มข้น 10.2 และ 13.3 mM ตามลำดับ นอกจากนี้ในกลุ่มพิวเว โนคูมารินไกลโคไซด์
 พบว่า feronielloside แสดงฤทธิ์ยับยั้งเอนไซม์ได้ดีที่สุดที่ระดับความเข้มข้น 16.9 mM.



สถาบันวิทยบริการ จุฬาลงกรณ์มหาวิทยาลัย

ภาควิชา.....เคมี.....ลายมือชื่อนิสิต.....*จลวยลักษณ์ ภูษิณนันท*
 สาขาวิชา.....เคมี.....ลายมือชื่ออาจารย์ที่ปรึกษา.....*ปริษา ภูวไพริศิศา*
 ปีการศึกษา.....2550.....

##4872253123: MAJOR CHEMISTRY

KEY WORD: ACETYLCHOLINESTERASE INHIBITORS / *Feroniella lucida* /
COUMARINS

CHALOUYLUK PHOOPICHAYANUN: ACETYLCHOLINESTERASE
INHIBITORS FROM ROOTS OF *Feroniella lucida*. THESIS ADVISOR:
ASST. PROF. PREECHA PHUWAPRAISRISAN, Ph.D., 63 pp.

The chemical study of acetylcholinesterase (AChE) inhibitory activity compounds from BuOH crude extract from roots of *Feroniella lucida* in the family Rutaceae led to the isolation of four new furanocoumarins, named feronielloside, feronielllic acid A, feronielllic acid B and feronielllic acid C along with twelve known coumarins, glucopsoralen, bergaptol-O- β -D-glucopyranoside, aesculetin glycoside, 2'', 3''-epoxyanisolactone, anisolactone, marmesin, feroniellin A, feroniellin C, xanthoarnol, gosferol, 7-demethylsaberossine and haploperoside. Their structures were elucidated by the combination of spectroscopic method as well as comparison with previous literature data and chemical evidence. All the isolated coumarins were tested for AChE inhibitory activity by Ellman spectroscopic method. Of the isolated coumarins, gosferol was showed strong inhibitory effect against AChE with IC₅₀ value of 8.3 mM. In addition, xanthoarnol and marmesin were also found to be active in inhibiting AChE with IC₅₀ values of 10.2 and 13.3 mM, respectively. Of coumarin glycosides, feronielloside was the most active AChE inhibitor with IC₅₀ value of 16.9 mM.

สถาบันวิทยบริการ
จุฬาลงกรณ์มหาวิทยาลัย

Department.....Chemistry..... Student's signature..... *C. Phoopichayanun*
Field of study.....Chemistry..... Advisor's signature..... *P. Phuwapraisrisan*
Academic year.....2007.....

ACKNOWLEDGEMENTS

This thesis would not have been possible to complete without the support of the following individuals. Firstly, I would like to express my greatest gratitude to my advisor, Assistant Professor Preecha Phuwapraisirisan, for invaluable guidance during the course of this work.

I would like to express my heartfelt thank to Professor Dr. Udom Kokpol for his usual kind support over the accomplishment of my thesis as well as Associate Professor Santi Tip-pyang, Dr. Luksana Dubas and Dr. Wimolpun Rungprom, members of the thesis committee for extending cooperation over my presentation.

I would like to express my gratitude to Natural Products Research Unit, Department of Chemistry, Faculty of Science, Chulalongkorn University for providing the chemicals and facilities throughout the course of study.

The special thank to Dr. Wanchai Pluempanupat and Ms. Kamjira Saisin for their technical assistance. Furthermore, all of my friends in the laboratory for their friendships and help during the course of my graduate research.

Finally, I would like to thank 90th Anniversary of Chulalongkorn University Fund for the financial supports.



สถาบันวิทยบริการ
จุฬาลงกรณ์มหาวิทยาลัย

CONTENTS

	Page
ABSTRACT (IN THAI)	iv
ABSTRACT (IN ENGLISH)	v
ACKNOWLEDGEMENTS	vi
CONTENTS	vii
LIST OF TABLES	ix
LIST OF FIGURES	x
LIST OF SCHEMES	xii
LIST OF ABBREVIATIONS	xiii
CHAPTER	
I INTRODUCTION	1
II ISOLATION AND CHARACTERIZATION OF ISOLATED	
COUMARINS FROM <i>feroniella lucida</i>	14
2.1 Extraction and isolation of <i>Feroniella lucida</i>	14
2.2 Structure elucidation of feronielloside	16
2.3 Structure elucidation of feronielllic acid A-C.....	20
2.4 Experiment section.....	26
2.4.1 General experimental procedure.....	26
2.4.2 Plant material.....	26
2.4.3 Extraction and purification.....	26
2.4.4 Preparation of feronielloside pentaacetate.....	27
2.4.5 Hydrolysis of feronielloside.....	27
2.4.6 Modified Mosher's analysis.....	28
2.4.7 Anti dihydroxylation of 5 under acid condition.....	28
2.4.8 Syn dihydroxylation of 6 under Upjohn condition.....	29
III INVESTIGATION OF ACETYLCHOLINESTERASE	
INHIBITORY ACTIVITY OF ISOLATED COUMARINS	33
3.1 Acetylcholinesterase inhibition assay method	33
3.2 Result and discussion	34
3.3 Chemical and equipment.....	36

CONTENTS

	Page
3.4 Procedures.....	36
IV CONCLUSION.....	37
REFERENCES.....	40
APPENDICES.....	43
VITA.....	63



สถาบันวิทยบริการ
จุฬาลงกรณ์มหาวิทยาลัย

LIST OF TABLES

Table	Page
2.1 ^1H and ^{13}C NMR data for feronielloside (1) in CD_3OD	19
2.2 $\Delta\delta_{\text{H}}$ values of model compound (5a or 5b), 11 , 12 and 13	23
2.3 ^1H and ^{13}C NMR data of feronielic acid A-C (11-13) in CDCl_3	25
3.1 AChE inhibitory activity of isolated coumarins from roots of <i>Feroniella lucida</i>	35



สถาบันวิทยบริการ
จุฬาลงกรณ์มหาวิทยาลัย

LIST OF FIGURES

Figure	Page
1.1 Schematic diagram of a neuron representing altered neurotransmission in AD..	2
1.2 The proposed neurotransmission with AChE inhibitors.....	3
2.1 Selected HMBC correlations of 1	17
2.2 Diagnostic HMBC correlations observed in 1a	18
2.3 $\Delta\delta_{SR}$ values for the MTPA esters (1c and 1d) of 1b	19
2.4 Selected HMBC correlations of 11	20
2.5 ^1H NMR spectra of 11-13 in range of 4.2-5.3 ppm.....	21
2.6 ^1H NMR spectra of model compound and 11 in range of 1.8-7.2 ppm.....	23
2.7 $\Delta\delta$ sign distribution model for the MTPA esters of the possibilities of 1, 4-diol	24
2.8 Δ_{SR} values of the MTPA esters (5c and 5d) of 5a or 5b	24
3.1 Reaction mechanism of ACh	33
1 The ^1H NMR (CD ₃ OD) spectrum of feronielloside (1).....	44
2 The ^1H NMR (CDCl ₃) spectrum of feronielloside pentaacetate (1a).....	44
3 The ^1H NMR (CD ₃ OD) spectrum of glucopsoralen (2).....	45
4 The ^1H NMR (CD ₃ OD) spectrum of bergaptol-O- β -D-glucopyranoside (3).....	45
5 The ^1H NMR (CD ₃ OD) spectrum of aesculetin glycoside (4).....	46
6 The ^1H NMR (CDCl ₃) spectrum of 2'', 3''-epoxyanisolactone (5).....	46
7 The ^1H NMR (CDCl ₃) spectrum of anisolactone (6).....	47
8 The ^1H NMR (CDCl ₃) spectrum of marmesin (7).....	47
9 The ^1H NMR (CDCl ₃) spectrum of feroniellin A (8).....	48
10 The ^1H NMR (CDCl ₃) spectrum of feroniellin C (9).....	48
11 The ^1H NMR (CDCl ₃) spectrum of xanthoarnol (10).....	49
12 The ^1H NMR (CDCl ₃) spectrum of feroniellic acid A (11).....	49
13 The ^1H NMR (CDCl ₃) spectrum of feroniellic acid B (12).....	50
14 The ^1H NMR (CDCl ₃) spectrum of feroniellic acid C (13).....	50
15 The ^1H NMR (CDCl ₃) spectrum of gosferol (14).....	51

Figure	Page
16 The ^1H NMR (CDCl_3) spectrum of 7-demethylsaberosine (15).....	51
17 The ^1H NMR (CD_3OD) spectrum of haploperoside D (16).....	52
18 The COSY (CD_3OD) spectrum of feronielloside (1).....	52
19 The HSQC (CD_3OD) spectrum of feronielloside (1).....	53
20 The HMBC (CD_3OD) spectrum of feronielloside (1).....	53
21 Mass spectrum of feronielloside (1).....	54
22 The COSY (CDCl_3) spectrum of feronielloside pentaacetate (1a).....	54
23 The HSQC (CDCl_3) spectrum of feronielloside pentaacetate (1a).....	55
24 The HMBC (CDCl_3) spectrum of feronielloside pentaacetate (1a).....	55
25 Mass spectrum of feronielloside pentaacetate (1a).....	56
26 The COSY (CDCl_3) spectrum of feroniellic acid A (11).....	56
27 The HSQC (CDCl_3) spectrum of feroniellic acid A (11).....	57
28 The HMBC (CDCl_3) spectrum of feroniellic acid A (11).....	57
29 Mass spectrum of feroniellic acid A (11).....	58
30 The COSY (CDCl_3) spectrum of feroniellic acid B (12).....	58
31 The HSQC (CDCl_3) spectrum of feroniellic acid B (12).....	59
32 The HMBC (CDCl_3) spectrum of feroniellic acid B (12).....	59
33 Mass spectrum of feroniellic acid B (12).....	60
34 The COSY (CDCl_3) spectrum of feroniellic acid C (13).....	60
35 The HSQC (CDCl_3) spectrum of feroniellic acid C (13).....	61
36 The HMBC (CDCl_3) spectrum of feroniellic acid C (13).....	61
37 Mass spectrum of feroniellic acid C (13).....	62

LIST OF SCHEMES

Schemes	Page
2.1 The isolated procedure of BuOH extract from roots of <i>Feroniella lucida</i>	16
2.2 Reaction reagents and conditions of feroneilloside (1).....	17
2.3 Reaction reagents and conditions of feronielllic acid A-C (11-13).....	22



สถาบันวิทยบริการ
จุฬาลงกรณ์มหาวิทยาลัย

LIST OF ABBREVIATIONS

AD	Alzheimer's disease
APP	Amyloid precursor protein
apo	Apolipoprotein
ACh	Acetylcholine
AcCoA	Acetyl coenzyme A
A β	Beta-amyloid
AChE	Acetylcholinesterase enzyme
AcCl	Acetyl chloride
ATCI	Acetylthiocholine iodine
BuChE	Butylcholinesterase
BuOH	Buthanol
brd	Broad doublet (NMR)
^{13}C NMR	Carbon-13 nuclear magnetic resonance
CDCl_3	Deuterated chloroform
CD_3OD	Deuterated methanol
COSY	Correlated spectroscopy
calcd	Calculated
CNS	Central nervous system
ChAT	Choline acetyltransferase
ChE	Cholinesterase
2D NMR	Two dimensional nuclear magnetic resonance
d	Doublet (NMR)
dd	Doublet of doublet (NMR)
DTNB	5, 5'-dithiobis (2-nitrobenzoic acid)
G1	Globular tetrameric form
G4	Globular monomeric form
^1H NMR	Proton nuclear magnetic resonance
HSQC	Heteronuclear single quantum correlation
HMBC	Heteronuclear multiple bond correlation experiment
HPLC	High performance liquid chromatography
Hz	Hertz

HRESIMS	High resolution electrospray ionization mass spectrum
HCl	Hydrochloric acid
IC ₅₀	Concentration that required for 50% inhibition in vitro
<i>J</i>	Coupling constant
L	Liter (s)
m	Multiplet (NMR)
mL	Milliliter (s)
M	Molar
MeOH	Methanol
<i>m/z</i>	Mass per charge
mAChR	Muscarinic ACh receptors
MTPACl	α -methoxy- α -(trifluoromethyl)-phenylacetyl chloride
<i>m</i> -CPBA	<i>m</i> -chloroperoxybenzoic acid
NMR	Nuclear magnetic resonance
NFT	Neurofibrillary tangle
nAChR	Nicotinic ACh receptor
NaOH	Sodium hydroxide
sAPP α	Soluble amyloid precursor protein
UV	Ultraviolet
U	Unit
VCC	Vacuum column chromatography
δ	Chemical shift
δ_C	Chemical shift of carbon
δ_H	Chemical shift of proton
λ_{\max}	Maximum wavelength
μL	Microliter (s)
ϵ	Molar extinction coefficient
$[\alpha]_D$	Specific optical rotation

CHAPTER I

INTRODUCTION

Neurodegenerative disease is a generic term applied to a variety of conditions arising from a chronic breakdown and deterioration of neurons, particularly those of the central nervous system (CNS). In addition, these neurons may accumulate aggregated proteins which cause dysfunction. Alzheimer's disease (AD) is the best-known disease of this group which is involved a decline in cognitive dysfunction, primarily memory loss and in the later stages of the disease language deficits, depression, agitation, mood disturbances and psychosis are often seen.

Although a definitive cause has not yet been determined, several have been proposed. Mutations in the amyloid precursor protein (APP) gene (chromosome 21), the presenilin 1 gene (chromosome 14) and the presenilin 2 gene (chromosome 1) produce an autosomal dominant pattern of inheritance. Because of overproduction or transcription errors, an abnormal subunit of APP (beta-amyloid) is produced. The accumulation of beta-amyloid initiates the contributing cell death, disruption of cell membranes, inflammatory response, neurofibrillary tangle (NFT) formation, cerebral amyloid angiopathy and neurofibrillary degeneration.

Apolipoprotein (Apo E), a normal protein involved in the metabolism of cholesterol and lipoprotein, has been linked to the development of AD. Apo E possesses 3 alleles: $\epsilon 2$, $\epsilon 3$, and $\epsilon 4$. Of those alleles, $\epsilon 4$ appears to significantly reduce brain cholinergic activity and increase the risk of AD. Current criteria for the pathologic diagnosis of AD require the presence of both neuritic plaques and NFTs, which correlate with neuron and synapse loss. Neuritic plaques consist of a central core of amyloid protein, often containing paired helical filaments. NFTs contain paired helical filaments of abnormally phosphorylated tau protein that occupy the cell body and extend into the dendrites. The damage caused by plaques, NFTs, and subsequent cell death leads to significantly reduced cholinergic activity in the brain.

Acetylcholine (ACh) is the primary neurotransmitter that facilitates learning and increases attention. The ACh deficiency seen in AD led to the formulation of the cholinergic hypothesis, which states that the inability to transmit neurologic impulses across brain synapses is the cause of cognitive.

Three major principles underlie the use of cholinergic agents to treat AD. The first is reduced activity of choline acetyltransferase (ChAT) in the cerebral cortex. Levels of ChAT depletion correlate with the extent of neuritic plaque formation. Second, a reduction occurs in presynaptic muscarinic type 1 and nicotinic receptors but postsynaptic muscarinic type 2 receptors are preserved. Third, the large neurons responsible for the supply of ACh to the cerebral cortex, important for attention and new learning, are lost. Neuropathologic studies have shown the presence of NFTs in these neurons. In addition, cholinergic agonists have been found to facilitate the learning process, which also supports the important role of ACh in attention and learning. Among the different types of drugs that are used to modify cholinergic neurotransmission, only the cholinesterase (ChE) inhibitors have been effective to date. Physostigmine, rivastigmine and galanthamine are unique ChE inhibitors that have been approved by the US Food and Drug Administration for the treatment of mild to moderate AD [1-3].

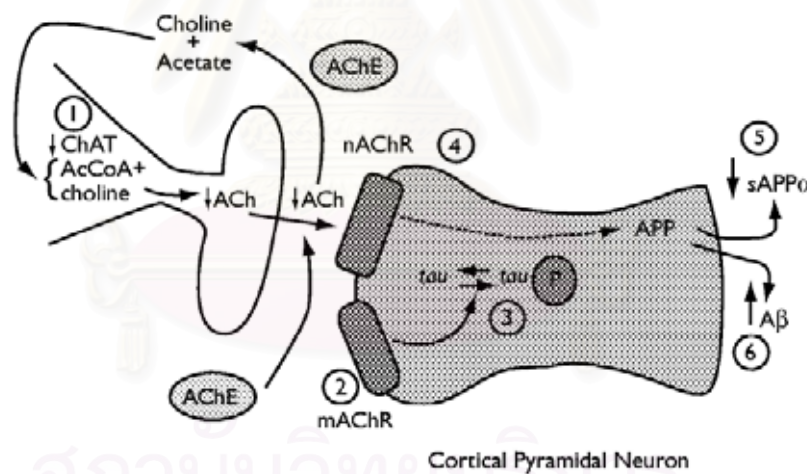


Figure 1.1. Schematic diagram of a neuron representing the altered neurotransmission in AD. (1) Substantial cortical deficits in the enzyme responsible for the synthesis of ACh from acetyl coenzyme A (AcCoA) and choline acetyltransferase (ChAT); therefore, release of ACh into the synaptic cleft is decreased. (2) Decreased coupling of second messengers to the muscarinic ACh receptors (mAChR). (3) Decreased coupling causing a shift of tau protein to the hyperphosphorylated state (precursor to neurofibrillary tangles). (4) Interaction of nicotinic ACh receptor (nAChR) with beta-amyloid ($A\beta$). (5) The interaction causing decreased secretion of soluble amyloid

precursor protein (sAPP α). (6) The interaction also increases production of A β protein. AChE and APP adapted with permission.

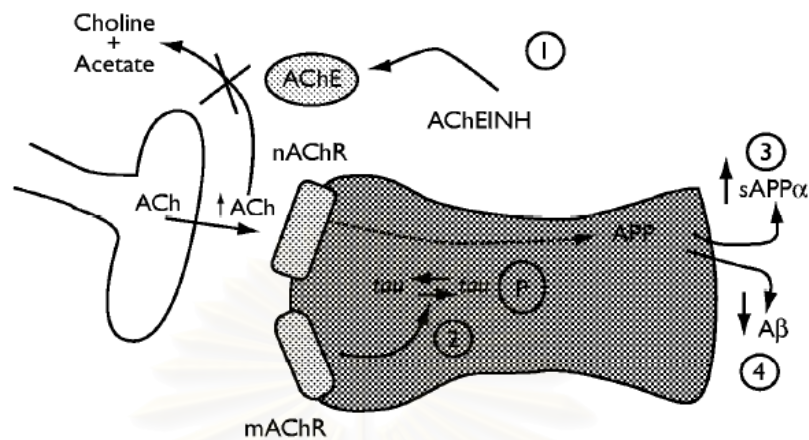
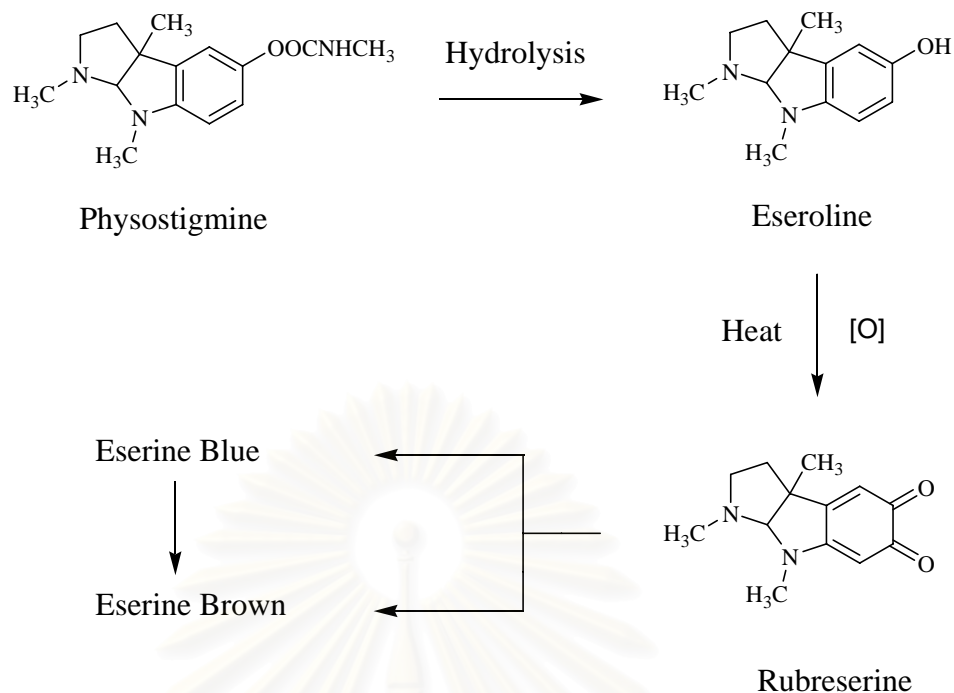


Figure 1.2. The proposed neurotransmission with AChE inhibitors. (1) ACh breakdown by AChE is inhibited because of addition of AChE inhibitor (AChEINH). Reduced phosphorylation of tau protein. (3). The secretion of soluble amyloid precursor protein (sAPP α) returning to normal. (4) The production of A β protein is reduced to normal. nAChR, APP and mAChR were adapted with permission.

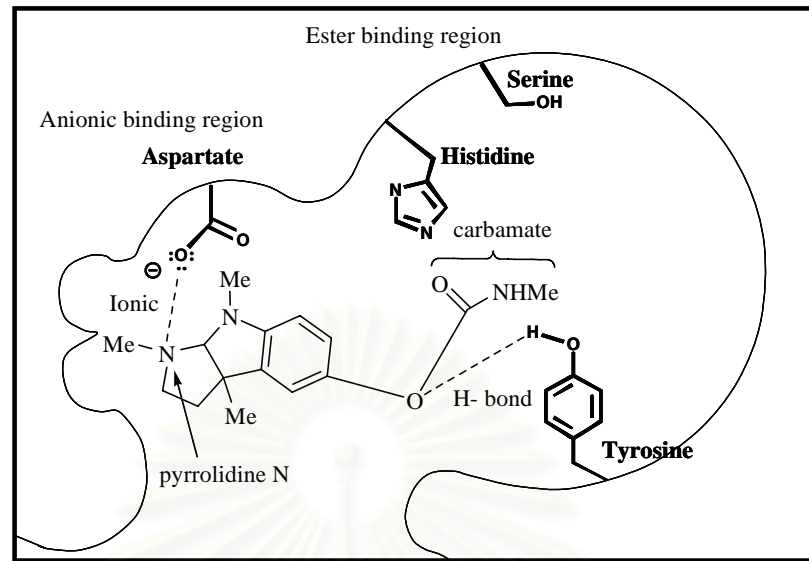
1.1 Acetylcholinesterase inhibitors from plants

The classic cholinesterase inhibitor is the alkaloid physostigmine (eserine). It was isolated from the seeds of *Physostigma venenosum* (Calabar bean) [4] that was discovered in the 19th century. Although other chemicals were discovered later, physostigmine still remains as the most valuable alkaloid and is soluble in organic solvents. Physostigmine is highly unstable, and turns a red compound, rubreserine which is converted into eserine blue or eserine brown upon exposure to light, air and especially heat. These major metabolic products are significantly less active inhibitors of AChE than physostigmine.

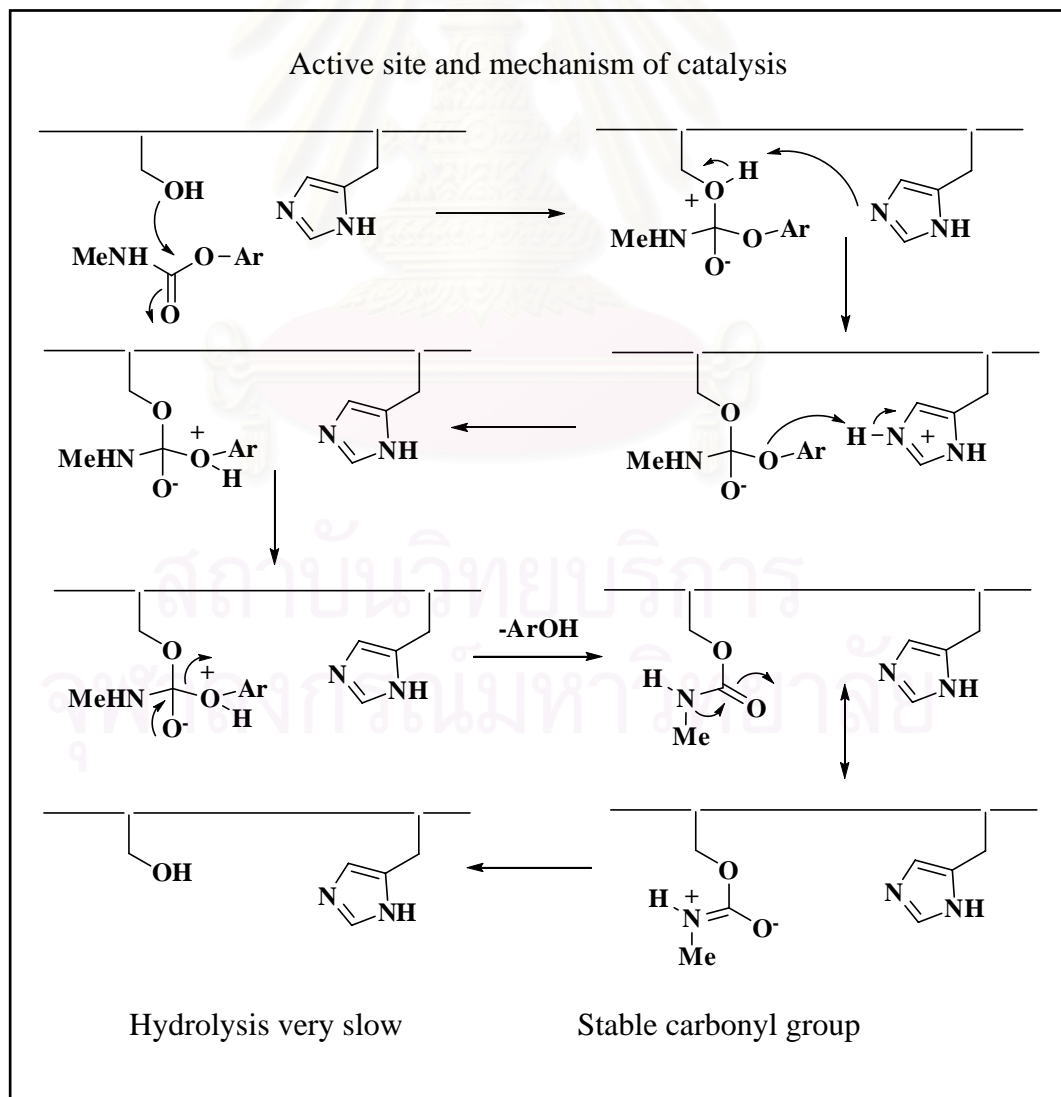


In recent years, the structure of AChE has been determined and the mode of binding for AChE inhibitors has also been elucidated. The particular amino acid residues which are considered to be the most important in the binding process and from this knowledge, structure-activity relationships of AChE inhibitors can be understood at the intermolecular level. The important regions of an inhibitor appear to be positively charged nitrogen (pyrrolidine N) of physostigmine, which binds to an aspartate residue, and a region, separated by a lipophilic area from the positive charge, which can form a hydrogen bond with a tyrosine or serine residue in the active site of AChE. Carbamate or urethane which can bind to a serine residue by histidine acting as a basic catalyst is formed as a deactivated carbonyl group and it is not surprising that physostigmine is a blocking hydrolysis of ACh.

Active site and binding interaction



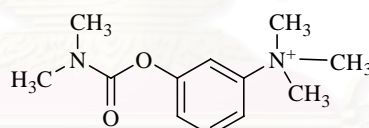
Active site and mechanism of catalysis



Since physostigmine was known to cross the blood-brain barrier, several *in vivo* studies were conducted which showed that it reduced symptoms of ACh deficiency in the CNS. Physostigmine was reported to protect mice against cognitive impairment caused by oxygen deficit and it improved learning in rats [5]. Clinical studies showed significant cognitive benefits in both normal and AD patients [6]. As well as inhibiting AChE, physostigmine also inhibited butylcholinesterase (BuChE), another enzyme found in the CNS.

Although the animal evidence suggests that physostigmine was a useful pretreatment for AD patients, there are several drawbacks to its use. Physostigmine has a relatively short half-life. Therefore, it must be given relatively frequently and in relatively high oral doses. In addition, physostigmine has been reported to have severe side effects, including nausea, vomiting and diarrhea.

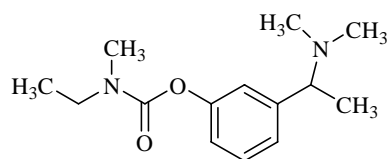
To improve its pharmacokinetic profile, there is a synthesis of analogues of physostigmine. These have been applied to the treatment of myasthenia gravis, neostigmine being the most widely used drug for this disease. Neostigmine is a quaternary amine and this feature severely impairs its ability to cross the blood-brain barrier and so be of value in treating AD [7].



Neostigmine

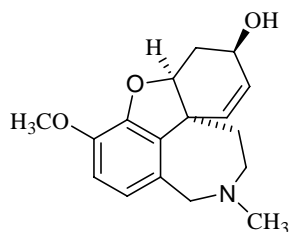
Rivastigmine tartrate (Exelon[®]) is a carbamate derivative that reversibly inhibits the metabolism of AChE and BuChE in the CNS and has been licensed as a treatment for symptomatic relief of AD since 2000. It binds to both the esteratic and ionic sites of AChE, preventing the enzyme from metabolizing ACh. Several isoforms of AChE have been identified, with identical amino acid sequence, but with different posttranslational modifications, anatomic and microanatomic locations and functions. The predominant form of AChE in the cortical and hippocampal regions of the normal brain is the membrane-bound globular tetrameric form, G4, with a small amount of the monomeric form, G1. Due to a selective loss of the G4 form in patients with dementia, the G1 form predominates. In AD patients, rivastigmine preferentially inhibits the G1 form of AChE compared with the G4 form. As a carbamate derivative,

rivastigmine is therefore contraindicated in patients with carbamate hypersensitivity risk such as asthma, bradycardia, sick sinus syndrome and epilepsy [8].

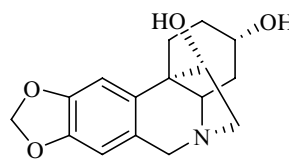


Rivastigmine

Galantamine was found in members of the Amaryllidaceae, such as the Chinese medicinal herb *Lycoris radiata* and the European *Galanthus nivalis* L. and *Narcissus* spp. A comprehensive report of the development of galantamine from *Galanthus nivalis* has been recently published [9]. Galantamine increases the availability of ACh in the cholinergic synapse by competitively inhibiting AChE and has more than a 10 fold selectivity for AChE relative to BuChE, which is in contrast to nonselective agents such as tacrine and physostigmine. Galantamine also potentiates cholinergic neurotransmission by positively modulating the response of nAChRs to ACh. Galantamine is an allosteric potentiation ligand because it acts at a site on the nAChR that is different from ACh-binding site [10]. Pharmacological studies showed that enhancing both pre- and post synaptic nAChR function by making nAChRs more sensitive to available ACh and submicromolar concentrations of galantamine increase the frequency of opening of nicotinic receptor ion channels, thereby potentiating submaximal ACh-activated currents and possibly enhancing cholinergic function and memory. This effect suggests that galantamine may have therapeutic advantages over other AChE inhibitors and its value in vascular dementia as well as AD. Several other alkaloids isolated from Iberian *Narcissus* species have been tested for cholinesterase activity. A study of two *Crinum* species used in Nigerian traditional medicine to help ailing memory resulted in the isolation of four alkaloids of which the most active was hamayne, although its IC₅₀ value of 250 μM was three orders of magnitude weaker than physostigmine, so it is likely that it would be present in sufficient quantity to have a strong therapeutic effect [11].

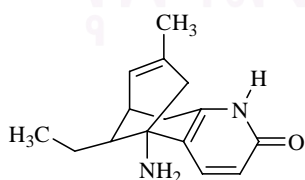


Galantamine

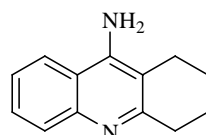


Hamayne

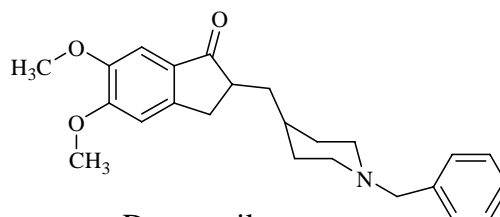
While physostigmine analogues and galantamine have entered the pharmacopoeia in the Western world, another natural cholinesterase inhibitor, huperzine A (Hup A) has been introduced in China for treating AD. Hup A is one of the alkaloids found from Qian Ceng Ta, a traditional Chinese medicine produced from the whole plant of the club moss *Huperzia serrata* Thumb. (Lycopodiaceae) which is used in various formulae in Chinese medicine to alleviate problems of memory loss, promote circulation and for fever and inflammation. Hup A is related to the quinolizidine alkaloids and reversibly inhibits AChE in vitro and in vivo. Hup A has been marketed in China as a new drug for AD treatment, and its derivative ZT-1 is being developed as anti-AD new drug candidate both in China and Europe. Hup A has been shown to improve memory in cognitively impaired rats and gerbils following ischemia. These observations suggest that Hup A has clinical potential in cerebrovascular disorders. Indeed, since it has also been shown to be neuroprotective, AChE inhibition may not be the only explanation for the clinical effects observed but also has been shown to be neuroprotective against β -amyloid peptide fragment and free radical-induced cytotoxicity and to attenuate apoptosis by inhibiting the mitochondria-caspase pathway. Hup A was reported to be more selective for AChE than BuChE and was less toxic than the synthetic AChE inhibitors donepezil and tacrine [12-13].



Huperzine A

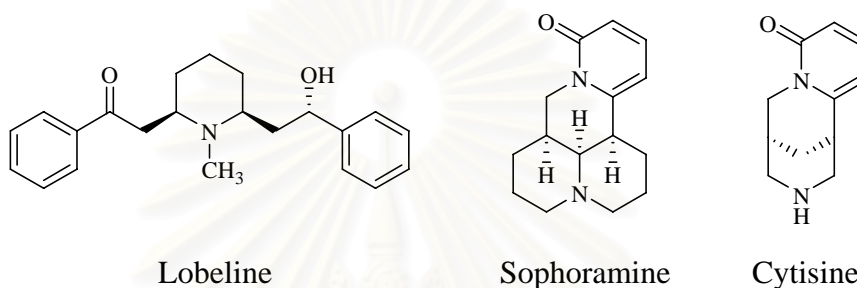


Tacrine

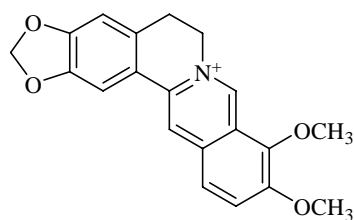


Donepezil

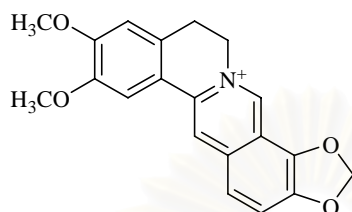
There are several other alkaloids which are nicotinic agonists at the cholinergic receptor. Lobeline from *Lobelia inflata* interacts with the nicotinic receptor and could also be exploited to influence cholinergic function in AD. Other alkaloids such as sophoramine and cytosine found in members of the Leguminosae, have nicotinic actions. Cytisine is used as a pharmacological tool because of its strong binding affinity to nicotinic receptors but it does not appear to have been developed for any pharmaceutical purposes, probably because of its toxicity [14].



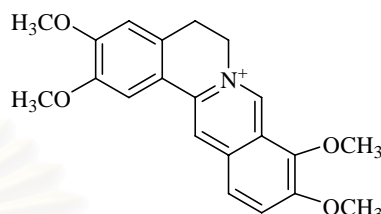
Other alkaloids have shown AChE activity and most of these have been isolated from plants used in traditional medicine. *Coptis chinensis* Franch. (Ranunculaceae) has been used for several conditions including age-related cognitive and memory decline. Some alkaloids found in this species, such as berberine, coptisine and palmatine, are also ChE inhibitors. Berberine has been shown to be selectively active against AChE compared with BuChE. Rutaecarpine is the major alkaloid found in *Evodia rutaecarpa* (Juss.) Benth. (Rutaceae); the unripe fruit of which was used in inhibitory COX-2 activity in vitro, and was anti-inflammatory in vivo. Dehydroevodiamine, another alkaloid found in the same plant, inhibited AChE in vitro and reversed scopolamine induced memory impairment in rats. Solanidine and related compounds, steroidal alkaloids produced in genus *Solanum*, have been known for AChE inhibition but these alkaloids have not been investigated for any usefulness clinically, presumably because of their toxicity such as sweating, palpitations and CNS disturbance including hallucinations [15].



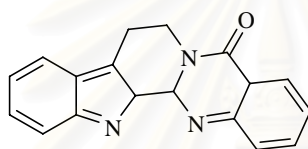
Berberine



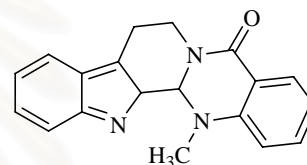
Coptisine



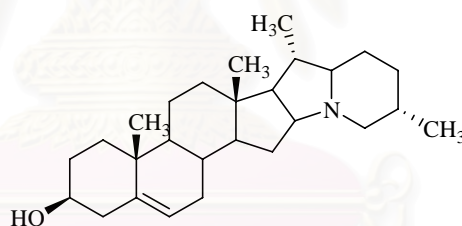
Palmatine



Rutaecarpine

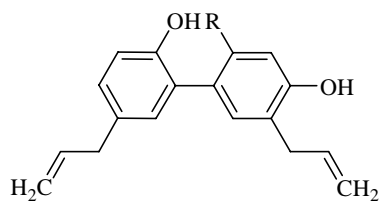


Dehydroevodiamine



Solanidine

There are many types of phenolic compounds, but the only ones which have been shown to possess AChE inhibitory activity are neolignans from *Magnolia officinalis*. The root and stem bark of *Magnolia officinalis* Rehd. have been used to treat anxiety and nervous disturbances. *M. officinalis* contains the biphenolic lignans, honokiol and magnolol. Both lignans increased ChAT activity and inhibited AChE activity in vitro and increased hippocampal ACh release in vivo. Honokiol and magnolol showed anxiolytic effects and these appear to be due to their ability to potentiate GABAergic neurotransmission. These two compounds also have antioxidant, anti-inflammatory and neuroprotective properties and such polyvalency in activity is of interest in their potential use in treating AD [16].



Honokiol: R = H

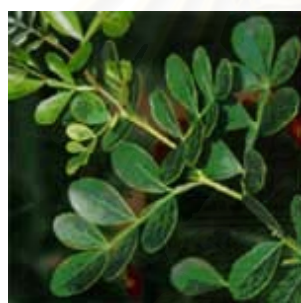
Magnolol: R = OH

Since the recent report of AChE inhibitors from plant origin, several inhibitors have attracted the attention of neuropharmacologists. Unfortunately, the potential effectiveness offered is limited by the appearance of central and peripheral side effect and their toxic properties. Recent data focus on the other natural inhibitory compounds and disclose the involvement of other neurotransmitters that highly enhance memory and are not toxic to AD patients.

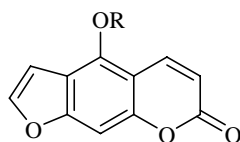
1.2 *Feroniella Lucida*

Feroniella lucida or Ma sang is a plant in the family Rutaceae. The genus of *Feroniella* was categorized into the subtribe Balsmocitrinae. Leaves are small 2-5- (usually 3-4-) paired; rachis pubescent, articulate at the node, internodes more or less winged above, petioles very short, pubescent. Leaflets elliptic or obovate, obtuse at the apex, often cuneate at base, entire or subscrenulat, margins recurve, shining and glabrous above, below opaque pubescent all over or only at the veins, pellucid-punctate over the whole surface, but having a single series of larger glands near the margin. Panicles loose, made up of 3-flowered cymes, often 2 or 3 grouped in the axils, pubescent, shorter than the leaves. Flowers large, hermaphrodite, or staminate by abortion of the stigma and ovules; flower-buds opening early with all parts continuing to grow. Calyx lobes linear, pubescent, deciduous; petals acuminate, margins reflexed at base, opening erect, then recurving, glabrous; stamens 16-25 in mature flowers, exserted; anthers oblong, 4-cornered, cordate at the base, truncate-mucronulate at the apex; pollen round with 3-4 pores, with granulose exine; ovary globose, glabrous; style in perfect flowers elongate, terete, glabrous with an exerted persistent fusiform stigma; in the majority of the flowers the style is very short, the stigma deformed or aborted; Fruits with a very thick woody epicarp. Seeds immersed in glutinous pulp arising from the placenta and the endocarp. This species is native in

central Java, usually growing at less than 400 meters altitude. It is a medium-sized tree, 10 to 15 meters (30 to 49 feet) tall, with a straight trunk 20 to 30 cm in diameter. It is common in stands of teak (*Tectona grandis*). It sometimes occurs in situations where the soil is periodically very dry. In Cambodia and India, this species is popularly cultivated as an ornamental plant, while the leaves and fruit are used as foods and medicines.



The first photochemical investigations of *Feroniella lucida* revealed coumarins having highly oxygenated C₁₀ moieties, feroniellins A-C from the roots. Feroniellins A and B were cytotoxic against human KB with IC₅₀ values of 0.13 and 0.23 mM respectively and HeLa carcinoma cells with IC₅₀ values of 0.14 and 0.19 mM, respectively [17]. Several furanocoumarins including feroniellamin inhibited lipid peroxidation with an IC₅₀ value of 52 μM [18].

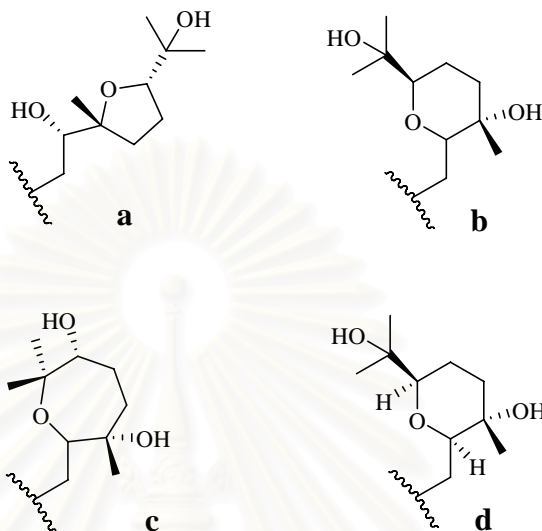


Feroniellin A: R = **a**

Feroniellin B: R = **b**

Feroniellin C: R = **c**

Feroniellamin: R = **d**



As a part of searching for natural inhibitors for AChE with TLC bioautographic assay method, the BuOH extract from roots of *Feroniella lucida* was the most active in AChE assay. Currently no AChE inhibitory activity has been reported from this species contains coumarin compounds. Therefore, for this purpose, the BuOH extract was examined in the efficient constitution. The objectives of this research can be summarized as followed:

1. To extract and isolate compounds from the BuOH extract of roots of *F. lucida* roots.
2. To elucidate the structures of all isolated compounds.
3. To determine the AChE inhibitory activity of the isolated compounds.

CHAPTER II

ISOLATION AND CHARACTERIZATION OF ISOLATED COUMARINS FROM *Feroniella lucida*

2.1. Isolation

The BuOH extract from roots of *Feroniella lucida* was divided into two parts. The first part of BuOH extract was separated through VCC technique. Repeated column chromatography over Sephadex LH-20 followed by silica gel and RP- HPLC afforded a new furanocoumarin glycoside named feronielloside (1) together with three known furanocoumarin glycosides, glucopsoralen (2), bergaptol-O- β -D-glucopyranoside (3) and aesculetin glycoside (4). The second part of BuOH extract was separated via Diaion HP-20 into acetone, MeOH and water soluble fractions. The acetone soluble fraction yielded six known coumarins, 2'', 3''-epoxyanisolactone (5), anisolactone (6), marmesin (7), feroniellin A (8), feroniellin C (9) and xanthoarnol (10). The MeOH soluble fraction led to the isolation of three new coumarins named feroniellin acid A-C (11-13) along with three known coumarins, gosferol (14), 7-demethylsaberose (15) and haploperoside D (16). The structures of known compounds were identified by comparison of their ^1H NMR and MS data with those reported in the literature. Isolation procedure was summarized in scheme 2.1.

สถาบันวิทยบริการ
จุฬาลงกรณ์มหาวิทยาลัย

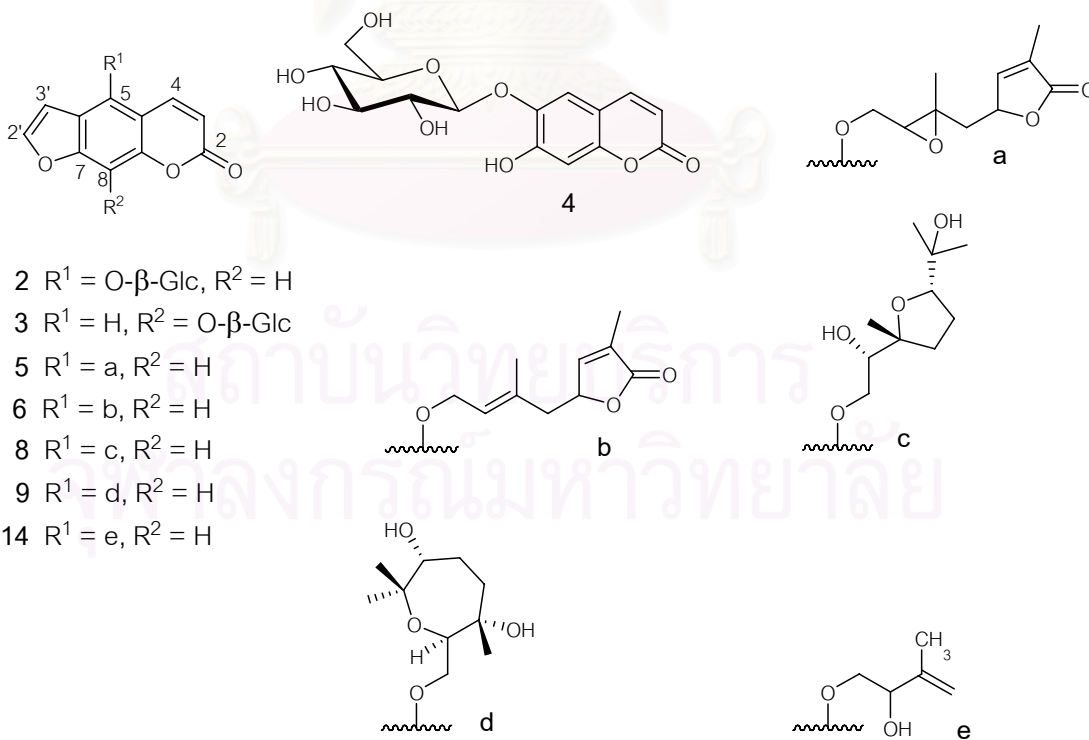
Air-dried roots of *Feroniella lucida* (3.75 kg)

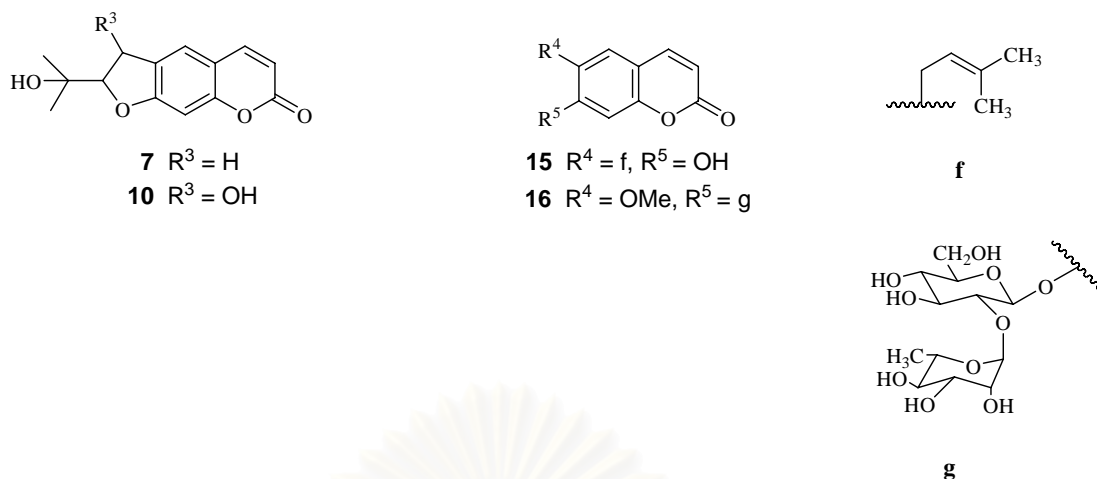
- 1) Soxhlet with MeOH
- 2) Extract with CH₂Cl₂ and *n*-butanol

BuOH extract (30 g)

- | | |
|---|---|
| <ol style="list-style-type: none"> 3) VCC with MeOH-CH₂Cl₂ 4) Sephadex LH-20
(<i>n</i>-hexane- CH₂Cl₂-MeOH) 5) Silica gel with MeOH-CH₂Cl₂ 6) ODS (MeOH-H₂O) | <ol style="list-style-type: none"> 3) Diaion HP-20 (H₂O, MeOH, Acetone) 4) Repeat silica gel and Sephadex LH-20 with MeOH-CH₂Cl₂ 5) Preparative TLC (MeOH-CH₂Cl₂) |
|---|---|

- | | |
|--|--|
| <p>Feronielloside (1: new, 50 mg)
 Glucopsoralen (2, 12.5 mg)
 Bergaptol-O-β-D-glucopyranoside (3, 60 mg)
 Aesculetin glycoside (4, 17 mg)</p> | <p>2'', 3''-Epoxyanisolactone (5, 5 mg)
 Anisolactone (6, 3.8 mg)
 Marmesin (7, 2.5 mg)
 Feroniellin A (8, 1.8 mg)
 Feroniellin C (9, 1.3 mg)
 Xanthoarnol (10, 2.1 mg)
 Feroniellin acid A (11: new, 1.1 mg)
 Feroniellin acid B (12: new, 1.2 mg)
 Feroniellin acid C (13: new, 1.1 mg)
 Gosferol (14, 2.0 mg)
 7-Demetylsaberosine (15, 3.2 mg)
 Haploperoside D (16, 5.4 mg)</p> |
|--|--|



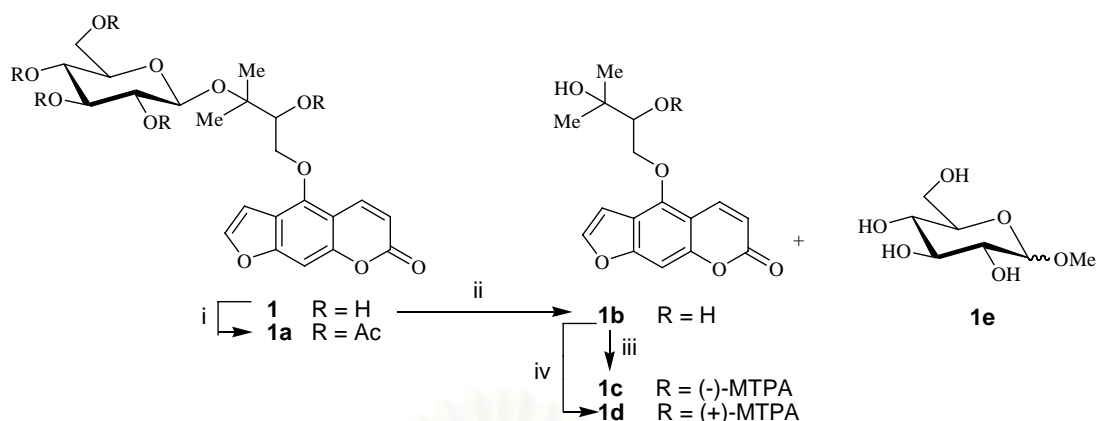


Scheme 2.1. The isolation procedure of BuOH extract from roots of *Feroniella lucida*.

2.2. Structure elucidation of Feronielloside (1)

Feronielloside was isolated as white powder. The molecular formula $C_{22}H_{26}O_{11}$ was deduced by HRESIMS in conjugation with ^{13}C NMR data. The UV absorptions ($\log \epsilon$) at 250 (3.73) and 309 (3.61) were indicative of coumarin moiety. The 1H NMR data of **1** in CD_3OD (table 2.1) revealed the presence of five methine signals to a 3,4-unsubstituted furanocoumarin [δ_H 6.28 (1H, d, $J = 10.0$ Hz; H-3), 8.43 (1H, d, $J = 10$ Hz; H-4), 7.20 (1H, s; H-8), 7.69 (1H, d, $J = 2.0$ Hz; H-2'), 7.26 (1H, d, $J = 2.0$ Hz; H-3')]. The ^{13}C NMR spectrum showed 22 signals; eleven of which belong to a furanocoumarin nucleus. The remaining carbon signals were ascribable to a geranyl derived portion and sugar moieties on the basis of 2D NMR data analysis. Interpretation of 2D NMR data suggested that the spin system of O-CH₂-CH-O was flanked by the quaternary carbon [δ_C 78.6] which was in turn accommodated by two singlet signals of methyl groups [δ_H 1.34 (3H, s, CH₃-4''), 1.38 (3H, s, CH₃-5'')].

The sugar moiety was identified to be glucose by NMR and chemical methods. A typical large coupling constant ($J = 7.8$ Hz) of anomeric proton 4.58 (1H, d, $J = 7.8$ Hz, H-1''') pointed out a β - glucosidic linkage. Methyl glucopyranosides (**1e**) obtained by hydrolysis (scheme 2.2) was identified by comparing with an authentic sample as D-glucose.



Scheme 2.2. Reagents and conditions: (i) AcCl, pyridine, rt; (ii) HCl/MeOH, reflux; (iii) (*S*)-MTPACl, pyridine; (iv) (*R*)-MTPACl, pyridine.

The HMBC correlation (figure 2.1) indicated the connectivity of the two singlet methyl [δ_{H} 1.34 ($\text{CH}_3\text{-4''}$), 1.38 ($\text{CH}_3\text{-5''}$)] and two methylene signals [δ_{H} 4.41 (H-1''a) and 4.90 (H-1''b)] to C-2'' (δ_{C} 75.9). The correlation between H-1'' and C-3'' confirmed the connectivity of glucose moiety and geranyl derived residue through ether linkage.

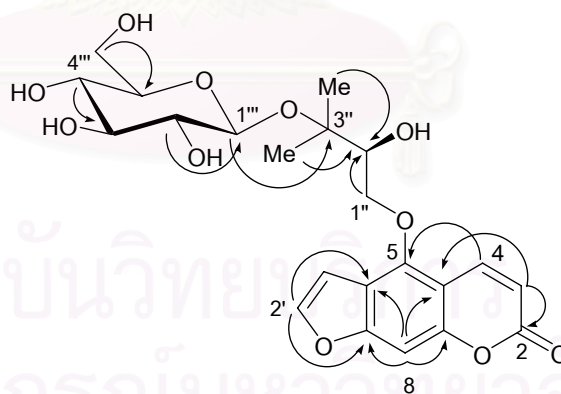


Figure 2.1. Selected HMBC correlations of **1**.

However, 2D NMR analysis addressing the position of geranyl derived moiety on the furanocoumarin was hampered because there was no HMBC cross peak observed between H-1'' and a carbon on the aromatic ring. This problem, which resulted from the signal overlapping with HOD residue, was circumvented by

formation of acetylated product. Treatment of **1** with AcCl in dry pyridine at ambient temperature afforded feronielloside pentaacetate (**1a**). The ^1H NMR spectrum of **1a** in CDCl_3 showed the shape signals of H-1'' at δ_{H} 4.52 and 4.78, which revealed HMBC correlations with C-5 of coumarin moiety (figure 2.2), thus completing the entire structure of **1**.

In previously proposed structure, the absolute configuration of C-2'' has remained unclear. Prior to applying Mosher's analysis, removal of glucose moiety from **1** was required (scheme 2.2), in order to eliminate unexpectedly combined anisotropic effects of four phenylacetic acid derivatives. Acid hydrolysis of **1** under reflux condition yielded oxypeucedamin hydrate (**1b**) and glucose residue (**1e**). Treatment of **1b** with *R*-(-)- and *S*-(+)-MTPA chlorides yielded (*S*)-(-)- and (*R*)-(+)-MTPA esters (**1c** and **1d**). The $\Delta\delta_{\text{SR}}$ distribution (figure 2.3) indicated *S* configuration of C-2''.

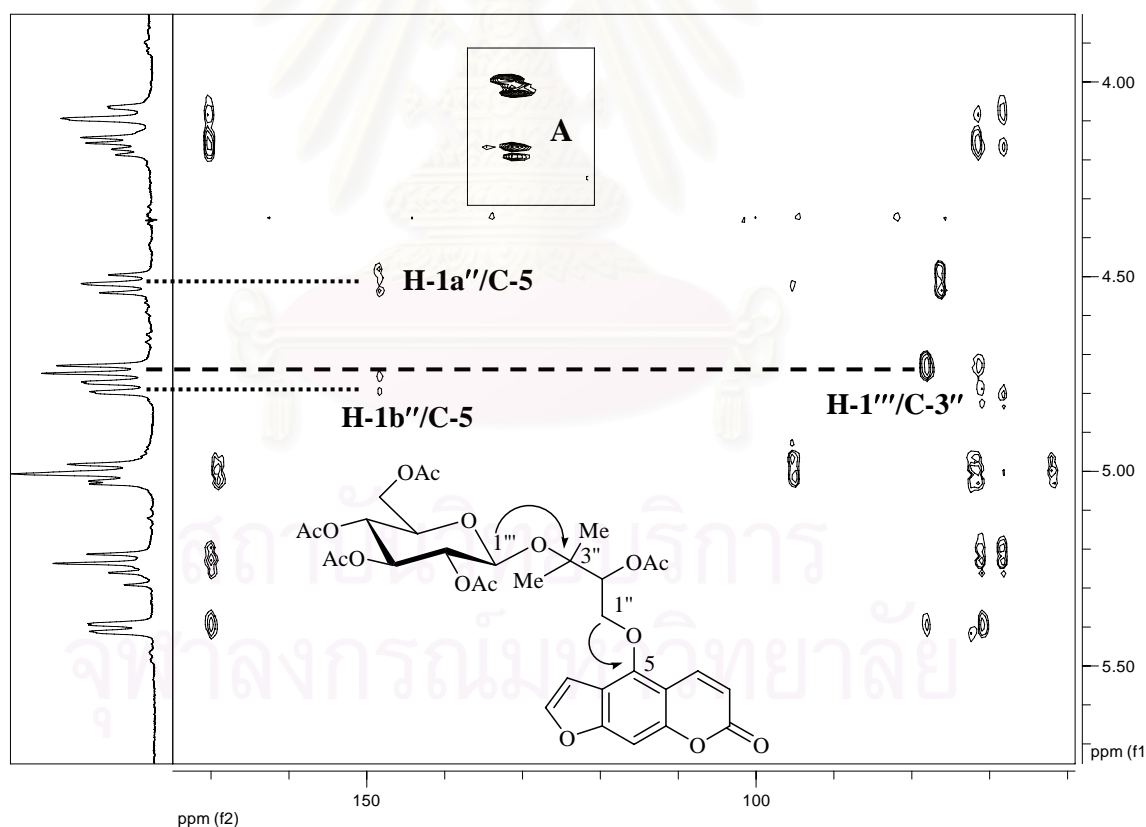


Figure 2.2. Diagnostic HMBC correlations observed in **1a**. Expansion (A) shows cross peaks of H-1a''/C-5 and H-1b''/C-5.

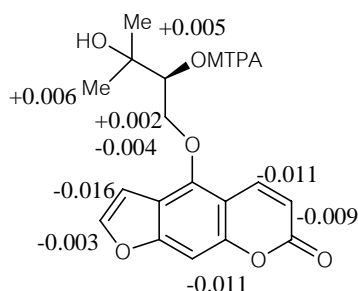


Figure 2.3. $\Delta\delta_{SR}$ values for the MTPA esters (**1c** and **1d**) of **1b**.

Table 2.1. NMR data of feronielloside (**1**, CD₃OD) and feronielloside pentaacetate (**1a**, CDCl₃).

position	1		1a^a	
	δ_C	δ_H (mult, <i>J</i> in Hz)	δ_C	δ_H (mult, <i>J</i> in Hz)
2	161.8		161.2	
3	111.4	6.28 d (10.0)	112.8	6.26 d (10.0)
4	140.3	8.43 d (10.0)	139.2	8.04 d (10.0)
4a	107.0		106.7	
5	149.4		148.5	
6	114.2		113.0	
7	158.3		158.2	
8	93.2	7.21 s	94.2	7.14 s
8a	152.2		152.6	
2'	145.2	7.69 d (2.0)	145.0	7.62 d (2.0)
3'	105.0	7.26 d (2.0)	105.1	7.03 d (2.0)
1''	74.3	4.41 dd (8.8, 8.2)	71.1	4.52 dd (8.0, 10.2)
		4.90 ^b		4.78 dd (1.2, 10.2)
2''	75.9	3.89 dd (1.6, 8.2)	76.7	5.40 dd (1.2, 8.0)
3''	78.6		78.8	
4''	20.9	1.34 s	22.1	1.27 s
5''	23.0	1.38 s	24.5	1.35 s
Glc				
1'''	97.0	4.58 d (7.8)	95.3	4.74 d (7.8)
2'''	73.7	3.16 dd (7.8, 8.8)	71.5	5.00 dd (7.8, 8.9)
3'''	76.5	3.30 m	5.02	5.02 m
4'''	76.3	3.38 m	72.6	5.24 m
5'''	70.1	3.28 m	71.8	3.72 m
6'''	61.3	3.62 d (10.6)	62.2	4.08 dd (5.6, 11.8)
		3.81 d (11.8)		4.17 dd (5.6, 11.8)

^aSignals of acetates resonated at δ_H 1.98, 1.99, 2.01, 2.02 and 2.09; δ_C 20.3, 20.6 (4 × CH₃), 170.2 (4 × C=O) and 169.4.

^bOverlapped by HOD residue.

2.3. Structure elucidation of Feronielliac acids A-C (11-13)

Feronielliac acid A (**11**) had a molecular formula of $C_{21}H_{22}O_9$ as analyzed by HRESIMS. Its UV absorption at 261 and 310 nm suggested the presence of coumarin moiety. The 1H NMR spectrum exhibited two doublet signals of H-3 [δ_H 6.33] and H-4 [δ_H 8.17] and a pair of furan protons at δ_H 7.63 (H-2') and δ_H 6.96 (H-3') which were indicative of unsubstituted furanocoumarin. In addition to two singlet methyls [δ_H 1.25 and 1.82], the signals in olefinic [δ_H 7.07] and oxygenated [δ_H 4.2-4.6] regions were similar to those of 2'', 3''-epoxyanisolactone (**5**). A significant lowfield shift of H-2'' [δ_H 4.20 of **11** and δ_H 3.29 of **5**] indicated that the epoxide ring in **5** was replaced by a 1, 2-diol moiety in **11**. The presence of carboxylic acid at C-8'' and secondary alcohol at C-5'' was implied from a larger 36 amu (MS 418 for **11** and 382 for **5**), thus accounting for the molecular formula established for **11**. The C-6''-C-7'' olefin was assigned to be *E* geometry, based on typical upfield shift of C-10'' [δ_C 10.1] [19]. Moreover, the gross structure of **11** was confirmed by 2D NMR.

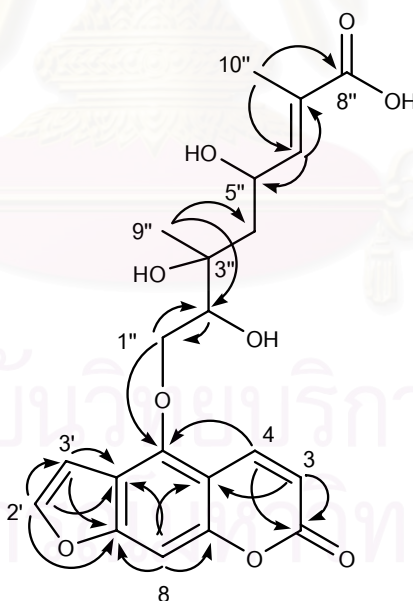


Figure 2.4. Selected HMBC correlations of **11**.

Feronielllic acids **B** and **C** (**12-13**) had the same the molecular formula, $C_{21}H_{22}O_9$. In the 1H and ^{13}C NMR spectra (table 2.2), there were the characteristic signals of 3, 4-unsubstituted coumarin moiety, a pair of furan protons at H-2' and H-3', an oxygenated methylene protons, methylene protons, three methine protons of C-2'', 5'' and 6'' and two singlet methyls. In fact **12** and **13** demonstrated 1H NMR signals nearly identical to those of **11**, except for oxygenated methines and methylenes in range of 4.2-5.3 ppm. These data suggested that **11-13** were isomeric different to each other only in stereochemistry of C-2'', 3'' and 5''.

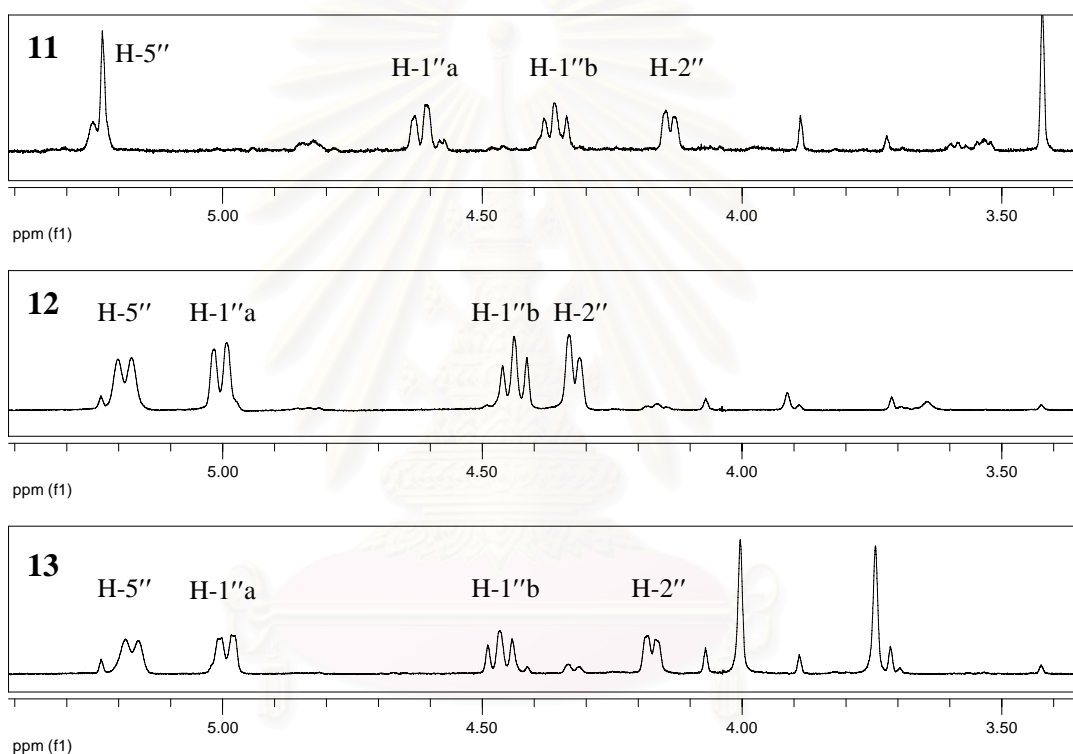
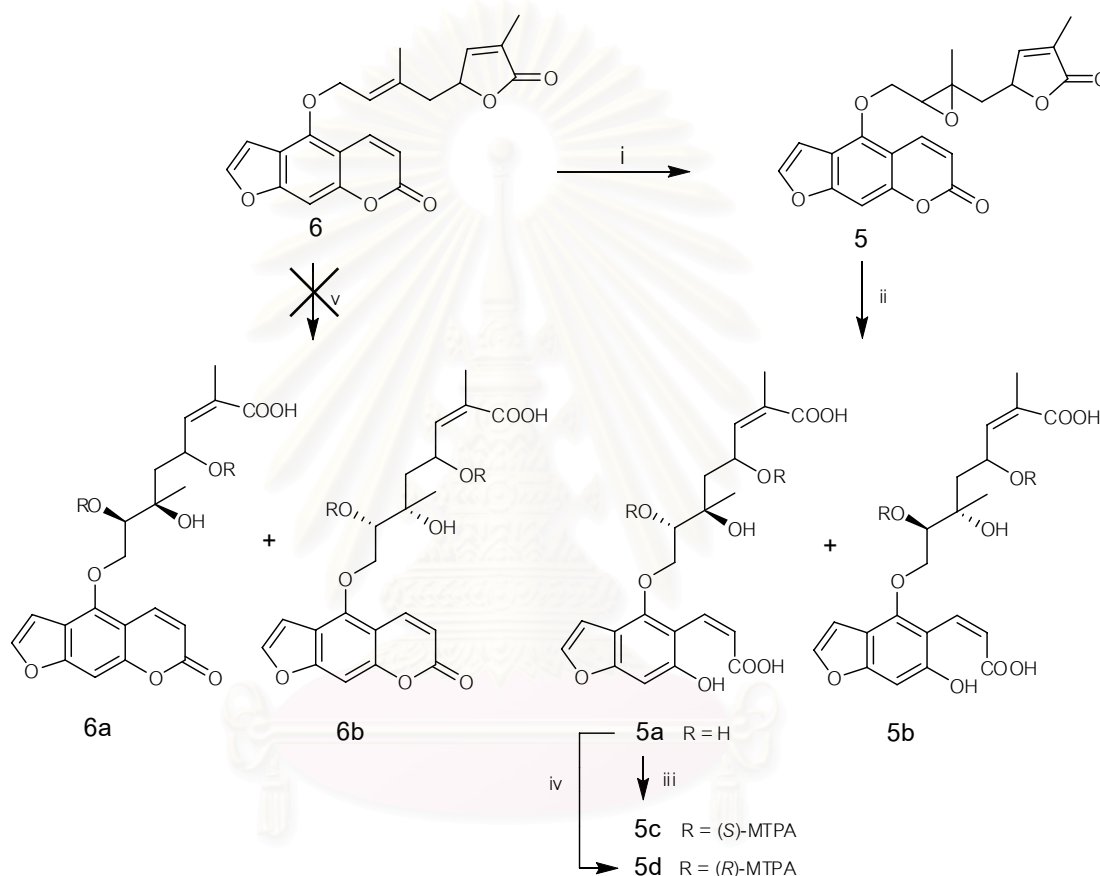


Figure 2.5. 1H NMR spectra of **11-13** in range of 4.2-5.3 ppm.

An attempt to address stereochemistry of these chiral centers was impossible due to the limited amount of samples (~ 1 mg). This problem could be resolved by constructing model compounds that allow direct comparison with **11-13** through 1H NMR.

Anisolactone (**6**), a major component isolated in this experiment, was used as a starting material. All possible stereomers (**5a**, **5b**, **6a** and **6b**) could be generated by hydroxylation of double bond at C-2''-C-3'' using two different routes (scheme 2.3).

Epoxidation of **6** with *m*-CPBA produced **5**, which was identical to 2'', 3''-epoxyanisolactone. Acid-catalyzed epoxide ring opening of **5** afforded a single *anti*-diol product, **5a** or **5b**. On the other hand, a plane to generate *syn*-diol products (**6a** and **6b**) was conducted using OsO₄. Various hydroxylation conditions such as Upjohn method (OsO₄/NMO) [20] were unsuccessful to produce desired products, possibly due to preference of OsO₄ for less steric alkene.



Scheme 2.3. Reagents and conditions: (i) *m*-CPBA, CH₂Cl₂, rt; (ii) 0.75 M H₂SO₄, *t*-BuOH, reflux; (iii) (-)-MTPACl, pyridine; (iv) (+)-MTPACl, pyridine; (v) OsO₄, NMO, 4:1 acetone-water, rt.

The ¹H NMR spectrum of the model compound (**5a** or **5b**), particularly signals of H-1'' to H-6'' was nearly identical to that of **11** (Figure 2.6 and Table 2.2). This data indicated *anti*-diol for C-2'' and C-3'' of **11** and it was inevitable to assign 2'', 3''-*syn*-diol for **12** and **13**.

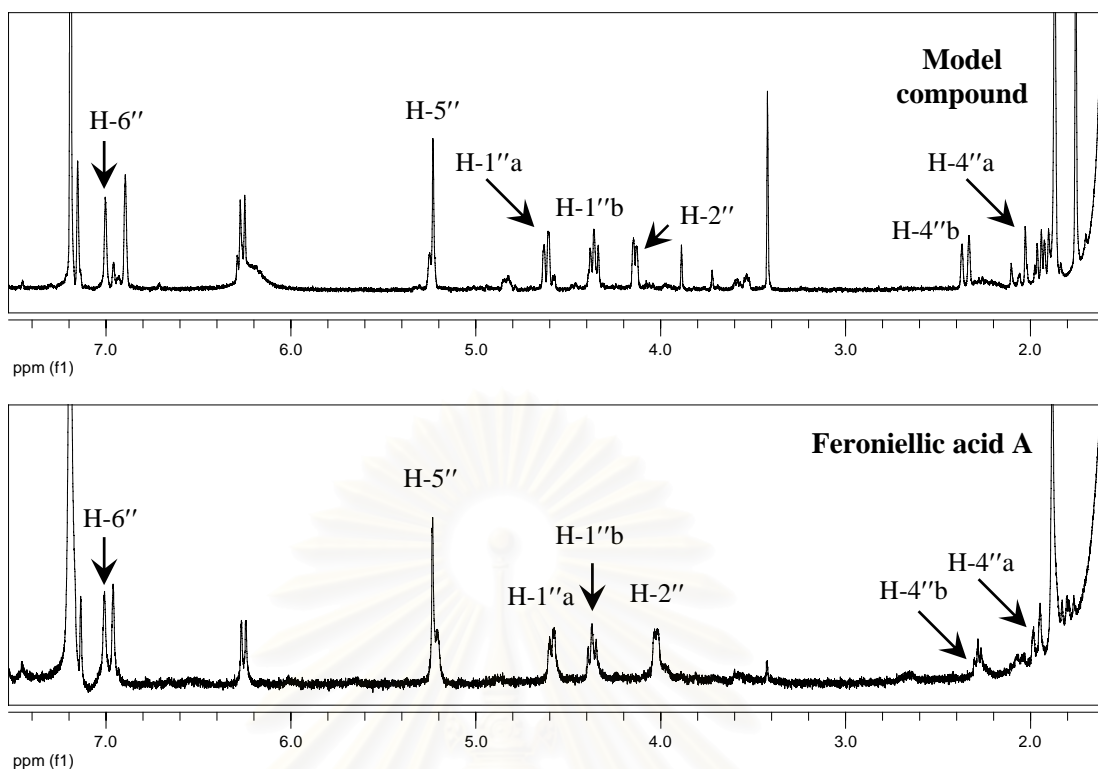


Figure 2.6. ^1H NMR spectra of model compound (**5a** or **5b**) and **11** in range of 1.8-7.2 ppm.

Table 2.2. $\Delta\delta_{\text{H}}$ values of model compound (**5a** or **5b**), **11**, **12** and **13**.

Position	$\Delta\delta_{5a/5b-11}$	$\Delta\delta_{5a/5b-12}$	$\Delta\delta_{5a/5b-13}$
H-1''a	0.003	-0.420	-0.392
H-1''b	0.008	-0.520	-0.331
H-2''	0.004	-0.305	-0.125
H-4''a	0.000	0.250	0.110
H-4''b	0.009	0.214	0.381
H-5''	0.000	0.034	0.093
H-6''	-0.001	-0.033	0.002

The absolute configuration of three chiral centers (C-2'', 3'' and 5'') was established by Mosher's method. Although this methodology was originally developed to determine the absolute configuration of monoalcohols, it has also been widely applied to polyols [21]. Recently, Riguera et al. [21] have validate this approach for the configurational assignment of acyclic 1, 2-, 1, 3-, 1, 4- and 1, 5-diol

by examining the combined anisotropy effects of two phenylacetic acid derivatives (e.g. MTPA).

Generally, it appears that four possible stereoisomer (types A-D) of a diol with two asymmetric carbons have a specific and characteristic distribution of $\Delta\delta_{SR}$ signs. For acyclic 1, 4-diol, $\Delta\delta_{SR}$ distribution patterns used to predict absolute configuration of two chiral centers are shown (Figure 2.7). Two bis- MTPA derivatives, **5c** and **5d**, were separately prepared by treating **5a** with (-) - and (+) -MTPACl in pyridine, and the $\Delta\delta_{SR}$ distribution was demonstrated in Figure 2.8. Apparently, an unequal $\Delta\delta_{SR}$ sign distribution, negative signs around C-2'' and positive signs around C-5'', was consistent with *anti*-1, 4-diol type C. Therefore absolute configuration of feroniellie acid A (**11**) was depicted.

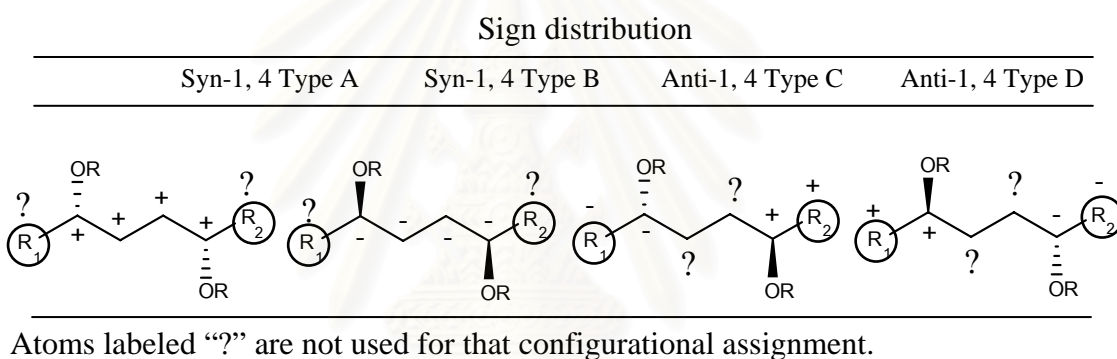


Figure 2.7. $\Delta\delta$ sign distribution model for the MTPA esters of the possibilities of a 1, 4-diol.

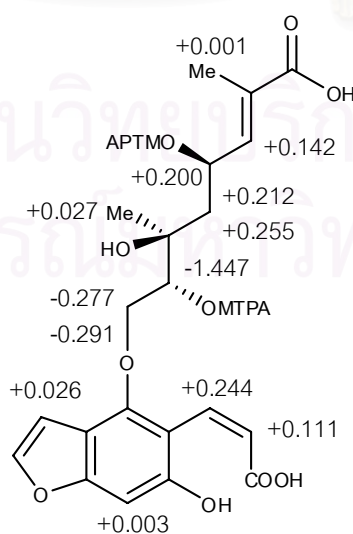


Figure 2.8. $\Delta\delta_{SR}$ values for the MTPA esters (**5c** and **5d**) of **5a** or **5b**.

Table 2.3. ^1H and ^{13}C data of **11-13** in CDCl_3 at 400 MHz.

position	11		12		13	
	δ_{C}	δ_{H} (mult, J in Hz)	δ_{C}	δ_{H} (mult, J in Hz)	δ_{C}	δ_{H} (mult, J in Hz)
2	161.0		161.5		161.0	
3	113.4	6.33 d (10.0)	113.5	6.32 d (10.0)	113.5	6.32 d (9.6)
4	139.0	8.17 d (9.6)	139.5	8.25 d (10.0)	139.0	8.24 d (9.6)
4a	107.5		107.5		107.5	
5	148.0		148.0		148.0	
6	114.5		114.5		114.5	
7	158.0		158.0		158.0	
8	95.2	7.22 s	95.2	7.21 s	95.0	7.20 s
8a	152.4		152.5		152.5	
2'	145.4	7.63 s	145.6	7.63 s	145.5	7.62 s
3'	104.2	6.96 s	104.5	6.96 s	104.5	7.00 s
1''a	73.6	4.67 dd (7.6, 9.2)	73.8	5.07 dd (9.6)	73.5	5.06 dd (2.8, 10.8)
1''b		4.43 dd (8.0, 8.4)		4.40 dd (8.0, 8.8)		4.53 dd (8.0, 8.8)
2''	77.4	4.20 dd (6.8, 1.20)	65.5	4.38 d (8.0)	66.0	4.24 d (6.4)
3''	73.5		72.0		73.8	
4''a	43.5	1.94 s	42.8	1.69 dd (11.2, 14.4)	43.4	1.83 dd (10.8, 14.8)
4''b		2.36 m		2.38 d (14.8)		2.33 d (14.8)
5''	77.8	5.30 s	77.5	5.25 d (10.4)	77.5	5.24 d (10.0)
6''	148.5	7.07 s	148.7	7.10 s	148.5	7.10 s
7''	130.5		130.0		130.0	
8''	173.5		173.0		173.0	
9''	29.5	1.25 s	23.5	1.42 s	22.0	1.49 s
10''	10.1	1.82 s	10.5	1.95 s	12.0	1.95 s

2.4. Experiment section

2.4.1. General Experimental Procedures

Optical rotations were measured on a Jasco P-1010 polarimeter. UV spectra were measured on Shimadzu UV-160A photodiode array spectrophotometer. NMR spectra were recorded with a Varian model Mercury⁺ 400 which operated at 400 MHz for ¹H and 100 MHz for ¹³C nuclei. The chemical shift in δ (ppm) was assigned with reference to the signal from the residual protons in deuterated solvents and using TMS as an internal standard in some cases. EIMS and HRESIMS were obtained from Mass Spectrometer Model VG TRIO 2000 and a Micromass LCT mass spectrometer, respectively. HPLC was conducted on Water[®] 600 controller equipped with a Water[®] 2996 photodiode array detector (USA). Cosmosil 5C18-ARII column (10 × 250 mm) was used for separation purpose. Sephadex LH-20 and silica gel 60 Merck cat. No. 7734 and 7729 were used for open column chromatography. Thin layer chromatography (TLC) was performed on precoated Merck silica gel 60 F₂₅₄ plates (0.25 mm thick layer).

2.4.2. Plant material

Roots of *Feroniella lucida* were collected in April 2005 from Roi-Et province, Thailand. The specimens (Voucher number BCU.O.T. 968) were identified by Professor Dr. Thaweesakdi Boonkerd, Plant of Thailand Research Unit, Department of Botany, Faculty of Science, Chulalongkorn University.

2.4.3. Isolation procedure

The air-dried chopped roots of *Feroniella lucida* (3.75 kg) were extracted with MeOH in Soxhlet extractor to yield MeOH extract which was suspended in MeOH-H₂O (1:1). The crude extract was extracted with CH₂Cl₂ (3 × 1 L). The aqueous layer was concentrated and extracted with saturated *n*-BuOH (3 × 700 mL) to yield BuOH extract (30 g). The first part of BuOH extract (15.5 g) was separated through VCC using MeOH-CH₂Cl₂ (1:9, 1:4, 1:1 and 1:0). Repeat column chromatography over

Sephadex LH-20 using *n*-hexane-CH₂Cl₂-MeOH (3:1.5:0.5 and 2:2:0.5) followed by silica gel CC (1:9 MeOH-CH₂Cl₂) and RP-HPLC (1:1 MeOH-H₂O) to afford a new furanocoumarin glycoside named feronielloside (**1**) (*R*_t = 31.5 min), together with three known furanocoumarin glycosides, glucopsoralen (**2**) (*R*_t = 22.0 min), bergaptol-O-β-D-glucopyranoside (**3**) (*R*_t = 24.3 min), aesculetin glycoside (**4**) (*R*_t = 10.5 min).

The second part of BuOH extract (15 g) was separated via Diaion HP-20 into acetone, MeOH and water soluble fractions. The acetone soluble fraction was chromatographed on silica gel CC (MeOH-CH₂Cl₂ 1:9) followed by Sephadex LH-20 (MeOH-CH₂Cl₂ 1:9) and preparative TLC developed with 1:99 MeOH-CH₂Cl₂ to yield six known compounds, 2'', 3''-epoxyanisolactone (**5**), anisolactone (**6**), marmesin (**7**), feroniellin A (**8**), feroniellin C (**9**) and xanthoarnol (**10**).

The MeOH soluble fraction was separated on Sephadex LH-20 (MeOH-CH₂Cl₂ 1:9) followed by silica gel CC (MeOH-CH₂Cl₂ 1:9) and preparative TLC developed with 1:99 MeOH-CH₂Cl₂ to afford three new coumarins named feroniellinic acids A-C (**11-13**), along with three known coumarins, gosferol (**14**), 7-demethylsaberosine (**15**) and haploperoside D (**16**).

2.4.4. Preparation of feronielloside pentaacetate (**1a**)

To a solution of **1** (5 mg) in dry pyridine (10 μL) was added with acetylchloride (5 μL). The reaction mixture was stirred for 2 h at room temperature. After completion of reaction, the reaction mixture was then dissolved with CH₂Cl₂ and extracted with 1M HCl (5 × 2 mL). The combined organic layers were dried over anhydrous Na₂SO₄ and evaporated under vacuum to afford **1a** (4.3 mg).

2.4.5. Hydrolysis of feronielloside (**1**)

A solution of **1** (20 mg) in MeOH was added with 2M HCl in MeOH (500 μL). The reaction mixture was refluxed for 4 h. After cooling, it was neutralized with NaHCO₃. After removal of MeOH, the reaction mixture was extracted with EtOAc (3 × 2 mL) and H₂O (3 × 2 mL). The combined organic layers were dried over anhydrous Na₂SO₄, evaporated under vacuum to dryness to afford **1b** (8 mg), in

which the hydrosate of **1** gave R_f value (0.56, CH_2Cl_2 -MeOH- H_2O 6:4:0.5) identical to methyl glucopyranoside (**1e**) prepared from authentic D-glucose.

2.4.6. Modified Mosher's analysis

(*R*)- α -methoxy- α -(trifluoromethyl)-phenylacetyl chloride (5 μL , 26 μM) was added to 5 mg of **1** in 10 μL dry pyridine. After being stirred at room temperature for 3 h, the mixture was extracted with CH_2Cl_2 (3×2 mL) and washed with 1M HCl (3×2 mL). The aqueous layer was dried with anhydrous NaSO_4 . The residue was evaporated to dryness and purified to give *S*-(-)-MTPA ester. (*S*)- α -methoxy- α -(trifluoromethyl)-phenylacetyl chloride was also prepared in the same protocol to afford *R*-(+)-MTPA ester.

2.4.7. Anti dihydroxylation of **5** under acid condition

A solution of **6** (20 mg) in CH_2Cl_2 and *m*-chloroperoxybenzoic acid (*m*-CPBA, 10 mg) was stirred for 5 h at room temperature. The residue was diluted with H_2O and extracted with CH_2Cl_2 (4×2 mL). The CH_2Cl_2 layer was washed with 1 M NaOH (4×2 mL) and then dried with anhydrous Na_2SO_4 . The residue was evaporated to dryness and afforded the crude product which was purified by Sephadex LH-20 to furnish **5** (12 mg). All the chemical data of this compound were found identical with that of the natural 2'', 3''-epoxyanisolactone.

To a solution of **5** (12 mg) in *t*-BuOH (3 mL) and water (1 mL) mixture was added with 0.75 M H_2SO_4 (2 mL). The reaction mixture was then heated at reflux for 1 h. After completion of the reaction (as monitored by TLC), it was cooled to room temperature and treated with NaHCO_3 and concentrated under vacuum to remove *t*-BuOH. The residue was diluted with CH_2Cl_2 (3×2 mL) and purified by Sephadex LH-20 to afford **5a/5b** as a yellow viscous liquid.

2.4.8 Syn dihydroxylation of **6** under Upjohn condition

To a stirred solution of **6** (15 mg) and *N*-methylmorpholine-*N*-oxide monohydrate (NMO) in 4:1 acetone-water was added OsO₄ and the solution stirred until complete (TLC analysis, cal~4 h). The reaction mixture was extract with 1M HCl (3 × 2 mL) and CH₂Cl₂ (3 × 2 mL). The aqueous layer was dried with anhydrous NaSO₄ and solvent was then evaporated under reduced pressure. The products should be **6a/6b**.

Feronielloside (**1**): amber gum, $[\alpha]_D^{27} +6.0^\circ$ (*c* 0.05, MeOH); UV (MeOH) λ_{\max} (log ϵ) 250 (3.73), 309 (3.61); HRESIMS *m/z* [M+Na]⁺ 489.1370 (calcd for C₂₂H₂₆O₁₁Na, 489.1373); ¹H NMR (CD₃OD, 400 MHz) and ¹³C NMR (100 MHz) see table 2.1.

Feronielloside pentaacetate (**1a**): dark yellow liquid, $[\alpha]_D^{27} -45.6^\circ$ (*c* 0.05, MeOH); UV (MeOH) λ_{\max} (log ϵ) 267 (3.96), 310 (3.89); HRESIMS *m/z* [M+Na]⁺ 699.1902 (calcd for C₃₂H₃₆O₁₆Na, 699.1901); ¹H NMR (CDCl₃, 400 MHz) and ¹³C NMR (100 MHz) see table 2.1.

Glucopsoralen (**2**): yellow liquid; ¹H NMR (CD₃OD, 400 MHz) δ_H 6.31 (1H, d, *J* = 10.0 Hz; H-3), 8.54 (1H, d, *J* = 9.6 Hz, H-4), 7.23 (1H, s; H-8), 7.70 (1H, s; H-2'), 7.20 (1H, s; H-3'), 5.00 (1H, d, *J* = 3.6 Hz; H-1''), 3.52 (1H, m; H-2''), 3.36 (1H, s; H-3''), 3.27 (1H, m; H-4''), 3.34 (1H, m; H-5''), 3.76 (1H, m; H-6''a), 3.63 (1H, m; H-6''b).

Bergaptol-O- β -D-glucopyranoside (**3**): yellow liquid; ¹H NMR (CD₃OD, 400 MHz) δ_H 6.39 (1H, d, *J* = 9.6 Hz; H-3), 8.04 (1H, d, *J* = 9.6 Hz, H-4), 7.50 (1H, s; H-5), 7.80 (1H, s; H-2'), 6.85 (1H, s; H-3'), 5.66 (1H, d, *J* = 7.6 Hz; H-1''), 3.58 (1H, m; H-2''), 3.34 (1H, s; H-3''), 3.47 (1H, m; H-4''), 3.60 (1H, m; H-5''), 3.74 (1H, m; H-6''a), 3.84 (1H, m; H-6''b).

Aesculetin glycoside (**4**): yellow liquid; ¹H NMR (CD₃OD, 400 MHz) δ_H 7.89 (1H, d, *J* = 9.2 Hz; H-4), 7.19 (1H, s; H-5), 7.17 (1H, s; H-8), 6.29 (1H, d, *J* = 9.2 Hz; H-3),

5.07 (1H, d, $J = 7.2$ Hz; H-1''), 3.32 (1H, m; H-2''), 3.40 (1H, m; H-3''), 3.42 (1H, m; H-4''), 3.44 (1H, m; H-5''), 3.76 (1H, m; H-6''a), 3.62 (1H, m; H-6''b).

2'', 3''-Epoxyanisolactone (**5**): colourless crystal solid; ^1H NMR (CDCl_3 , 400 MHz) δ_{H} 8.26 (1H, d, $J = 9.6$ Hz; H-4), 7.62 (1H, d, $J = 2.0$ Hz; H-3'), 7.61 (1H, brs; H-2'), 7.18 (1H, s; H-8), 7.08 (1H, s; H-6''), 6.32 (1H, d, $J = 9.6$ Hz; H-3), 5.08 (1H, m; H-5''), 4.44 (1H, dd, $J = 11.0, 6.6$ Hz; H-1''a), 4.70 (1H, dd, $J = 11.4, 4.6$ Hz; H-1''b), 3.29 (1H, t, $J = 8.4$ Hz; H-2''), 1.93 (3H, s; CH_3 -10''), 1.66 (2H, m; H-4''), 1.49 (3H, s; CH_3 -9'').

Anisolactone (**6**): colourless crystal solid; ^1H NMR (CDCl_3 , 400 MHz) δ_{H} 8.15 (1H, d, $J = 10.0$ Hz; H-4), 7.61 (1H, d, $J = 2.0$ Hz; H-2'), 7.17 (1H, s; H-8), 6.98 (1H, s; H-6''), 6.95 (1H, d, $J = 1.2$ Hz; H-2'), 6.29 (1H, d, $J = 9.6$ Hz; H-3), 5.67 (1H, t, $J = 6.4$ Hz; H-2''), 5.50 (1H, m; H-5''), 4.96 (2H, d, $J = 6.8$ Hz; H-1''), 2.46 (1H, dd, $J = 10.4, 5.0$ Hz; H-4''b), 2.35 (1H, dd, $J = 14.4, 8.2$ Hz; H-4''a), 1.92 (3H, s; CH_3 -10''), 1.79 (3H, s; CH_3 -9'').

Marmesin (**7**): colourless flakes; ^1H NMR (CDCl_3 , 400 MHz) δ_{H} 7.60 (1H, d, $J = 9.6$ Hz; H-4), 7.22 (1H, s; H-5), 6.75 (1H, s; H-8), 6.22 (1H, d, $J = 9.6$ Hz; H-3), 4.74 (1H, t, $J = 8.8$ Hz; H-2'), 3.21 (2H, m; H-3'), 1.37 (3H, s; CH_3 -1''), 1.23 (3H, s; CH_3 -1'').

Feroniellin A (**8**): pale yellow powder; ^1H NMR (CDCl_3 , 400 MHz) δ_{H} 8.22 (1H, d, $J = 10.0$ Hz; H-4), 7.60 (1H, d, $J = 2.0$ Hz; H-2'), 7.17 (1H, s; H-8), 7.01 (1H, d, $J = 1.6$ Hz; H-3'), 6.29 (1H, d, $J = 9.6$ Hz; H-3), 4.37 (1H, dd, $J = 8.0, 10.0$ Hz; H-1''a), 4.58 (1H, dd, $J = 2.8, 10.0$ Hz; H-1''b), 4.04 (1H, dd, $J = 2.4, 8.0$ Hz; H-2''), 3.84 (1H, m; H-7''), 1.75 (1H, m; H-5''a), 2.16 (1H, m; H-5''b), 1.91 (1H, m; H-6''), 1.24 (3H, s; CH_3 -4''), 1.26 (3H, s; CH_3 -9''), 1.16 (3H, s; CH_3 -10'').

Feroniellin C (**9**): brown liquid; ^1H NMR (CDCl_3 , 400 MHz) δ_{H} 8.16 (1H, d, $J = 9.6$ Hz; H-4), 7.48 (1H, d, $J = 2.0$ Hz; H-2'), 7.02 (1H, s; H-8), 7.02 (1H, brs; H-3'), 6.18 (1H, d, $J = 9.6$ Hz; H-3), 4.68 (1H, brd, $J = 8.4$ Hz; H-1''b), 4.21 (1H, m; H-1''a), 4.16

(1H, m; H-2''), 3.72 (1H, brd, $J = 7.6, 5.0$ Hz; H-7''), 2.04 (1H, brt, $J = 12.4, 8.2$ Hz; H-5''a), 1.86 (1H, m; H-6''a), 1.76 (1H, m; H-6''b), 1.59 (1H, m; H-5''b), 1.28 (3H, s; CH₃-9''), 1.22 (3H, s; CH₃-4''), 1.14 (3H, s; CH₃-10'').

Xanthoarnol (**10**): colourless flakes; ¹H NMR (CDCl₃, 400 MHz) δ_H 6.6.18 (1H, d, $J = 9.6$ Hz; H-3), 7.90 (1H, d, $J = 9.6$ Hz, H-4), 7.61 (1H, s; H-5), 6.70 (1H, s; H-8), 4.41 (1H, d, $J = 4.0$ Hz; H-2'), 5.45 (1H, d, $J = 4.0$ Hz; H-3'), 1.16 (3H, s; CH₃-4'), 1.15 (3H, s; CH₃-5').

Feronielllic acid A (**11**): yellow liquid, $[\alpha]_D^{26} +12.0^\circ$ (c 0.05, MeOH); UV (MeOH) λ_{max} (log ε) 261 (3.23), 310 (3.57); HRESIMS m/z [M+Na]⁺ 440.6700 (calcd for C₂₁H₂₂O₉Na, 441.1200); ¹H NMR (CDCl₃, 400 MHz) and ¹³C NMR (100 MHz) see table 2.3.

Feronielllic acid B (**12**): yellow liquid, $[\alpha]_D^{26} +52^\circ$ (c 0.05, MeOH); UV (MeOH) λ_{max} (log ε) 268 (3.10), 308 (3.27); HRESIMS m/z [M+Na]⁺ 440.8800 (calcd for C₂₁H₂₂O₉Na, 441.1200); ¹H NMR (CDCl₃, 400 MHz) and ¹³C NMR (100 MHz) see table 2.3.

Feronielllic acid C (**13**): yellow liquid, $[\alpha]_D^{26} -21.2^\circ$ (c 0.05, MeOH); UV (MeOH) λ_{max} (log ε) 268 (3.11), 308 (3.53); HRESIMS m/z [M+Na]⁺ 440.9300 (calcd for C₂₁H₂₂O₉Na, 441.1200); ¹H NMR (CDCl₃, 400 MHz) and ¹³C NMR (100 MHz) see table 2.3.

Gosferol (**14**): colourless crystal solid; ¹H NMR (CDCl₃, 400 MHz) δ_H 6.30 (1H, d, $J = 10.0$ Hz; H-3), 8.19 (1H, d, $J = 9.6$ Hz; H-4), 7.19 (1H, s; H-8), 7.61 (1H, s; H-2'), 6.98 (1H, s; H-3'), 4.40 (1H, d, $J = 7.6$ Hz; H-1''a), 4.34 (1H, d, $J = 7.6$ Hz; H-1''a), 4.49 (1H, m; H-2''), 5.08 (1H, s; H-4''a), 5.20 (1H, s; H-4''b), 1.83 (3H, s; CH₃-5'').

7-Demethylsaberrosine (**15**): colourless crystal solid; ¹H NMR (CDCl₃, 400 MHz) δ_H 6.23 (1H, d, $J = 9.6$ Hz; H-3), 7.63 (1H, d, $J = 9.6$ Hz; H-4), 7.19 (1H, s; H-5), 6.89 (1H, s; H-8), 3.38 (1H, d, $J = 7.2$ Hz; H-1'), 5.33 (1H, brs; H-2'), 1.79 (3H, s; CH₃-4''), 1.76 (3H, s; CH₃-5'').

Haploperoside D (**16**): yellow liquid; ^1H NMR (CD_3OD , 400 MHz) δ_{H} 6.33 (1H, d, $J = 9.6$ Hz; H-3), 8.04 (1H, d, $J = 9.6$ Hz, H-4), 7.20 (1H, s; H-5), 7.27 (1H, s; H-8), 4.95 (1H, d, $J = 7.6$ Hz; H-1'), 3.56 (1H, d, $J = 7.6$ Hz; H-2'), 3.50 (1H, m; H-3'), 3.36 (1H, m; H-4'), 3.65 (1H, m; H-5'), 3.52 (1H, m; H-6'a), 4.10 (1H, m; H-6'b), 4.70 (1H, m; H-1''), 3.89 (1H, m; H-2''). 3.95 (1H, s; H-3''), 3.40 (1H, s; H-4''), 3.67 (1H, m; H-5''), 3.91 (3H, s; OCH_3 -6''), 1.23 (3H, s; H-7'').



สถาบันวิทยบริการ
จุฬาลงกรณ์มหาวิทยาลัย

CHAPTER III

INVESTIGATION OF ACETYLCHOLINESTERASE INHIBITORY ACTIVITY OF ISOLATED COUMARINS

3.1. Acetylcholinesterase inhibition assay methods

Acetylcholinesterase (AChE) inhibitory activity of isolated coumarins was validated using Ellman colorimetric method [22] with slight modification. Briefly, AChE hydrolyzed the substrate acetylthiocholine iodide (ATCI), resulting in the product thiocholine which reacted with Ellman's reagent (DTNB) to produce 2-nitrobenzoate-5-mercaptothiocholine and 5-thio-2-nitrobenzoate (Figure 3.1). Therefore, the inhibitory effect of isolated coumarins towards AChE was quantified by UV (415 nm), in term of 5-thio-2-nitrobenzoate decline.

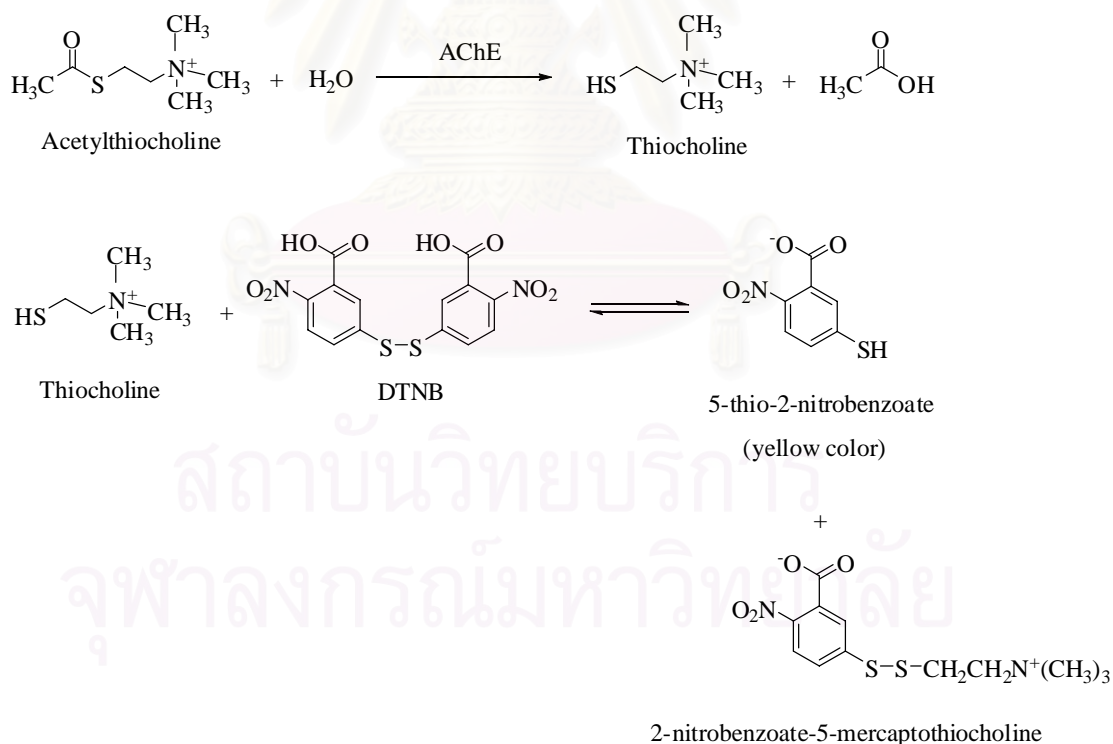


Figure 3.1. Reaction mechanism of ACh.

3.2. Results and Discussion

Thirteen coumarins were tested for the AChE inhibitory activity, and the results were shown in Table 3.1. Gosferol (**14**) was the most potent AChE inhibitor with IC_{50} value of 8.3 mM in a dose-dependent manner, while xanthoarnol (**10**) and marmesin (**7**) were also found to be active against AChE with slightly less extent ($IC_{50} = 10.2$ and 13.3 mM, respectively). The results suggested that simple coumarin having at least one hydroxyl group attached to aromatic moiety possessed enhanced inhibitory effect, which were consistent with those reported by Kang et al [23]. Of coumarin glycosides, feronielloside (**1**) was the most active AChE inhibitor with IC_{50} value of 16.9 mM. It appeared that a free hydroxyl group at C-2'' of prenyl derived moiety was important in exerting inhibitory effect. Interestingly, feronielloside pentaacetate (**1a**), which was structurally analogous to **1** (with acetate groups instead of hydroxyl groups), was a poor inhibitor with IC_{50} value of 489.0 mM. This data suggested that decrease in polarity and the lack of hydroxyl groups might be associated with inhibitory effect.

In addition, other coumarins such as 2'', 3''-epoxyanisolactone (**5**), anisolactone (**6**), feroniellin A (**8**) and feroniellin C (**9**) which were not dissolved in buffer solution, showed poor activity with IC_{50} values of 75.7, 72.0, 30.2 and 107.0 mM, respectively. It appears that solubility and polarity of these compounds had affect in inhibitory activity.

In conclusion, the enhanced activity found in simple coumarins containing at least one hydroxyl group at aromatic ring indicated that these structural features were associated with antagonizing active sites of AChE. This finding is consistent with previous independent work, which showed that a simple coumarin derivative containing a hydroxyl group bound to the peripheral site of AChE and inhibited AChE activity [24].

Table 3.1. AChE inhibitory activity of isolated coumarins from roots of *Feroniella lucida*.

Compounds	IC ₅₀ (mM)
Feronielloside (1)	16.9
Feronielloside pentaacetate (1a)	489.0
Glucopsoralen (2)	23.2
Bergaptol-O-β-D-glucopyranoside (3)	21.7
Aesculetin glycoside (4)	24.4
2'', 3''-Epoxyanisolactone (5)	75.7
Anisolactone (6)	72.0
Marmesin (7)	13.3
Feroniellin A (8)	30.2
Feroniellin C (9)	107.0
Xanthoarnol (10)	10.2
Feroniellic acid A (11)	n.d.
Feroniellic acid B (12)	n.d.
Feroniellic acid C (13)	n.d.
Gosferol (14)	8.3
7-Demethylsaberrosine (15)	20.0
Haploperoside D (16)	45.5
Physostigmine or eserine (standard)	4.79 × 10 ⁻³

n.d. = not determined

3.3 Chemical and equipment

The following buffers were used. Buffer A: 50 mM tris-HCl, pH 8; buffer B: 50 mM tris-HCl, pH 8, containing 0.1 % bovine serum albumin (BSA); buffer C: 50 mM tris-HCl, pH 8, containing 0.1 M NaCl and 0.02 M MgCl₂ ·6H₂O. Acetylcholinesterase from electric eel was purchased from Sigma (St. Louis, MO, USA). Enzymes was dissolved in buffer A to make 1000 U/ml stock solution, and further diluted with buffer B to get 0.22 U/ml. Acetylthiocholine iodide (ATCI) and 5, 5'-dithiobis-(2-nitrobenzoic acid) (DTNB) were purchased from Sigma (St. Louis, MO, USA). Bio-Rad microplate reader model 3550 UV was used to measure the absorbance at 415 nm for the enzyme reaction in the microplate assay.

3.4. Procedures

In the 96-well plate, 25 µl of 15 mM ATCI in Millipore water, 125 µl of 3 mM DTNB in buffer C, 50 µl of buffer B and 25 µl of isolated compounds in buffer A (50 mM Tris-HCl, pH 8) were added and the absorbance of resulting solution was measured at 415 nm every 30 s for five times [25]. After 25 µl of 0.22 U/ml enzyme solution was added, the absorbance was measured again every 30 s for eight times. The rate of reaction was calculated by Microsoft Excel[®]. An increase in absorbance due to the spontaneous hydrolysis of substrate (ATCI) was corrected by subtracting the rate of reaction before adding the enzyme from the rate of reaction after adding the enzyme. Percentage inhibition was expressed by comparing the rates for the sample to the blank (10% MeOH in buffer A) [26].

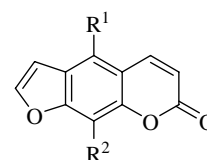
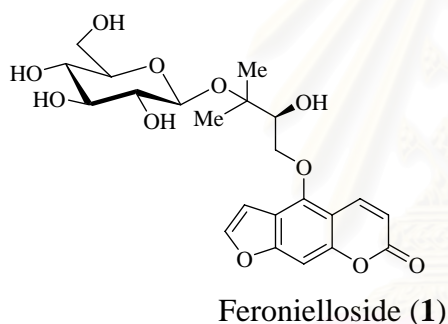
$$\% \text{ inhibition} = \left(\frac{\text{Rate of blank} - \text{Rate of sample}}{\text{Rate of Blank}} \right) \times 100$$

The IC₅₀ value was determined from a plot of percentage inhibition versus sample concentration [27, 28]. Eserine was used as a positive control and the experiment was performed in triplicate.

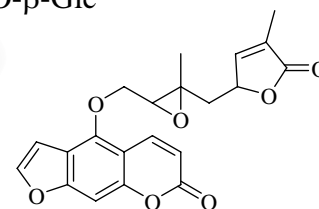
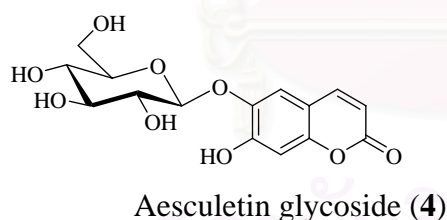
CHAPTER IV

CONCLUSION

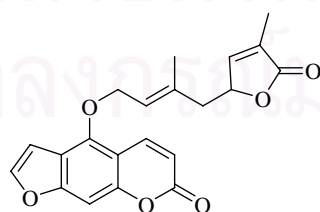
In this investigation, bioassay-guided fractionation using acetylcholinesterase (AChE) inhibitory activity led to the isolation of four new coumarins from BuOH extract of the roots of *Feroniella lucida*; feronielloside (1), feroniellic acid A (11), feroniellic acid B (12) and feroniellic acid C (13), along with twelve known coumarins, glucopsoralen (2), bergaptol-O-β-D-glucopyranoside (3), aesculetin glycoside (4), 2'', 3''-epoxyanisolactone (5), anisolactone (6), marmesin (7), feroniellin A (8), feroniellin C (9), xanthoarnol (10), gosferol (14), 7-demethylsaberosine (15) and haploperoside D (16).



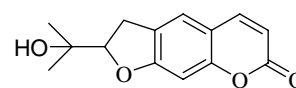
Glucopsoralen (2); $R^1 = O-\beta\text{-Glc}$, $R^2 = H$
Bergaptol-O-β-D-glucopyranoside (3);
 $R^1 = H$, $R^2 = O-\beta\text{-Glc}$



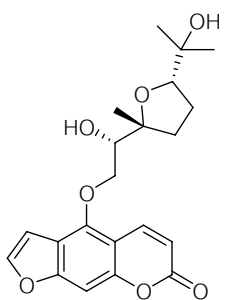
2'', 3''-Epoxyanisolactone (5)



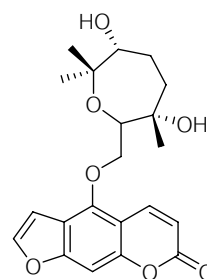
Anisolactone (6)



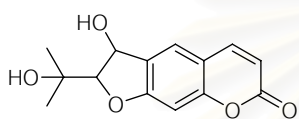
Marmesin (7)



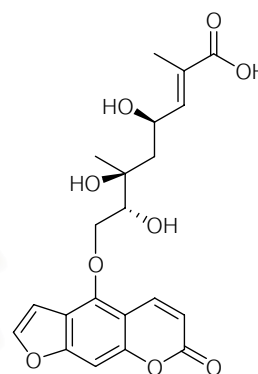
Feroniellin A (8)



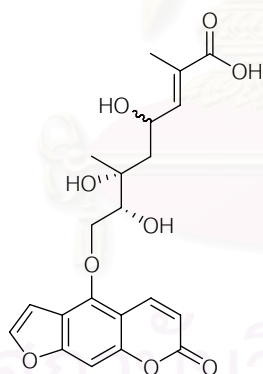
Feroniellin C (9)



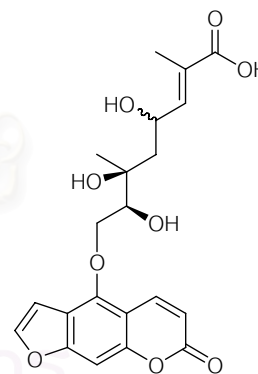
Xanthoarnol (10)



Feroniellinic acid A (11)

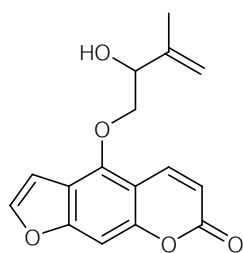
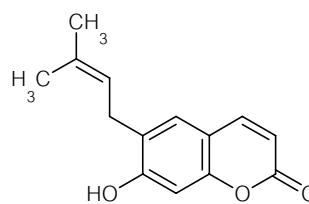
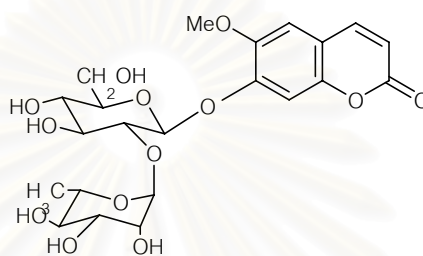


Feroniellinic acid B (12)



Feroniellinic acid C (13)

or

Gosferol (**14**)7-Demethylsaberose (**15**)Haploperoside D (**16**)

The investigation and evaluation for the AChE inhibitory activity using Ellman colorimetric method indicated that **14** was the most effective compound in inhibiting AChE with IC_{50} value of 8.3 mM. In addition, **10** and **7** were also found to be active in inhibiting AChE with IC_{50} values of 10.2 and 13.3 mM, respectively. Of coumarin glycosides, feronielloside (**1**) was the most effective AChE inhibitor with IC_{50} value of 16.9 mM.

สถาบันวิทยบริการ
จุฬาลงกรณ์มหาวิทยาลัย

REFERENCES

- [1] Williams, B.R.; Nazarians, A.; Giii, M.A. A reversible cholinesterase inhibitor. *Clin Ther.* **2003**, *25*, 1634-1653.
- [2] Small, D.H. Do acetylcholinesterase inhibitors boost synaptic scaling in Alzheimer's disease. *Trends Neurosci.* **2004**, *27*, 245-248.
- [3] Forstl, H.; Hentschel, F.; Sattel, H. Age-associated memory impairment and early Alzheimer's disease. *Drug Res.* **1995**, *45*, 394-397.
- [4] Batolini, M.; Bertucci, C.; Cavrini, V.; Andrisano, V. β -amyloid aggregation induced by human acetylcholinesterase: inhibition studies. *Biochem Pharmacol.* **2003**, *65*, 407-416.
- [5] Polinsky R.J. Clinical pharmacology of rivastigmine: A new-generation acetylcholinesterase inhibitor for the treatment of Alzheimer's disease. *Clin Ther.* **1998**, *20*, 634-647.
- [6] Sitaram, N.; Weingartner, H.; Gillin J.C. Physostigmine: Improvement of long-term memory processes in normal humans. *Science.* **1978**, *201*, 272-276.
- [7] Greig, N.H.; Utsuki, T.; Yu, Q.S. A new therapeutic target in Alzheimer's disease treatment: Attention to butyrylcholinesterase. *Curr Med Res Opin.* **2001**, *17*, 159-165.
- [8] Spencer, C.M.; Noble, S. Review of its use in Alzheimer's disease. *Drugs Aging.* **1998**, *13*, 391-441.
- [9] Bores, G.M.; Huger, F.P.; Petko, W. Pharmacological evaluation of novel Alzheimer's disease therapeutics: Acetylcholinesterase inhibitors related to galanthamine. *Am Soc Pharmacol Exp Ther.* **1996**, *277*, 728-738.
- [10] Fulton, B.; Benfield, P. Galantamine. *Drugs Aging.* **1996**, *1*, 60-65.
- [11] Lopez, S.; Bastida, J.; Viladomat, F. Acetylcholinesterase inhibitory activity of some Amaryllidaceae alkaloids and Narcissus extracts. *Life Sci.* **2002**, *71*, 2521-2529.
- [12] Zhou, J.; Zhang, H.Y.; Tang, X.C. Huperzine A attenuates cognitive deficits and hippocampal neuronal damage after transient global ischemia in gerbils. *Neurosci Lett.* **2001**, *313*, 137-140.
- [13] Jiang, H.; Luo, X.; Bai, D. Progress in clinical, pharmacological, chemical and structural biological studies of huperzine A: A drug of traditional Chinese

- medicine origin, in the treatment of Alzheimer's disease. *Curr Med Chem.* **2003**, *10*, 2231-2252.
- [14] Perry, N.S.; Bollen, C.; Perry, E.K. Salvia for dementia therapy: Review of pharmacological activity and pilot tolerability clinical trial. *Pharmacol Biochem Behav.* **2003**, *75*, 651-660.
- [15] Peng, W.H.; Heieh, M.T.; Wu, C.R. Effect of long-term administration of berberine on scopolamine-induced amnesia in rats. *J. Pharmacol.* **1997**, *74*, 261-266.
- [16] Kuznetsova, L.P.; Nikol, E.B.; Sochilina, E.E. Inhibition of human blood acetylcholinesterase and butyrylcholinesterase by some alkaloids. *J. Evol Biochem Physiol.* **2002**, *38*, 35-39.
- [17] Phuwapraisirisan, P.; Surapinit, S.; Sombund, S.; Siripong, P.; Tip-pyang, S. Feroniellins A-C, novel cytotoxic furanocoumarins with highly oxygenated C₁₀ moieties from *Feroniella lucida*. *Tetrahedron Lett.* **2006**, *47*, 3685-3688.
- [18] Phuwapraisirisan, P.; Surapinit, S.; Tip-pyang, S. A novel furanocoumarin from *Feroniella lucida* exerts protective effect against lipid peroxidation. *Phytother. Res.* **2006**, *20*, 708-710.
- [19] Sorek, H.; Rudi, A.; Benayahu, Y.; Ben-Califa, N.; Neumann, D.; Kashman, Y. Nuttingins A-F and Malonganeones D-H, Tetraprenylated alkaloids from the Tanzanian Gorgonian *Euplexaura nuttingi*. *J. Nat. Prod.* **2007**, *70*, 1104-1109.
- [20] Donohoe, T.J.; Blades, K.; Moore, P.R.; Waring, M.J.; Winter, J.G.; Helliwell, M.; Newcombe, N.J.; Stemp, G. Directed dihydroxylation of cyclic allylic alcohols and trichloroacetamides using OsO₄/TMEDA. *J. Org. Chem.* **2002**, *67*, 7946-7956.
- [21] Freire, F.; Manuel, J.; Quinoa, E.; Riguera, R. Determining the absolute stereochemistry of secondary/ secondary diols by ¹H NMR: basis and applications. *J. Org. Chem.* **2005**, *70*, 3778-3790.
- [22] Ellman, G.; Courtney, K.D.; Andres, V.; Featherstone, R.M. A new and rapid colorimetric determination of acetylcholinesterase activity. *Biochem Pharmacol.* **1961**, *7*, 88-95.
- [23] Kang, S.Y.; Lee, K.Y.; Sung, S.H.; Park, M.J.; Kim, Y.C. Coumarins isolated from *Angelica gigas* inhibit acetylcholinesterase: structure-activity relationships. *J. Nat. Prod.* **2001**, *64*, 683-685.

- [24] Radic Z.; Reiner, E.; Simeon, V. Binding sites on acetylcholinesterase for reversible ligands and phosphorylating agents. *Biochem Pharmacol.* **1984**, *33*, 671-677.
- [25] Orhan, I.; Kartal, M.; Naz, Q.; Ejaz, A.; Yilmaz, G.; Kan, Y.; Konuklugil, B.; Sener, B.; Choudhary, M.I. Antioxidant and anticholinesterase evaluation of selected Turkish *Salvia* species. *Food Chem.* **2007**, *103*, 1247-1254.
- [26] Anderson, A.; Gauguin, B.; Gudiksen, L.; Jager, A.K. Screening of plants used in Danish folk medicine to treat memory dysfunction for acetylcholinesterase inhibitory activity. *J. Ethnopharmacol.* **2006**, *104*, 418-422.
- [27] Rhee, I.K.; Meent, M.V.; Ingkaninan, K.; Verpoorte, R. Screening for acetylcholinesterase inhibitors from Amaryllidaceae using silica gel thin-layer chromatography in combination with bioactivity staining. *J. Chromatogr.* **2001**, *915*, 217-223.
- [28] Hu, M.K.; Wu, L.J.; Hsiao, G.; Yen, M.H. Homodimeric tacrine congeners as acetylcholinesterase inhibitors. *J. Med. Chem.* **2002**, *45*, 2277-2282.



APPENDICES

สถาบันวิทยบริการ
จุฬาลงกรณ์มหาวิทยาลัย

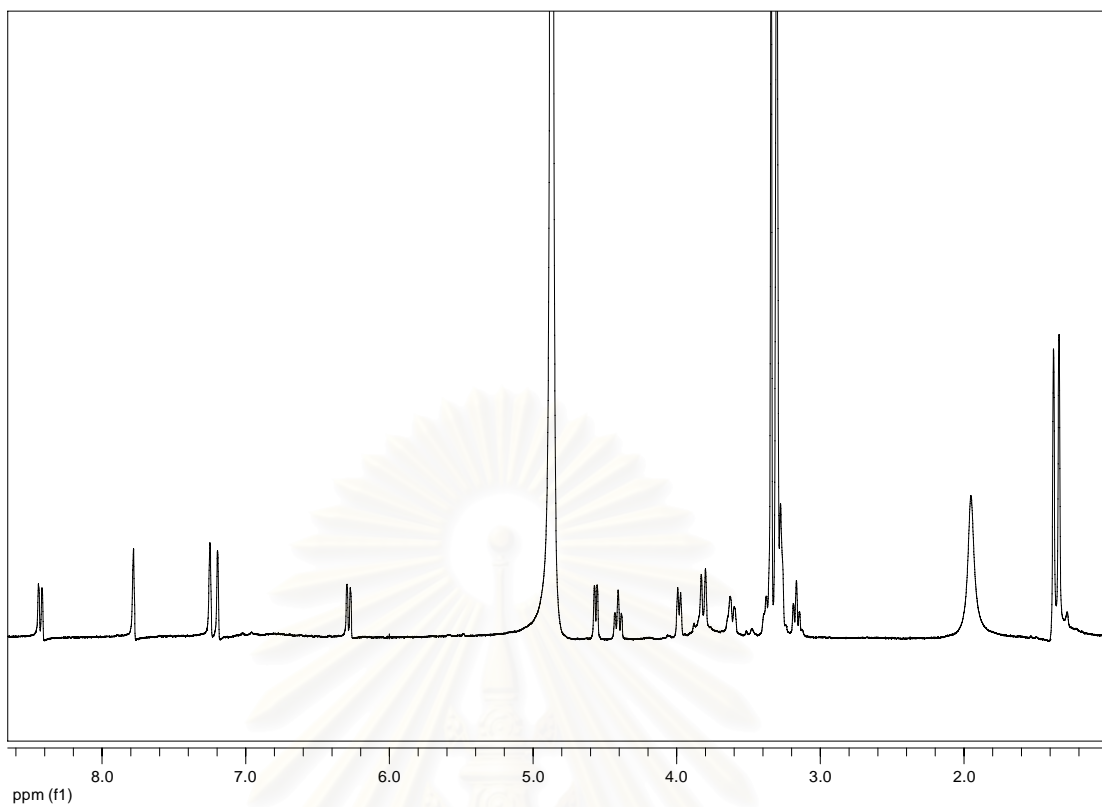


Figure 1. The ¹H NMR (CD₃OD) spectrum of feronielloside (**1**).

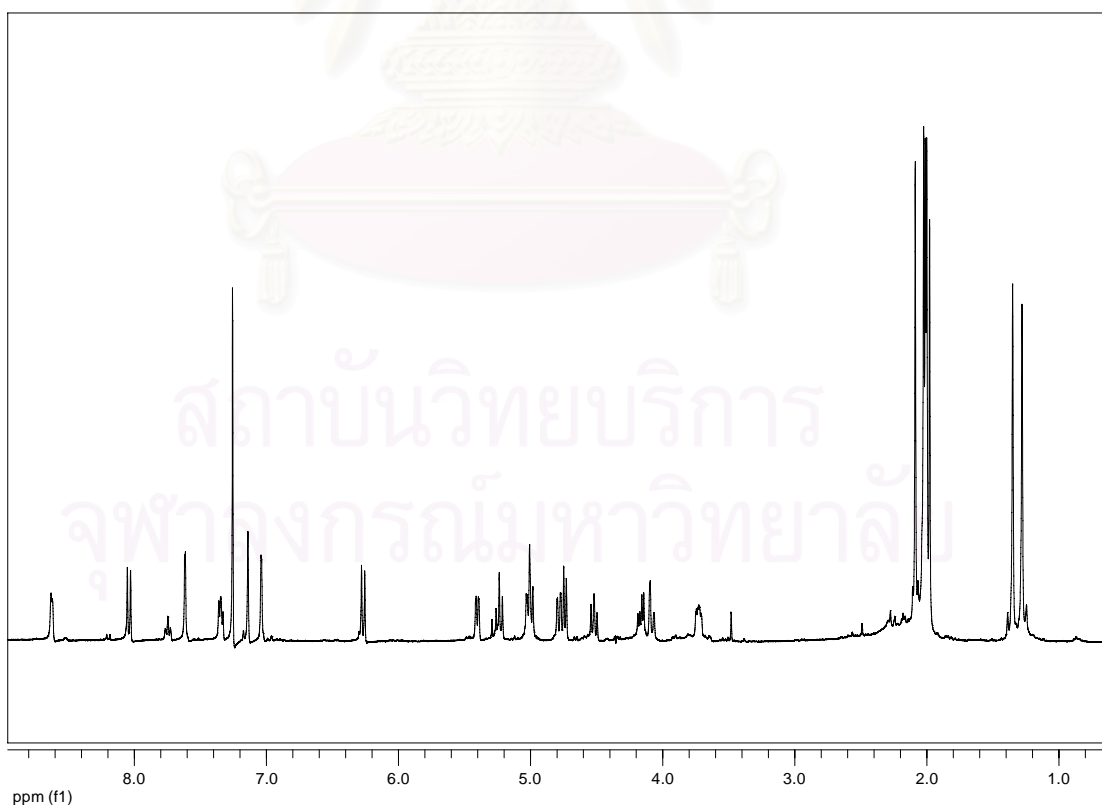


Figure 2. The ¹H NMR (CDCl₃) spectrum of feronielloside pentaacetate (**1a**).

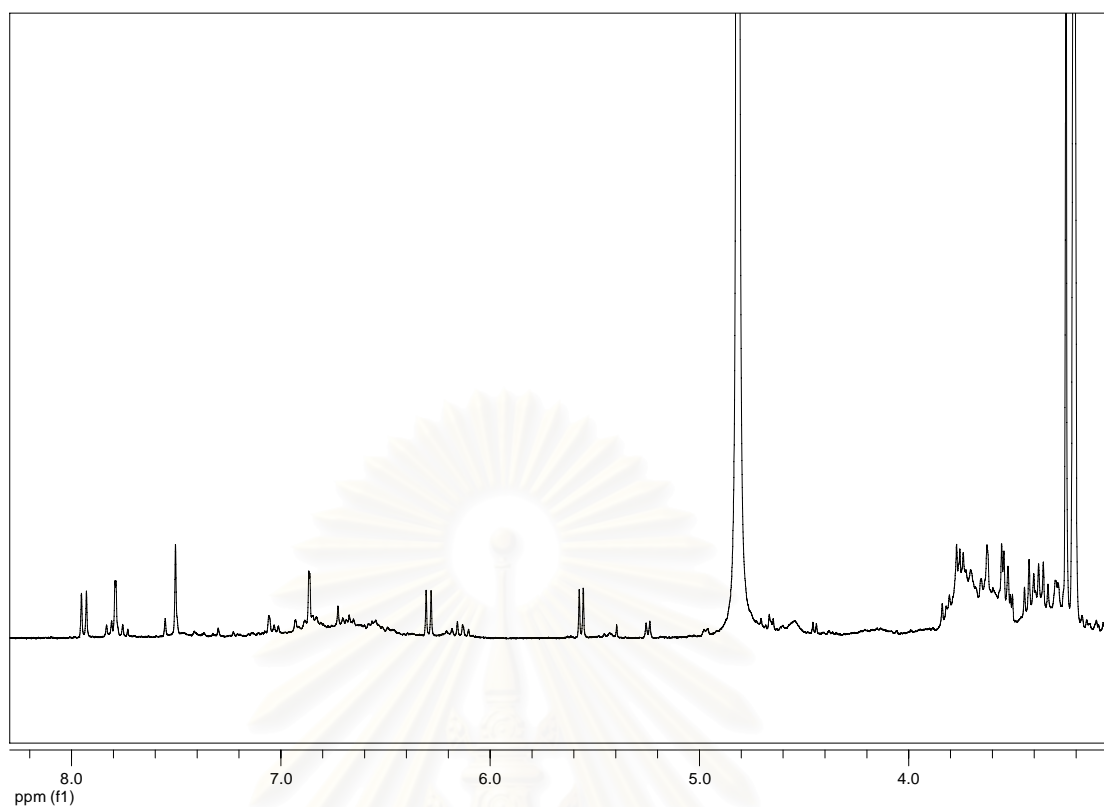


Figure 3. The ¹H NMR (CD₃OD) spectrum of glucopsoralen (2).

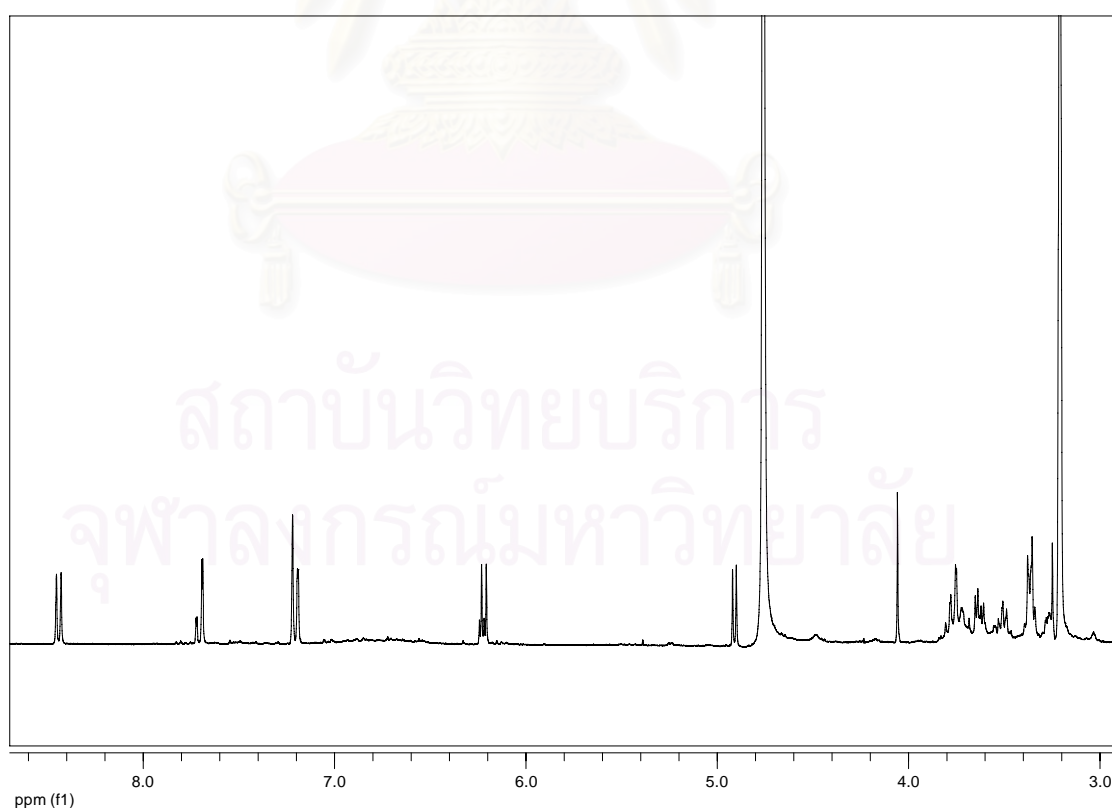


Figure 4. The ¹H NMR (CD₃OD) spectrum of bergaptol-O-β-D-glucopyranoside (3).

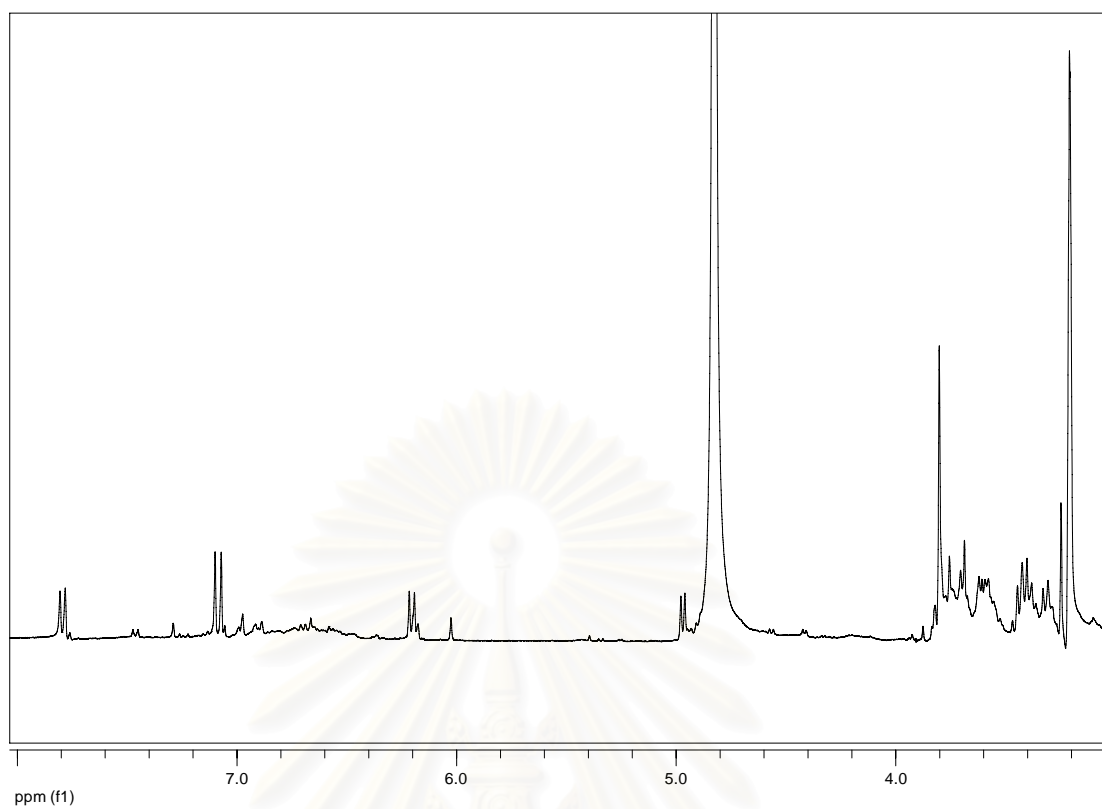


Figure 5. The ¹H NMR (CD₃OD) spectrum of aesculetin glycoside (4).

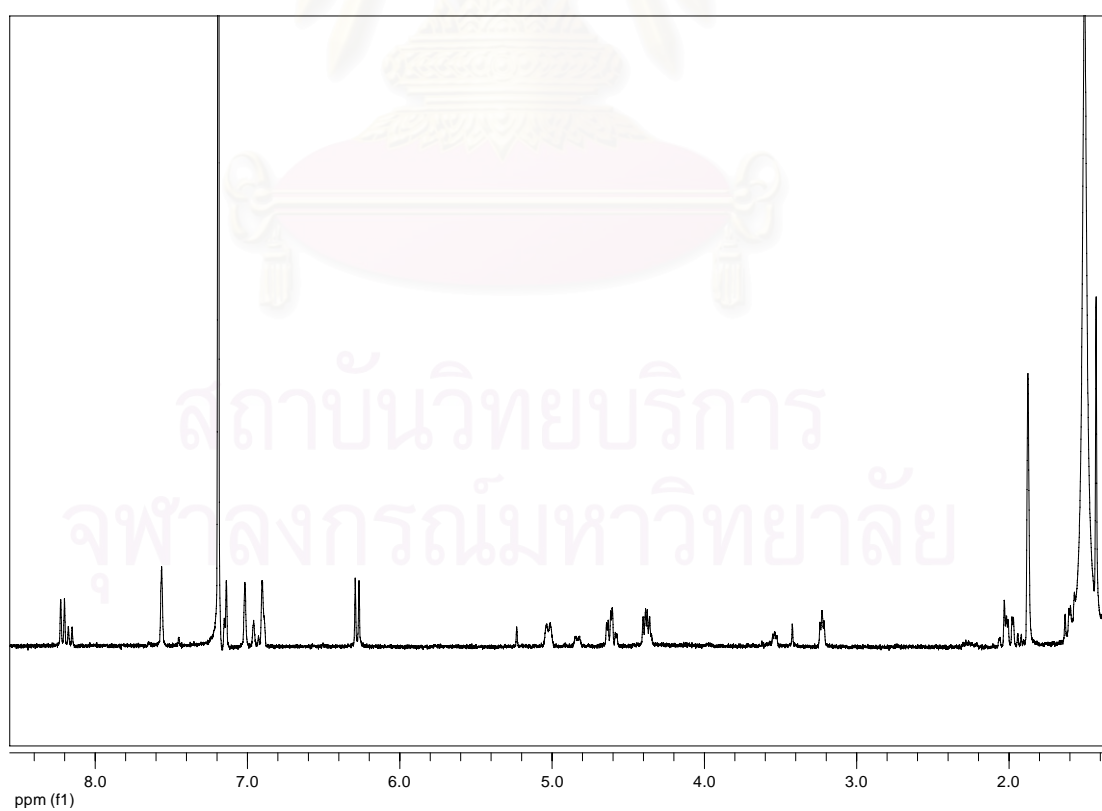


Figure 6. The ¹H NMR (CDCl₃) spectrum of 2'', 3''-epoxyanisolactone (5).

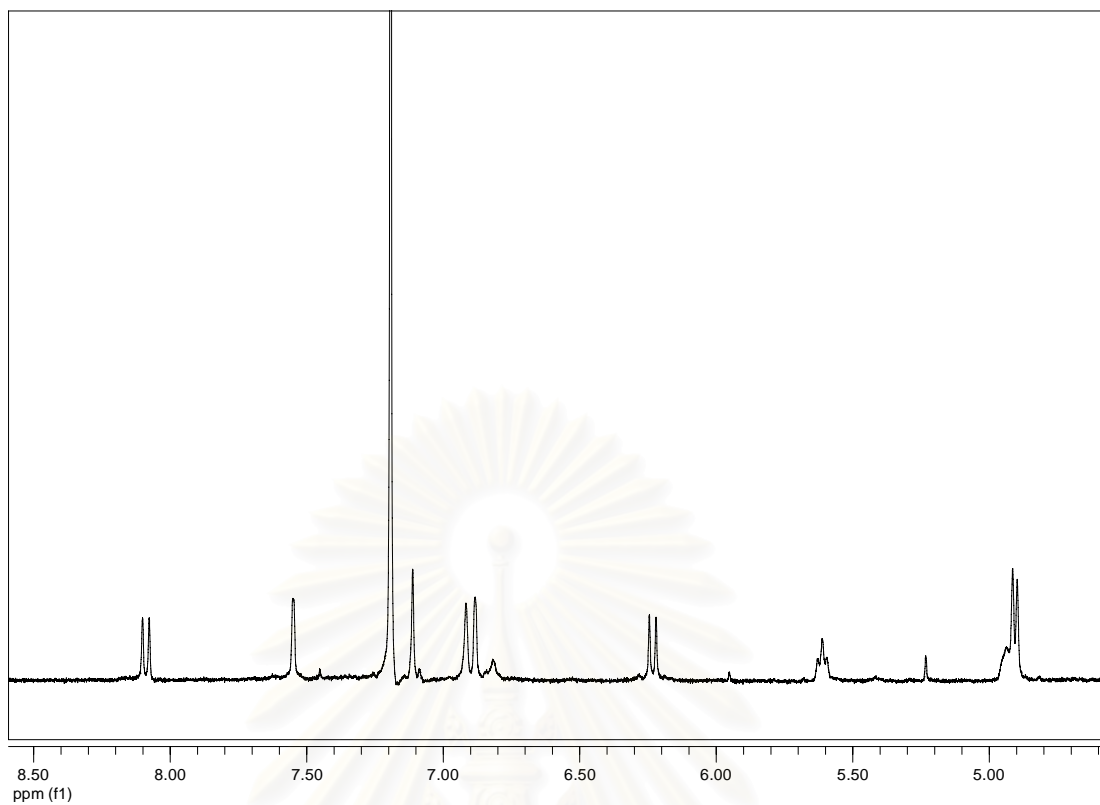


Figure 7. The ^1H NMR (CDCl_3) spectrum of anisolactone (**6**).

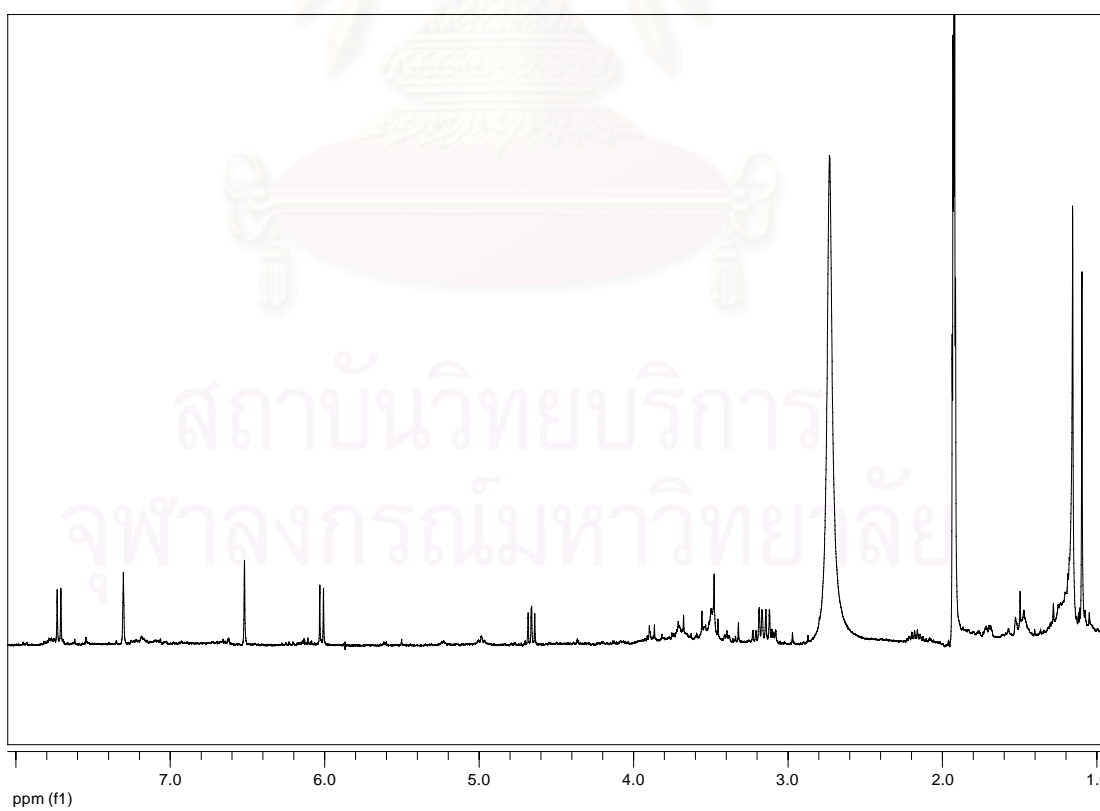


Figure 8. The ^1H NMR (CDCl_3) spectrum of marmesin (**7**).

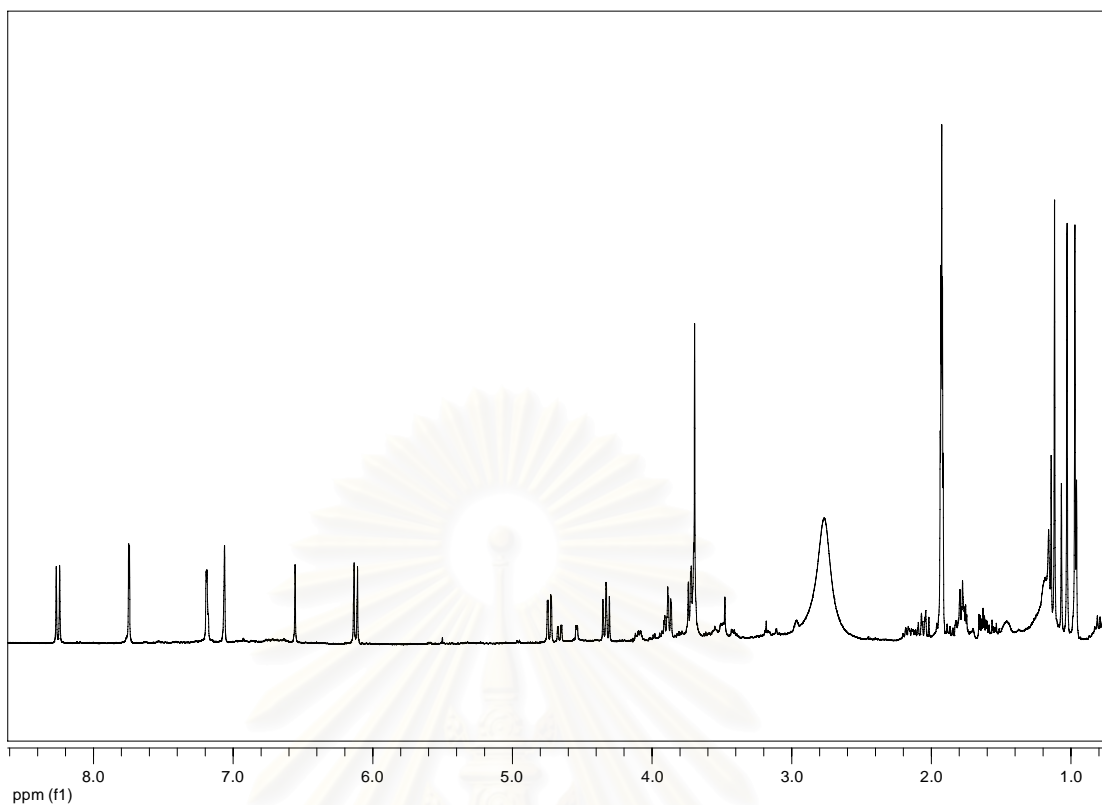


Figure 9. The ¹H NMR (CDCl₃) spectrum of feroniellin A (**8**).

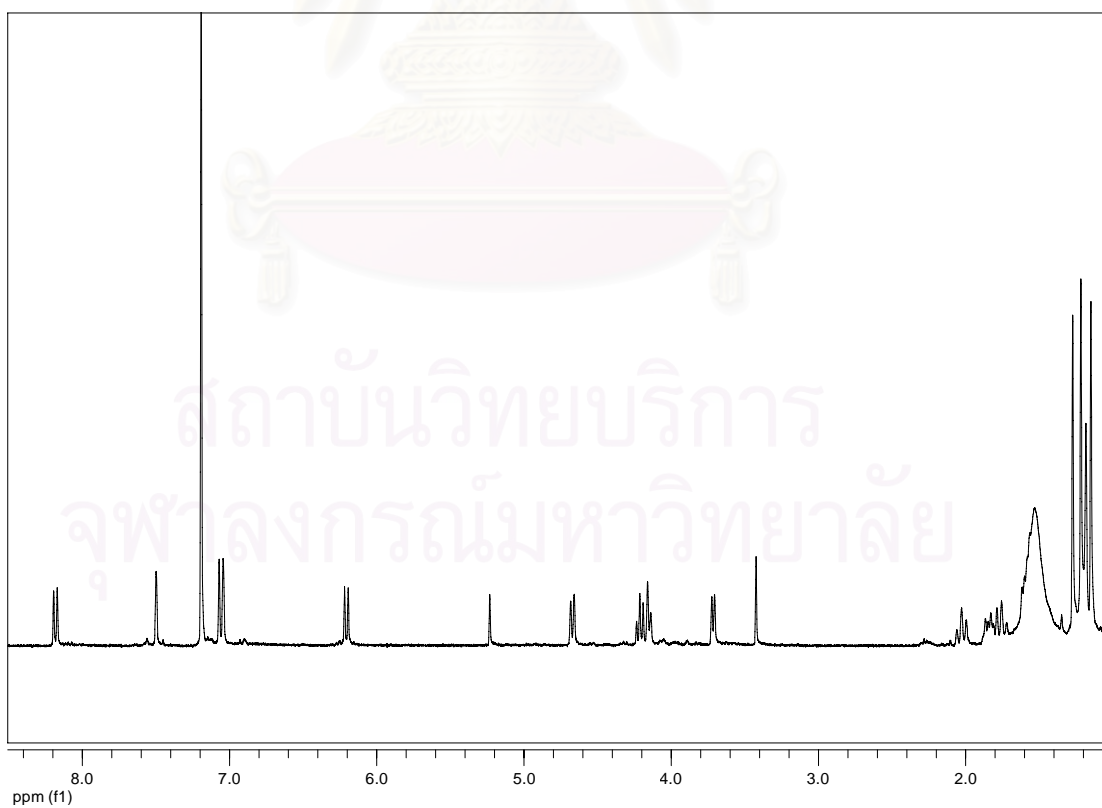


Figure 10. The ¹H NMR (CDCl₃) spectrum of feroniellin C (**9**).

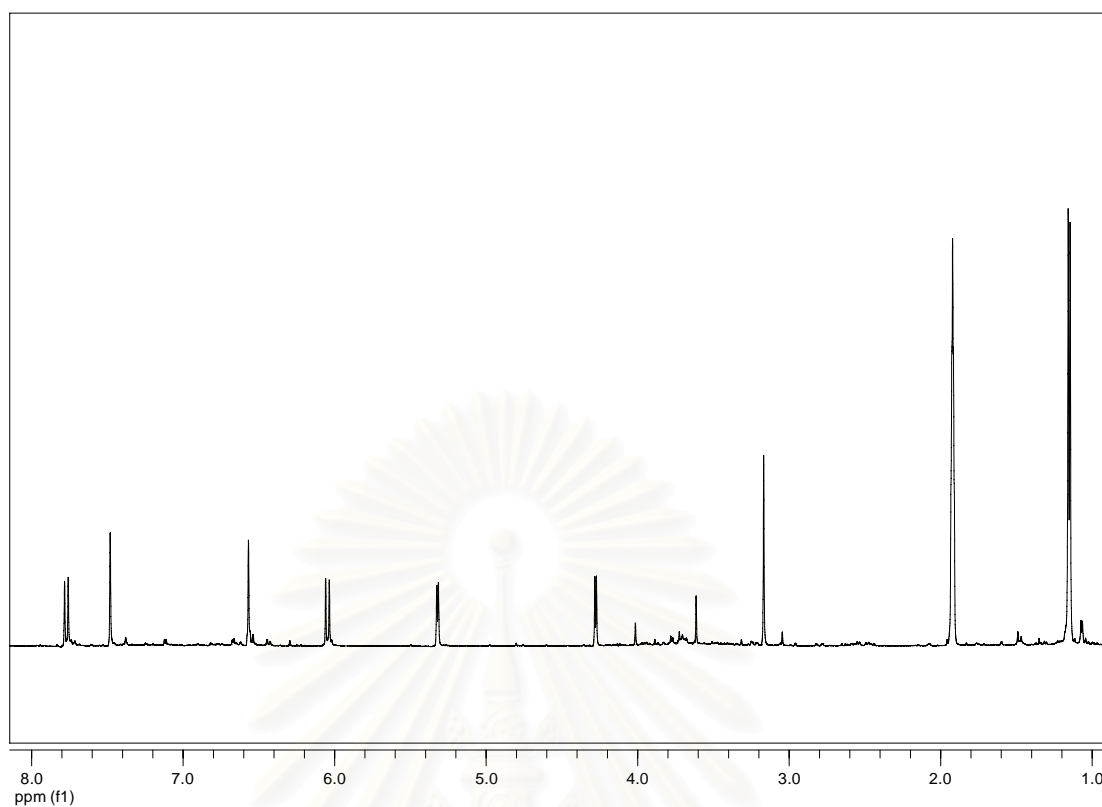


Figure 11. The ^1H NMR (CDCl_3) spectrum of xanthoarnol (**10**).

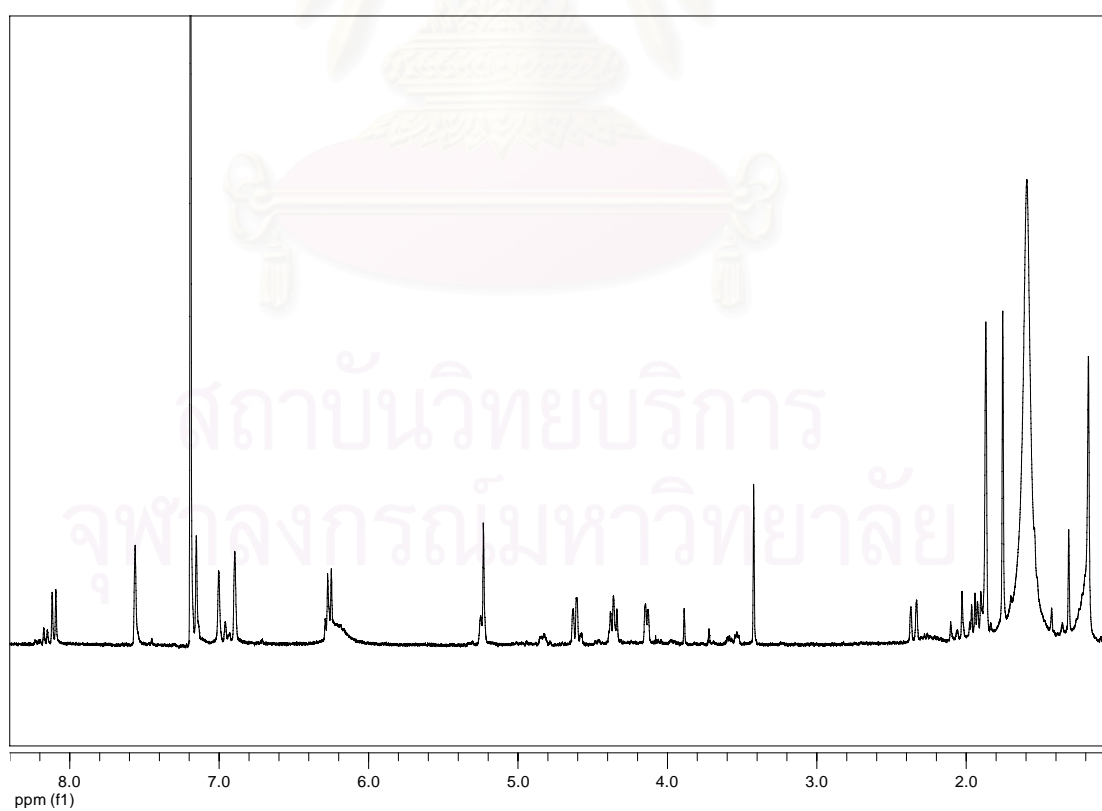


Figure 12. The ^1H NMR (CDCl_3) spectrum of feronielllic acid A (**11**).

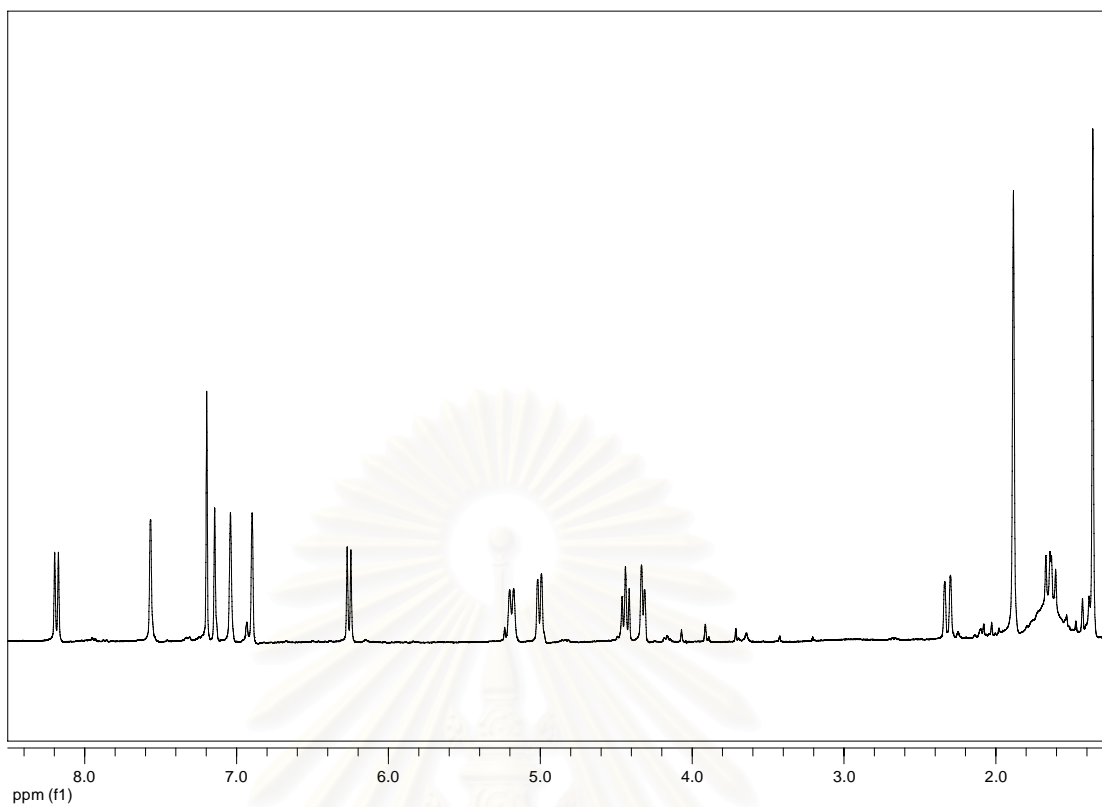


Figure 13. The ^1H NMR (CDCl_3) spectrum of feronielic acid B (**12**).

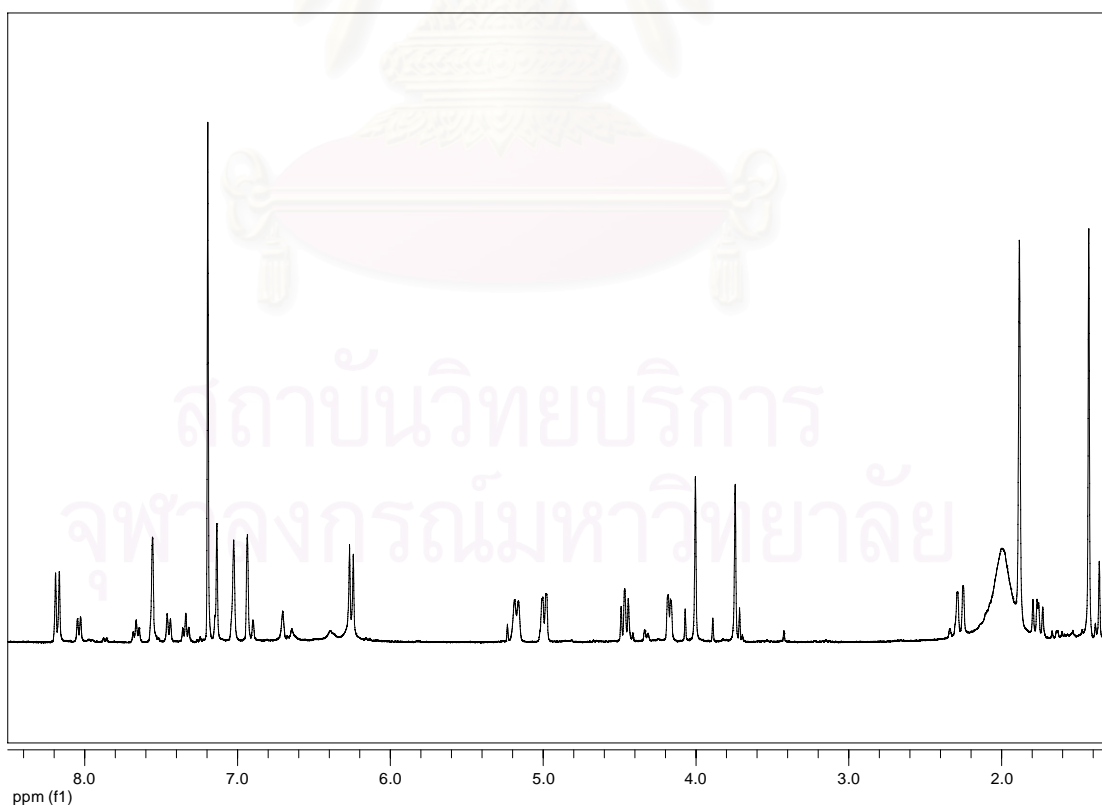


Figure 14. The ^1H NMR (CDCl_3) spectrum of feronielic acid C (**13**).

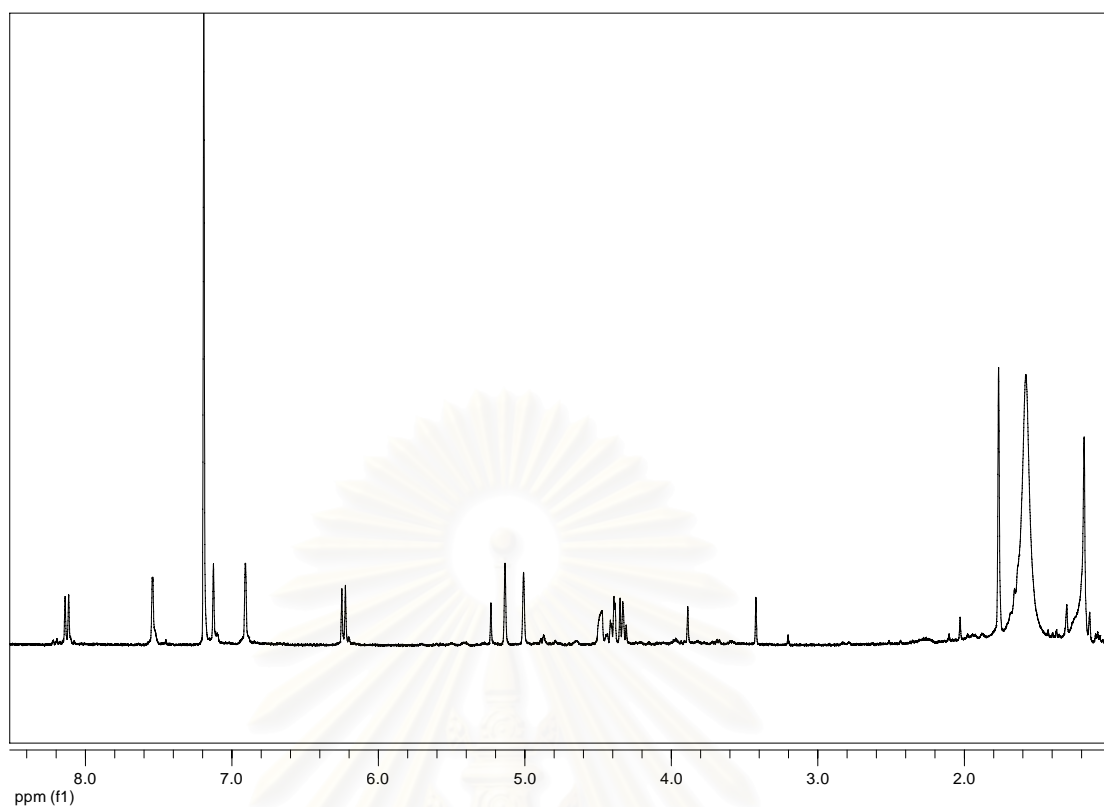


Figure 15. The ¹H NMR (CDCl₃) spectrum of gosferol (**14**).

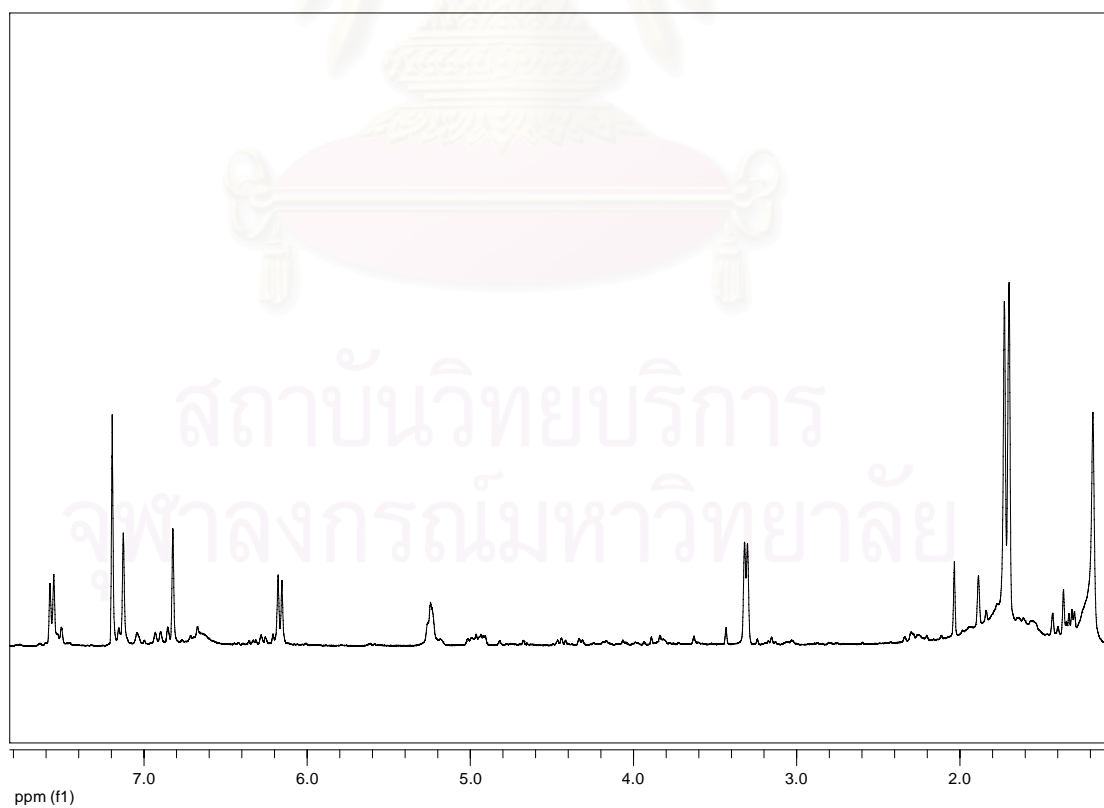


Figure 16. The ¹H NMR (CDCl₃) spectrum of 7- demethylsaberrosine (**15**).

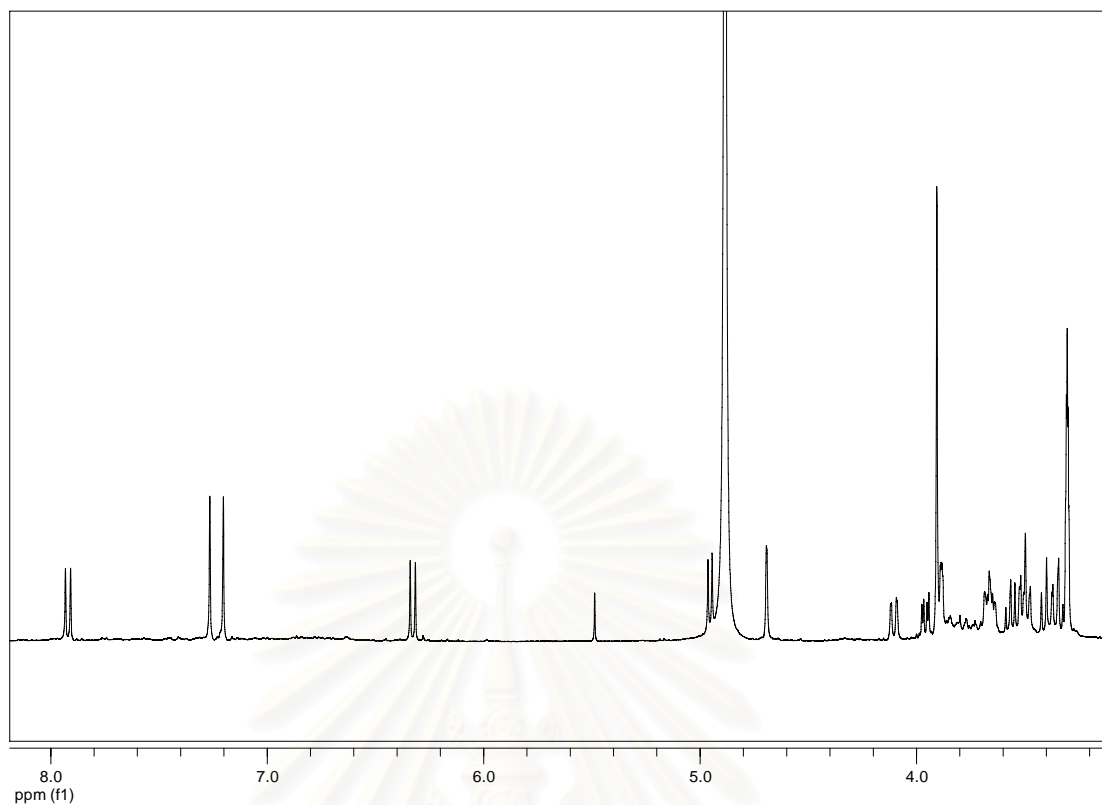


Figure 17. The ^1H NMR (CD_3OD) spectrum of haploperoside D (**16**).

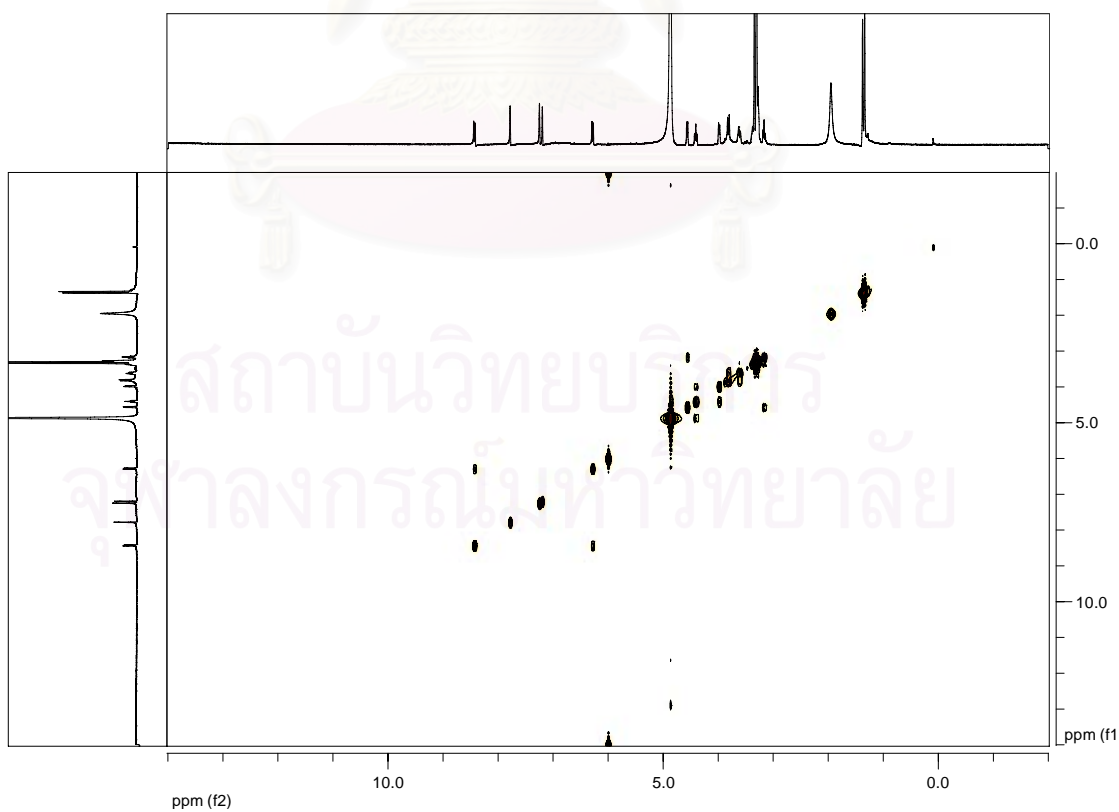


Figure 18. The COSY (CD_3OD) spectrum of feronielloside (**1**).

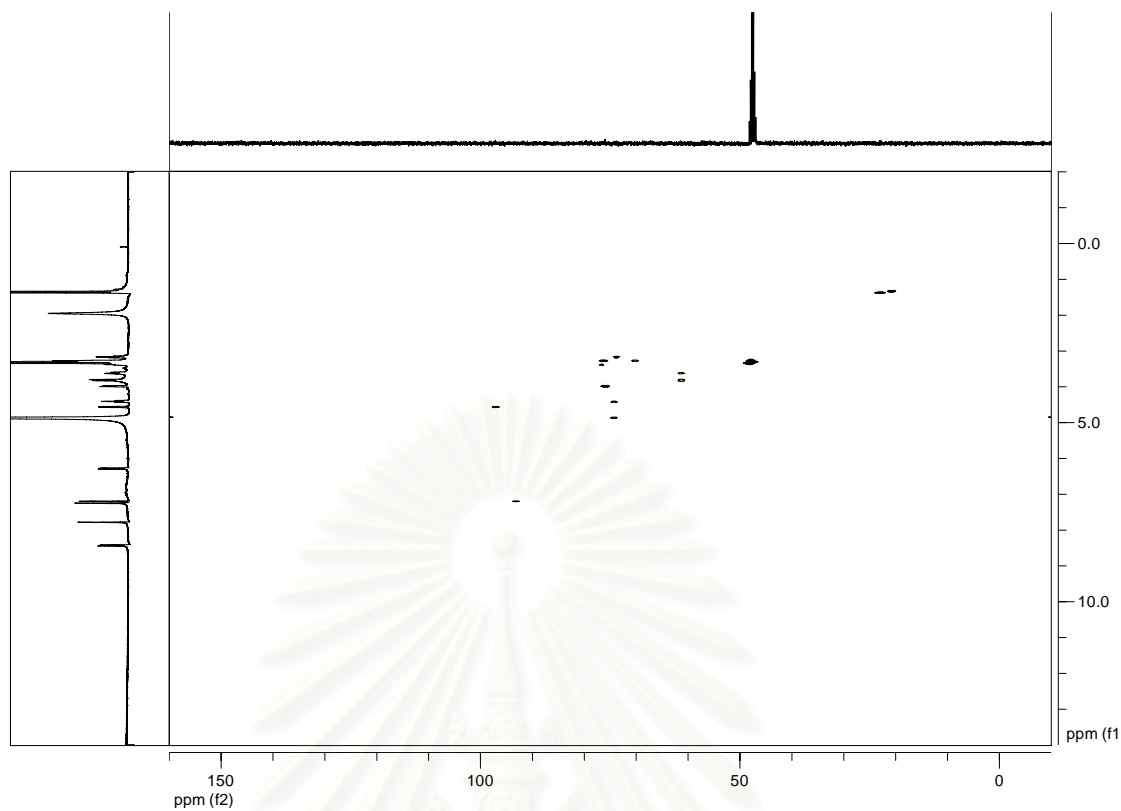


Figure 19. The HSQC (CD₃OD) spectrum of feronielloside (**1**).

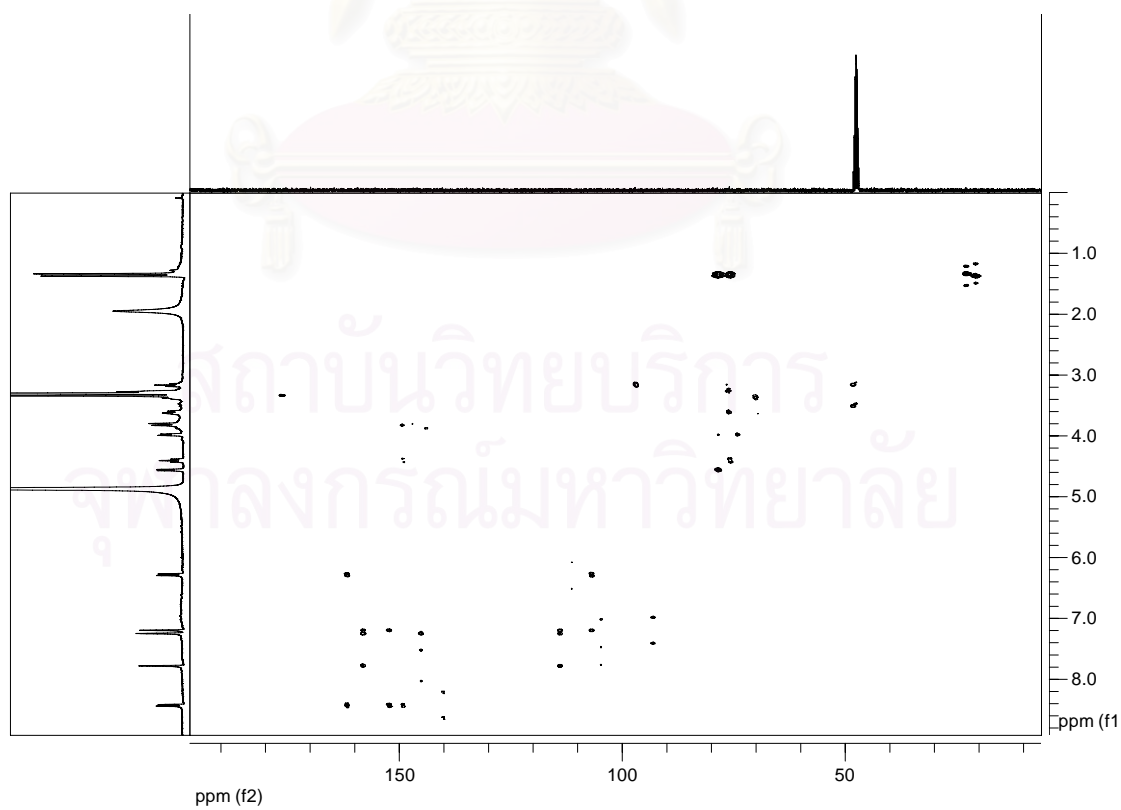


Figure 20. The HMBC (CD₃OD) spectrum of feronielloside (**1**).

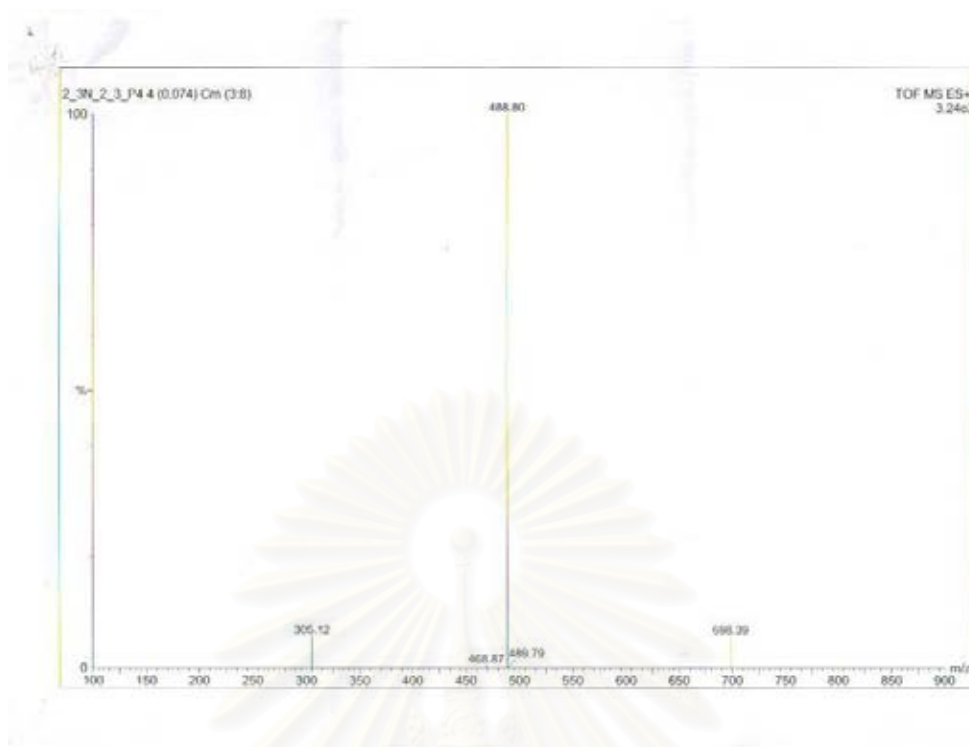


Figure 21. Mass spectrum of feronielloside (1).

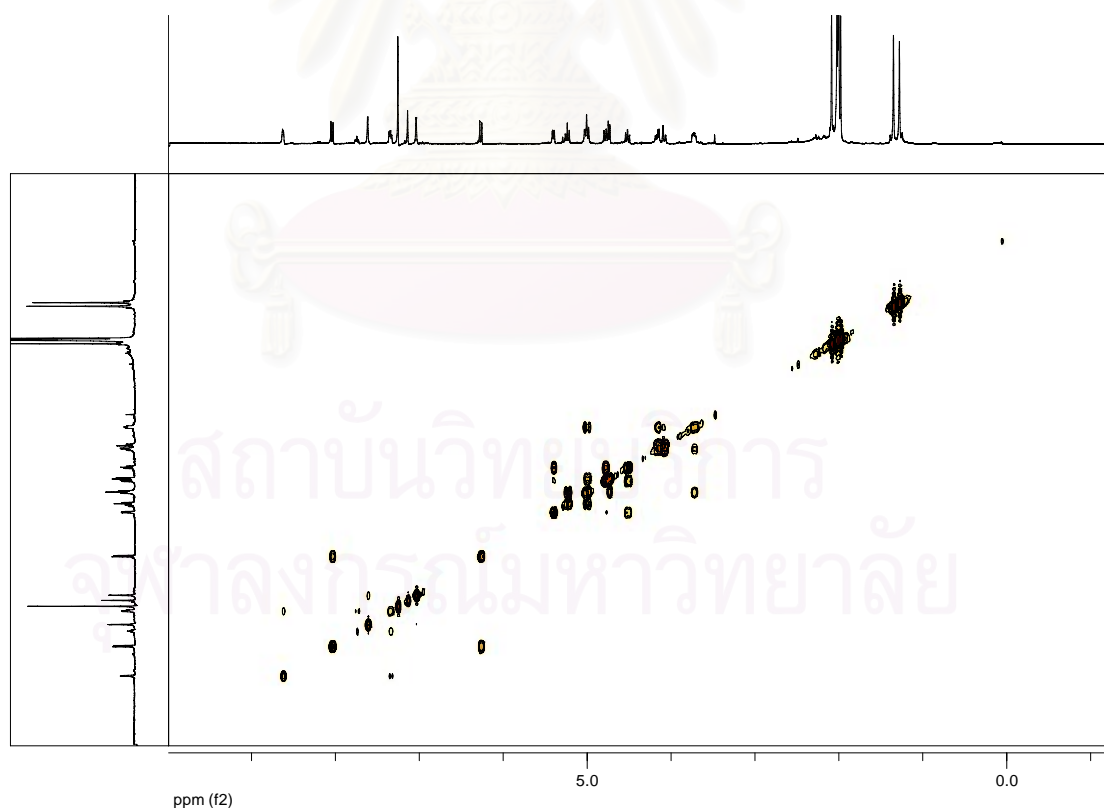


Figure 22. The COSY (CDCl₃) spectrum of feronielloside pentaacetate (1a).

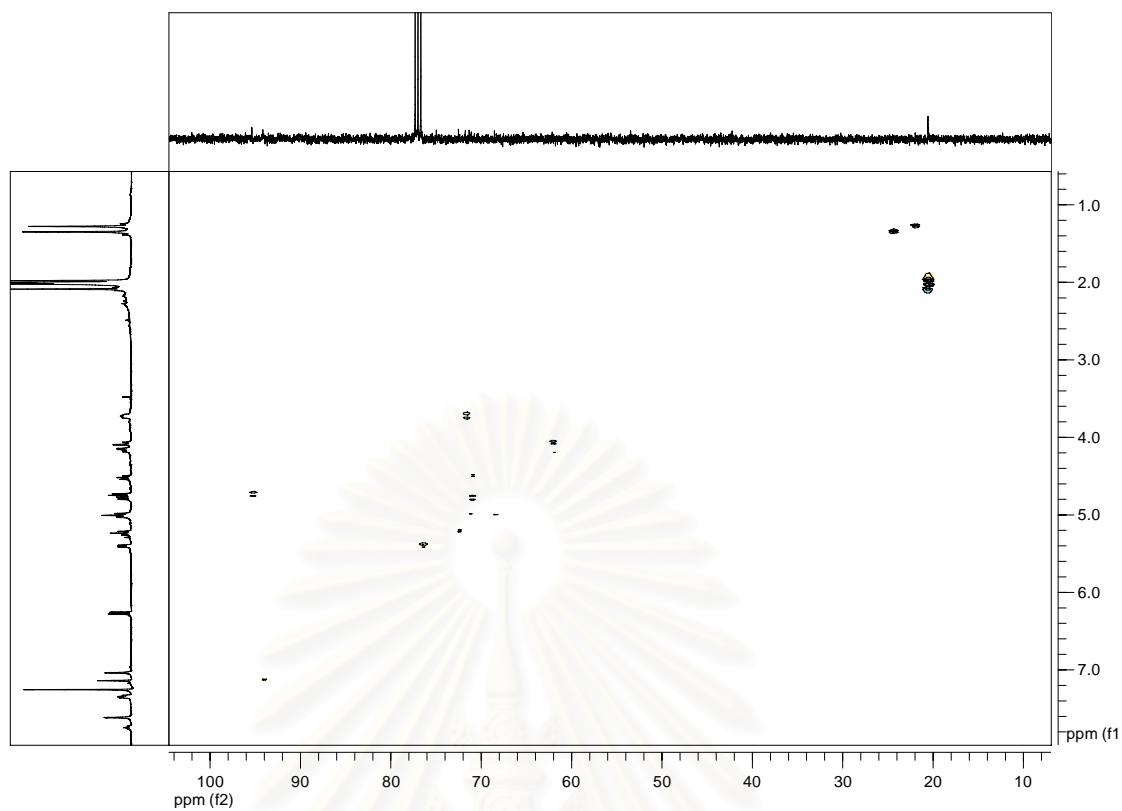


Figure 23. The HSQC (CDCl₃) spectrum of feronielloside pentaacetate (**1a**)

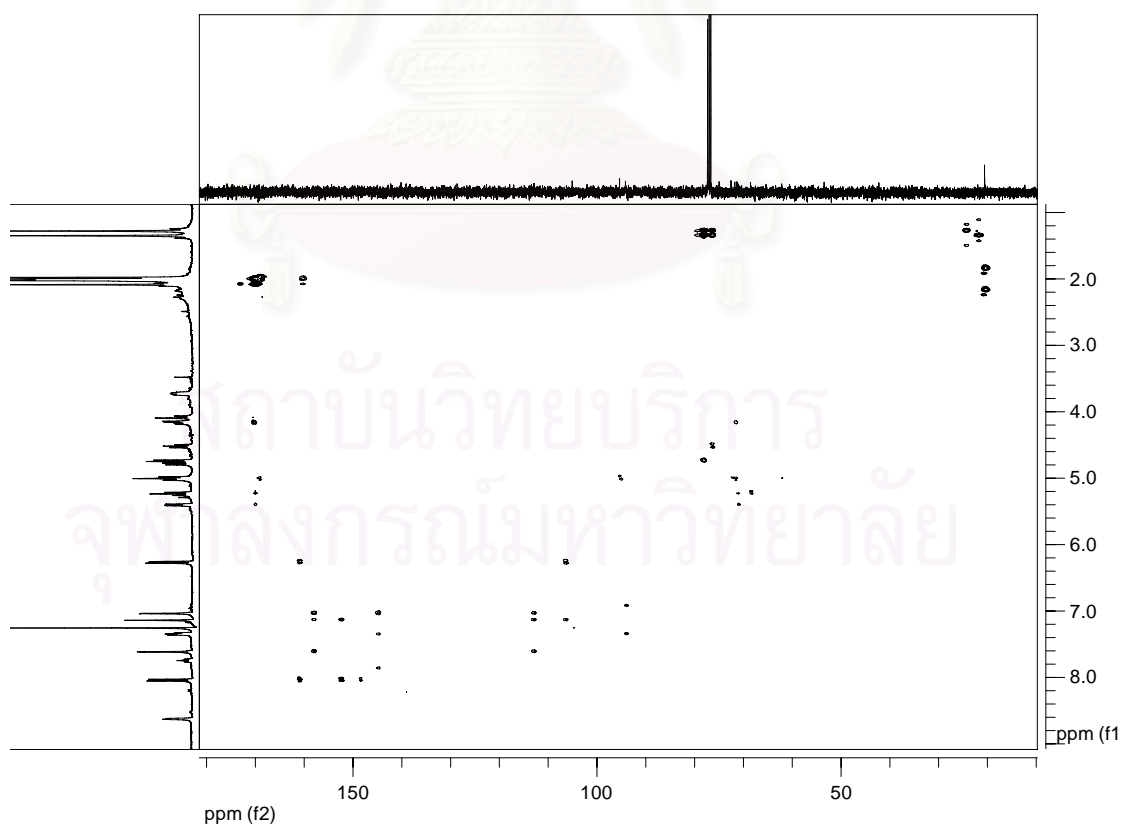


Figure 24. The HMBC (CDCl₃) spectrum of feronielloside pentaacetate (**1a**).

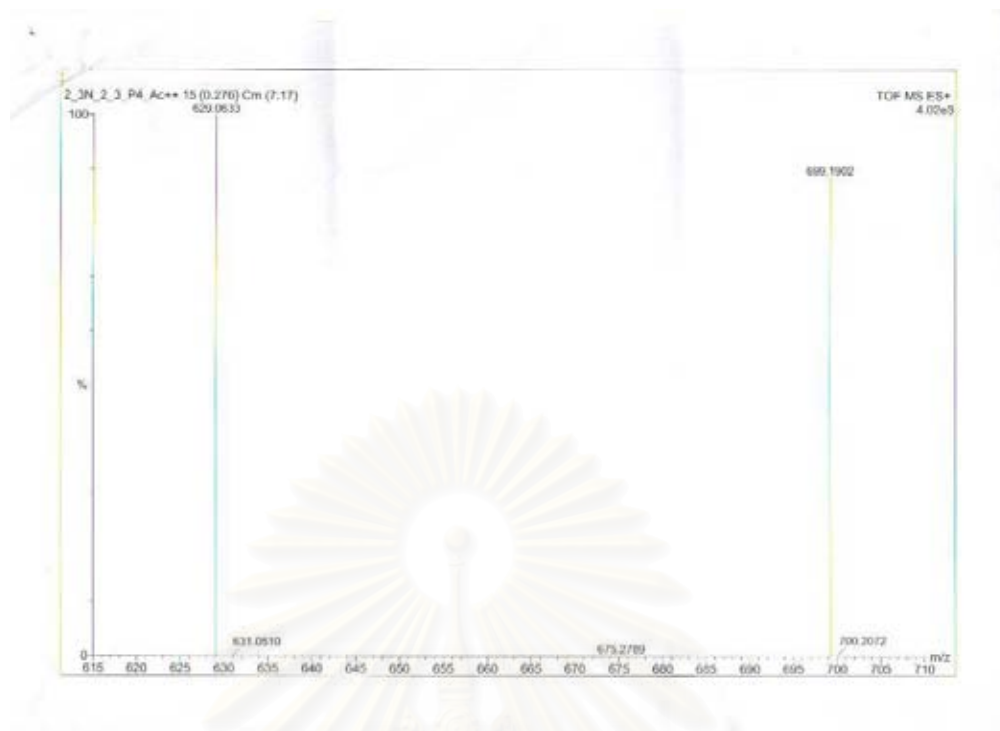


Figure 25. Mass spectrum of feronielloside pentaacetate (**1a**).

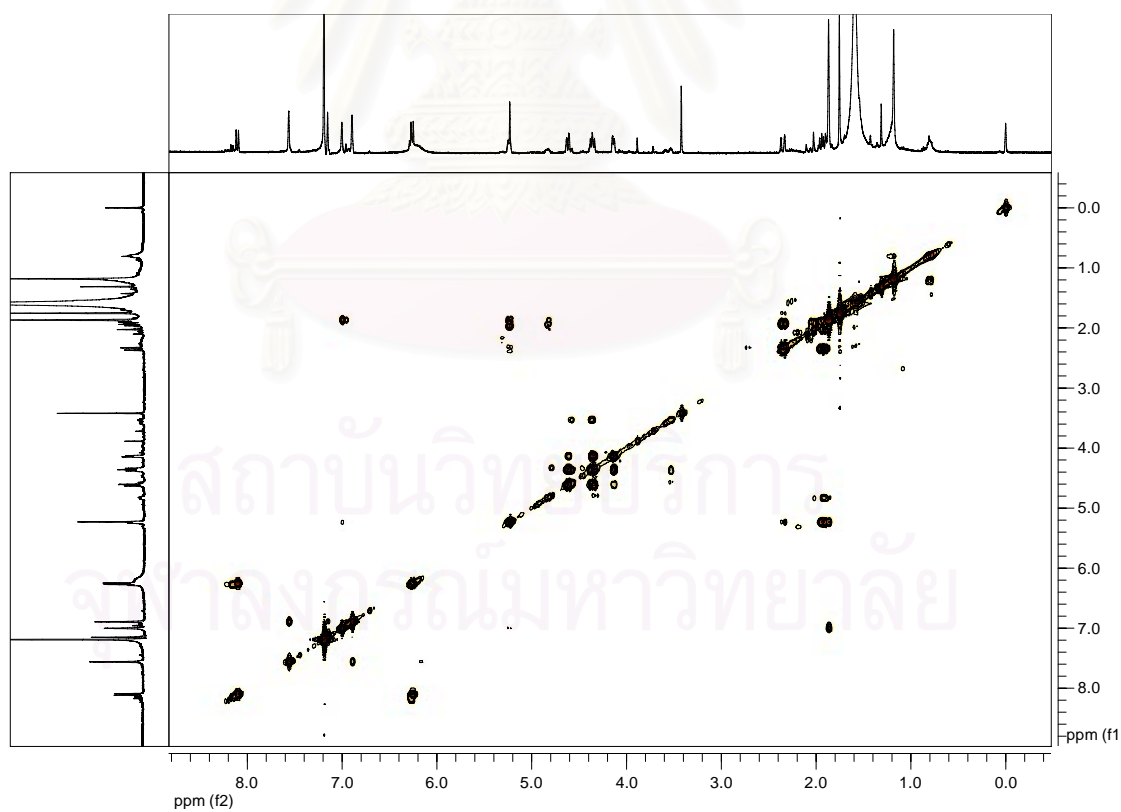


Figure 26. The COSY (CDCl_3) spectrum of feronielic acid A (**11**).

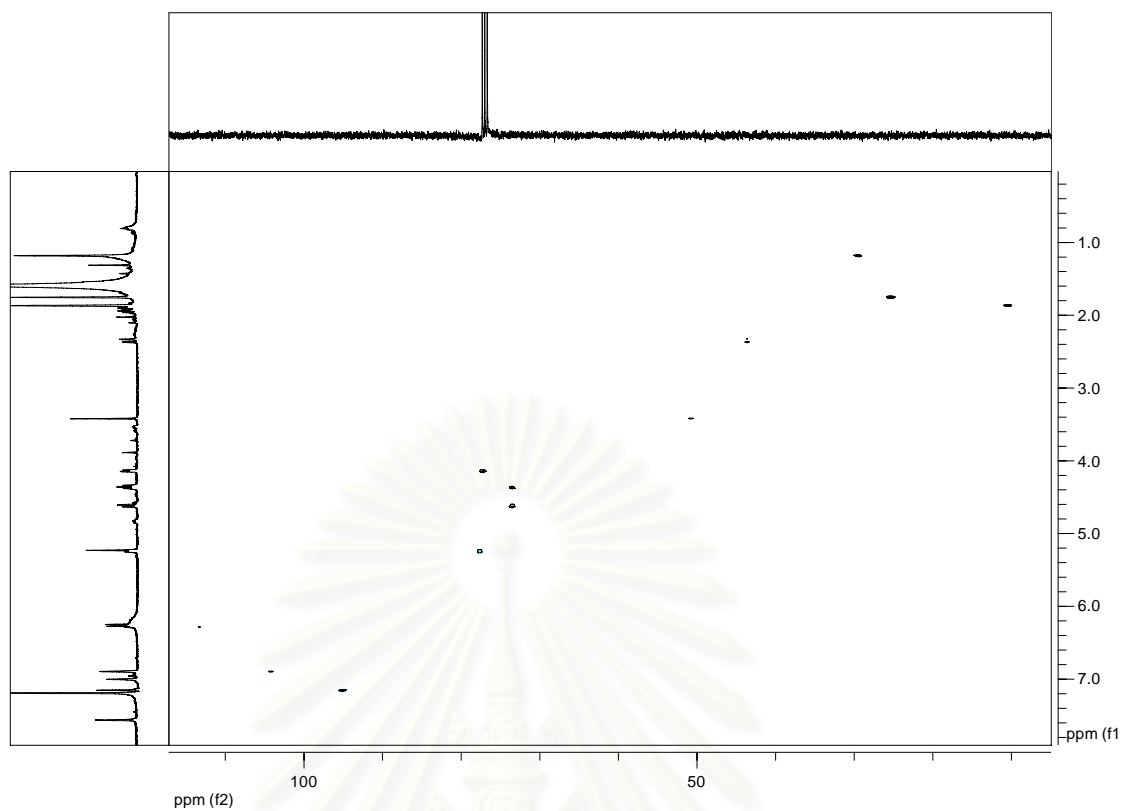


Figure 27. The HSQC (CDCl₃) spectrum of feronielllic acid A (**11**).

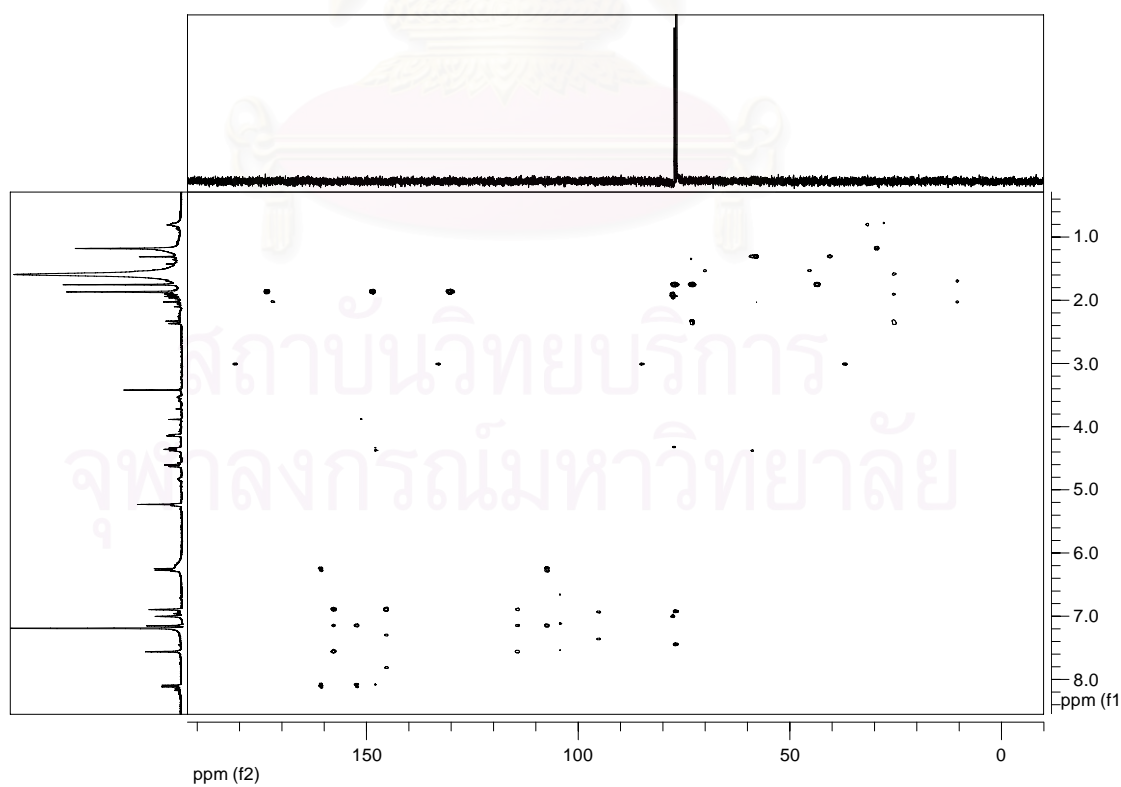


Figure 28. The HMBC (CDCl₃) spectrum of feronielllic acid A (**11**).

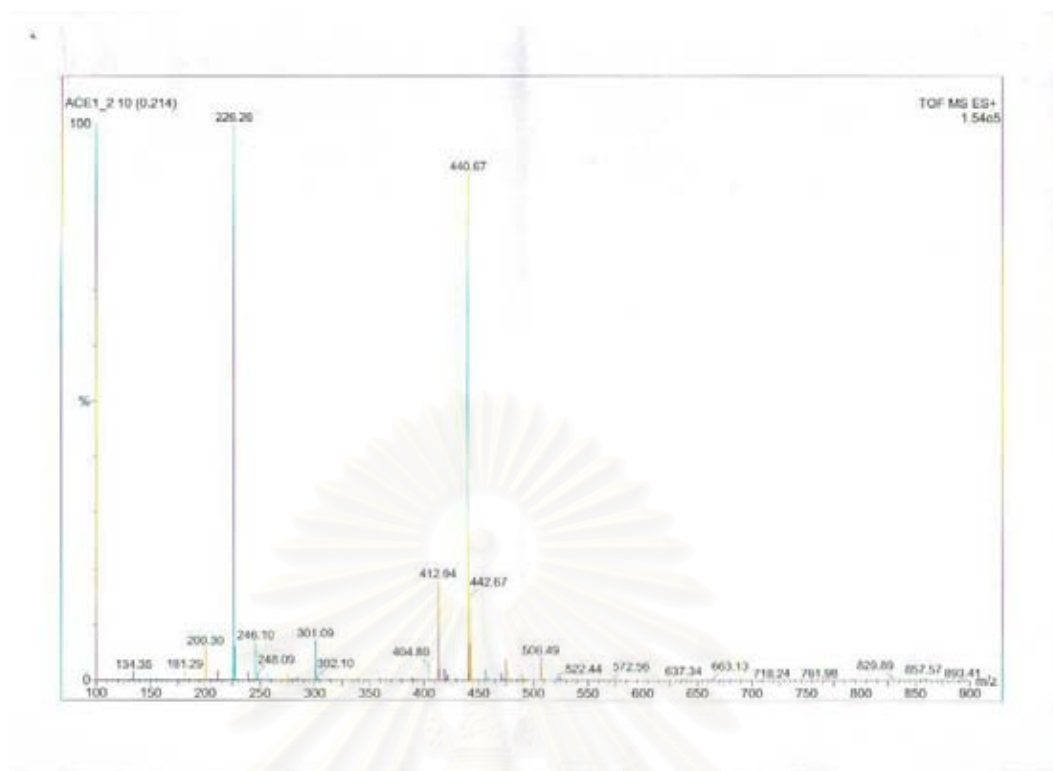


Figure 29. Mass spectrum of feronielllic acid A (**11**).

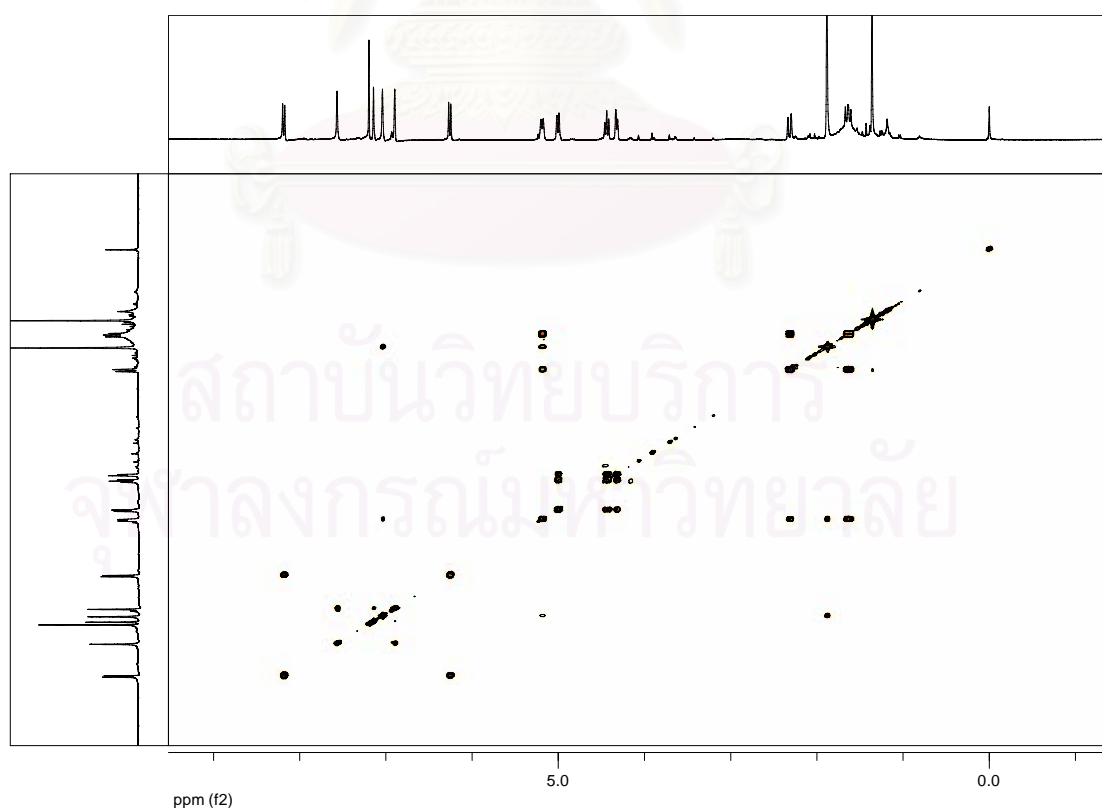


Figure 30. The COSY (CDCl₃) spectrum of feronielllic acid B (**12**).

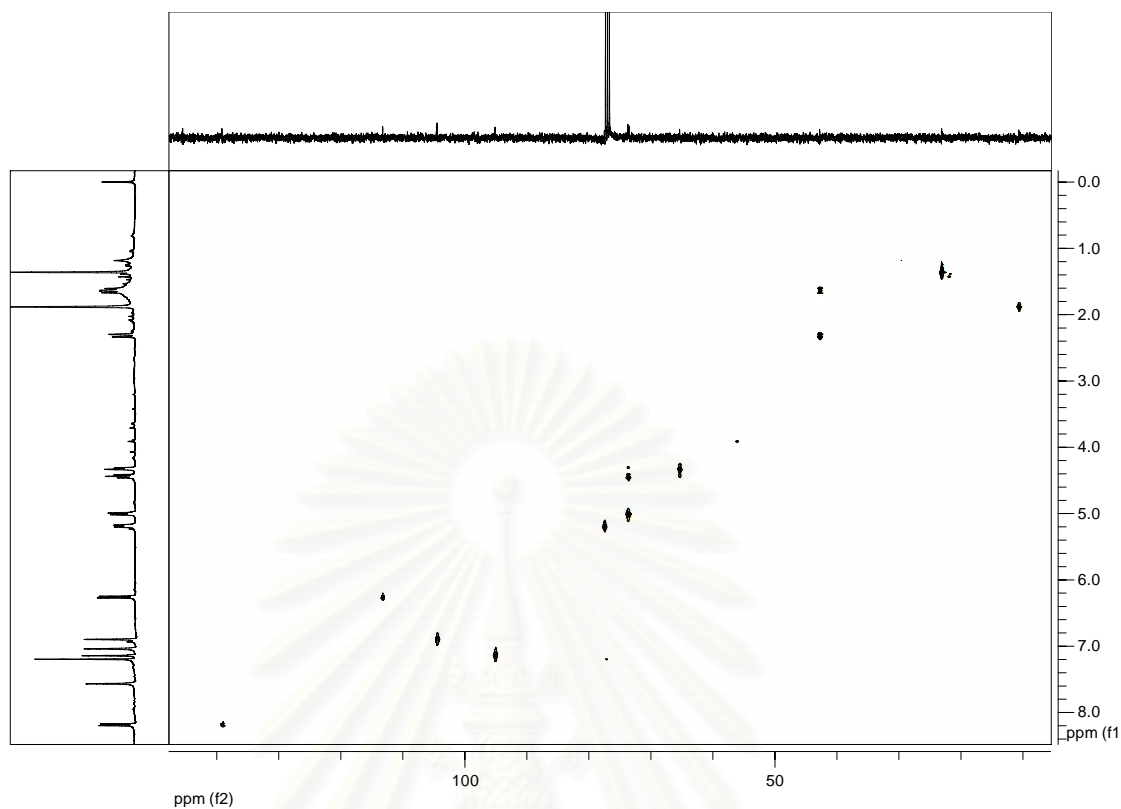


Figure 31. The HSQC (CDCl₃) spectrum of feronielllic acid B (**12**).

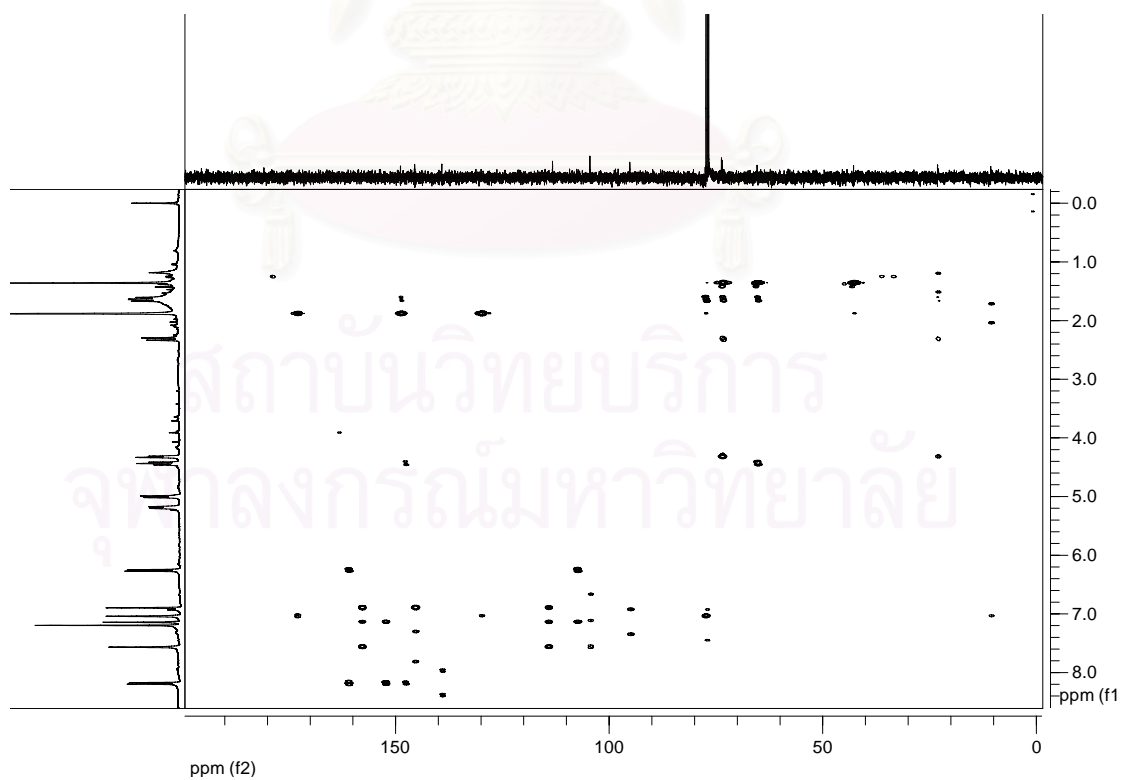


Figure 32. The HMBC (CDCl₃) spectrum of feronielllic acid B (**12**).

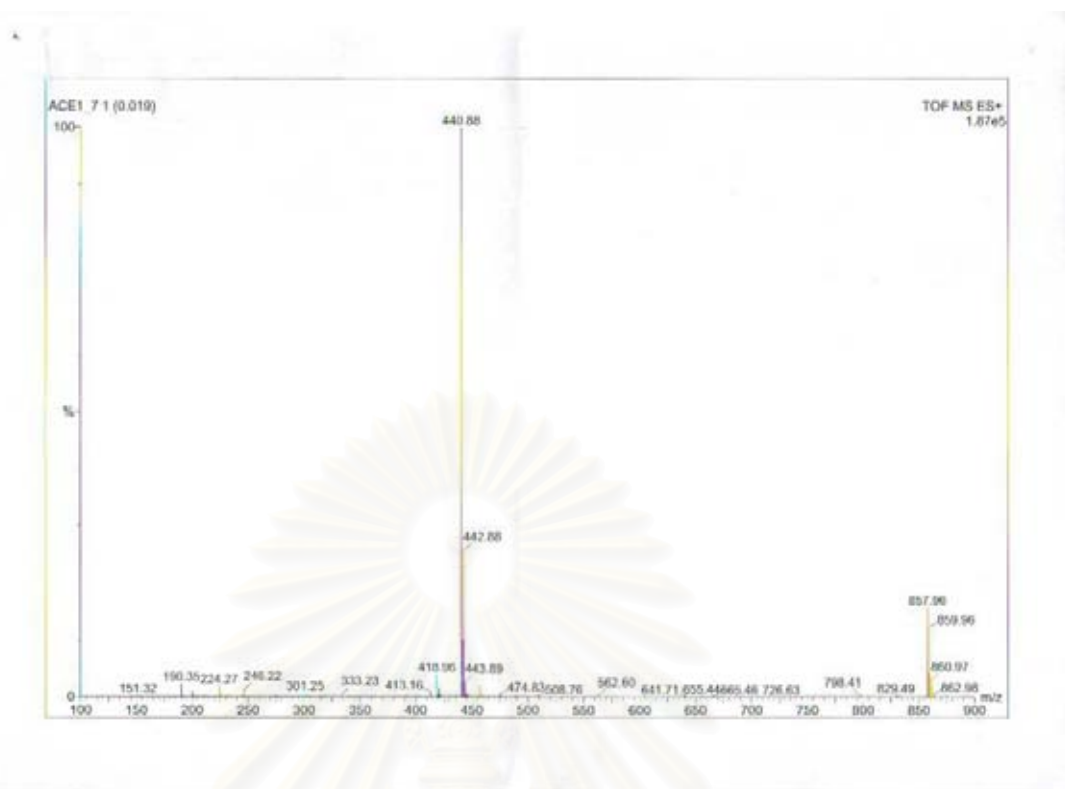


Figure 33. Mass spectrum of feronielic acid B (**12**).

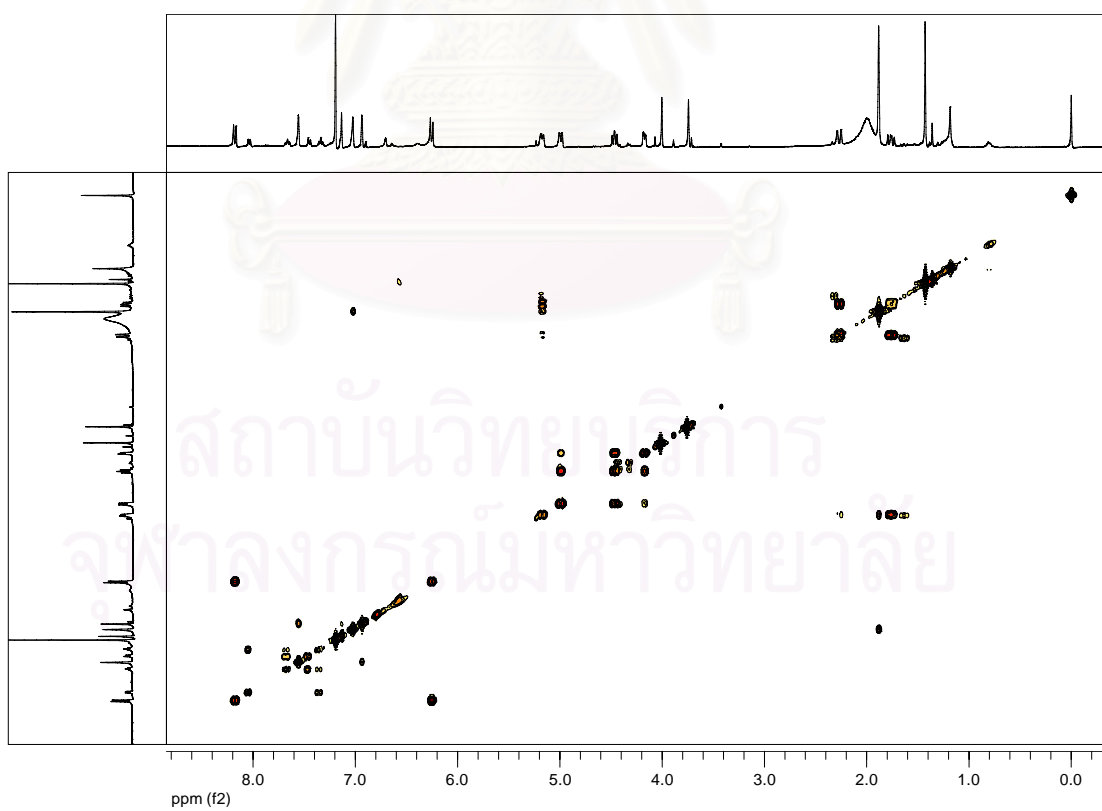


Figure 34. The COSY (CDCl₃) spectrum of feronielic acid C (**13**).

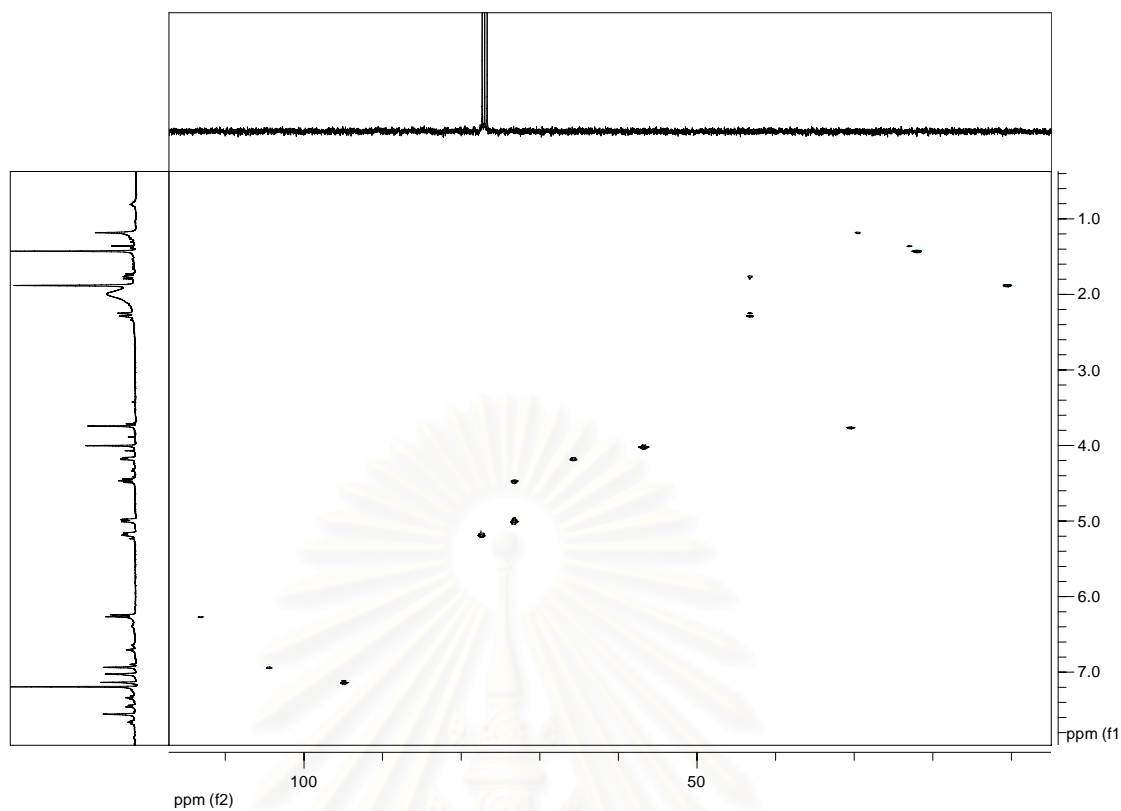


Figure 35. The HSQC (CDCl₃) spectrum of feronielic acid C (**13**).

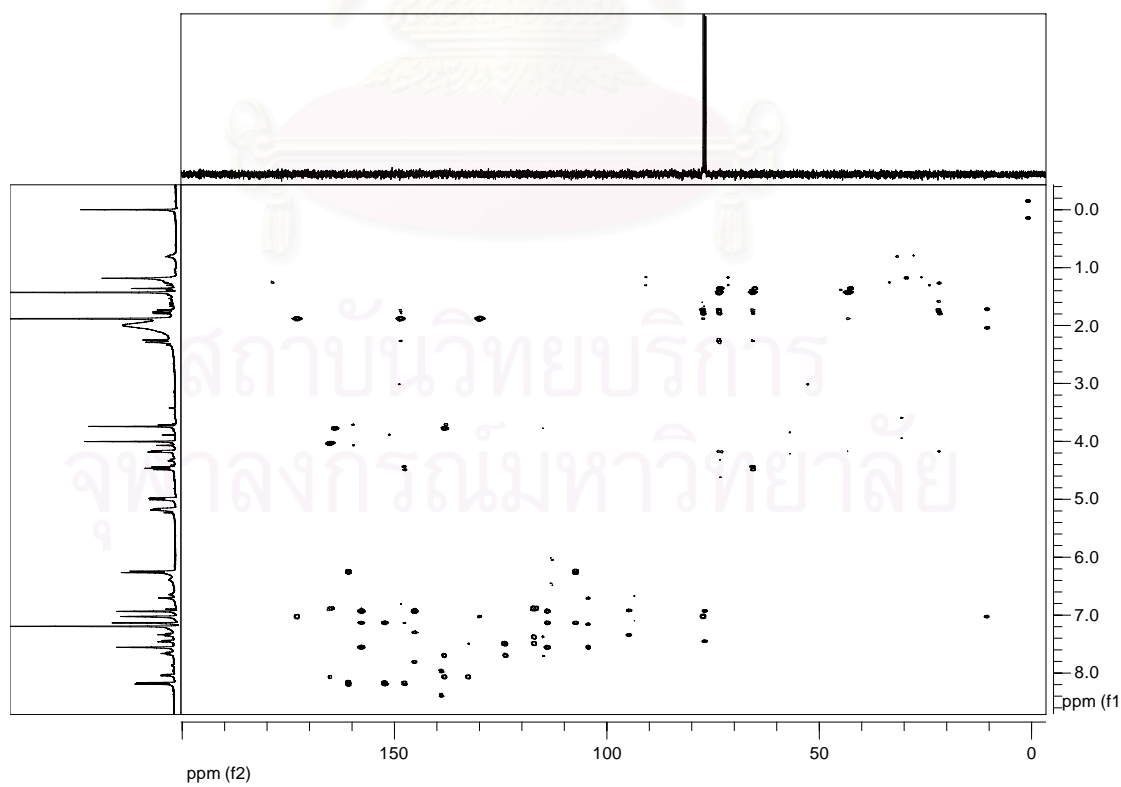


Figure 36. The HMBC (CDCl₃) spectrum of feronielic acid C (**13**).

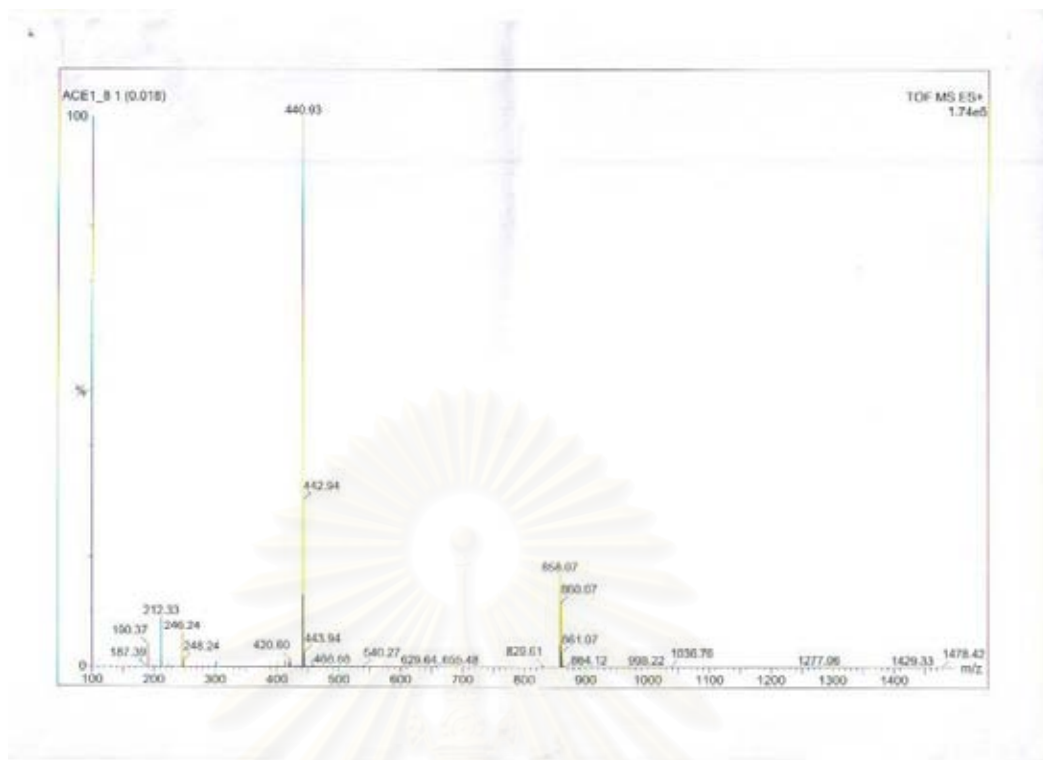


Figure 37. Mass spectrum of feronielllic acid C (**13**).

สถาบันวิทยบริการ
จุฬาลงกรณ์มหาวิทยาลัย

VITA

Ms. Chalouyluk Phoopichayanun was born on June 14, 1982 in Chonburi province, Thailand. She earned B.Sc. in Chemistry from Chulalongkorn University, in 2005. During studying in Master Degree in Department of Chemistry, she received the 90th Anniversary of Chulalongkorn University Fund (F-31-GS-ES13/29).



สถาบันวิทยบริการ
จุฬาลงกรณ์มหาวิทยาลัย